
# Phase Zero Final Report

## Recommendations on Composite Socket Fabrication based upon Experimental Results

**Christopher William Norfolk, PhD, and Jon Osborn, MS, MBA**
**SCRA / ARDI**
**20 June 2009**

# Report Documentation Page

*Form Approved*
*OMB No. 0704-0188*



| 1. REPORT DATE | 2. REPORT TYPE | 3. DATES COVERED |
|---|---|---|
| **19 JUN 2009** | **Final** | **21 Apr 2008 - 19 Jun 2009** |

| 4. TITLE AND SUBTITLE | 5a. CONTRACT NUMBER |
|---|---|
| **Prosthetics & Orthotics Manufacturing Initiative (POMI) Phase Zero Final Report: Recommendations on Composite Socket Fabrication based upon Experimental Results** | **N00014-06-D-0045** |
| | 5b. GRANT NUMBER |
| | 5c. PROGRAM ELEMENT NUMBER |
| 6. AUTHOR(S) **Norfolk, Christopher W; Osborn, Jon** | 5d. PROJECT NUMBER |
| | 5e. TASK NUMBER **DO 4/CLIN 12** |
| | 5f. WORK UNIT NUMBER |
| 7. PERFORMING ORGANIZATION NAME(S) AND ADDRESS(ES) **South Carolina Research Authority 91 Technology Dr, Suite 200 Anderson, SC 29625** | 8. PERFORMING ORGANIZATION REPORT NUMBER |
| 9. SPONSORING/MONITORING AGENCY NAME(S) AND ADDRESS(ES) **Mr. Neil Graf Office of Naval Research One Liberty Center 875 North Randolph Street, Suite 283 Arlington, VA 22203-1995** | 10. SPONSOR/MONITOR'S ACRONYM(S) **ONR** |
| | 11. SPONSOR/MONITOR'S REPORT NUMBER(S) |

12. DISTRIBUTION/AVAILABILITY STATEMENT
**Approved for public release, distribution unlimited**

13. SUPPLEMENTARY NOTES
**The original document contains color images.**

14. ABSTRACT
**The objective of was to gather quantitative data on the materials commonly used to manufacture definitive composite sockets. The purpose was to make informed recommendations to guide socket fabrication. Materials were fabricated into both flat panels and sockets. Flat panels were tested according to ASTM test protocols. Sockets were tested according to the static testing described by the ISO standard for lower limb prostheses.**

15. SUBJECT TERMS
**Prosthetics**

| 16. SECURITY CLASSIFICATION OF: | | | 17. LIMITATION OF ABSTRACT | 18. NUMBER OF PAGES | 19a. NAME OF RESPONSIBLE PERSON |
|---|---|---|---|---|---|
| a. REPORT | b. ABSTRACT | c. THIS PAGE | | | |
| **unclassified** | **unclassified** | **unclassified** | **UU** | **92** | |

# Executive Summary

The objective of was to gather quantitative data on the materials commonly used to manufacture definitive composite sockets. The purpose was to make informed recommendations to guide socket fabrication. Materials were fabricated into both flat panels and sockets. Flat panels were tested according to ASTM test protocols. Sockets were tested according to the static testing described by the ISO standard for lower limb prostheses.

It is important to note that the recommendations made in this report are on the basis of the static properties only. Fatigue testing was not performed as part of this work, and so the recommendations made must be implemented with care.

The major recommendations which stem from these static testing results are as follows:

- All failures observed from the static testing were observed at the attachment point, posterior. An analysis of the complex loading at this point indicates that the induced tensile forces at this point may be responsible for the failure. These failures were only observed when a single layer of reinforcement was tied into the plate, and never when more reinforcement was used. A good way to increase strength at this point without unnecessary weight is to use bi-directional carbon tape to add fibers in the most critical direction (0° to the socket's main axis).

- It was observed that adding reinforcement to just the distal three inches increased the static ultimate strength by at least 37% of the P4 loading requirement. In many cases, it may be preferable to use this partial layer, rather than a full layer, to increase strength but not add additional weight. This technique also adds low-angle fibers at the most critical area, and will result in greatly increased static strength.

- Higher vacuum pressures should be used for socket fabrication. The expected result is a reduction or elimination of resin-rich areas, especially those at undercuts in the socket. These resin-rich areas add weight without adding strength, and may serve as flaw initiation sites. This recommendation may require three additional actions:

    - Ensure a good seal of the inner vacuum bag. This may be most easily accomplished using the pre-sealed PVA bags now commercially available.

    - Prevent the collapse of the outer vacuum bag toward the mounting pipe by supporting it with a breather material. A simple felt material wrapped around the base of the mounting pipe would suffice. This material should be built up to the diameter of the residual limb mold, at least.

- Limit the physical manipulation of the resin into the fabric. This will prevent stretching of the PVA bag. Stretching of the bag will counteract the compaction forces applied by the vacuum.

- One of the most common failures of sockets observed in clinical practice is delamination failures near the brim of the socket. It is likely that these interlaminar failures are occurring at this secondarily bonded interface between a first and second infusion; to combat this, it is suggested that greater care be taken to the preparation of the surface of the initial infusion, especially in the area within 3-5 inches of the brim. This area should be roughed and cleaned as carefully as possible, using a relatively coarse grained sandpaper, and acetone or water for cleaning. This is expected to help address fatigue type delamination failures which are observed at the brim.

## Table of Contents



## List of Figures

# Introduction

Composite materials, which were first developed to meet the need of the aircraft industry after World War II, are an important class of materials which offer high strength and stiffness coupled with low weights. Prosthetics is one of the many areas which take advantage of these materials, presumably to easily fabricate a suitable socket with reduced weight and volume compared to what could be achieved by using other materials.

The fabrication of composite sockets involves many complex factors, and advanced materials, which need not be fully understood in order to fabricate suitable sockets. However, in order further increase the ease of fabrication, further reduce weight, and further reduce volume, a careful examination of the fabrication techniques and materials is merited. The goal is optimization of existing best practices.

In order to make recommendations, a discussion of fabrication methods is undertaken. Flat panels fabricated from materials commonly used in the prosthetics fields were tested according to ASTM standards in order to recommend one material over another. Sockets were fabricated and tested according to the ISO standard for testing lower limb prosthesis. These experimental results are meant to help improve already excellent practices.

An important limitation to the recommendations discussed below must be noted. All testing described herein are of static mechanical properties only. The mechanical properties over extended use, the fatigue properties, should also be similarly studied in order to fully test the mechanical properties of the materials. Since the fatigue properties were not studied, the recommendations suggested here must be implemented with care.

# Background

Sockets are fabricated using techniques which are similar to Vacuum Assisted Resin Transfer Molding (VARTM). A discussion of socket fabrication, traditional VARTM processing, and the important differences between the two, will provide an important background.

## Socket Fabrication

A positive mold is made of the patient's residual limb. This is normally done using plaster placed against the residual limb, creating a negative mold. The negative mold is used to create a positive mold by filling it with more plaster; a mounting pipe is inserted into the positive mold. After 'rectifying,' in which the prosthetists makes any changes to the positive mold deemed necessary for comfort, the mold is placed into a vise and manufacturing can begin. In the diagram below, the plaster positive mold is shown in solid gray, and the mounting pipe in black. A vacuum bag made of poly(vinyl alcohol) (PVA) (shown in light blue) is pulled over the mold. The top of it is sealed and the bottom is sealed to the mounting pipe using electrical tape (shown in black). A vacuum is pulled on the bag through a vacuum port in the

mounting pipe (shown in orange). This pulls the bag tightly around the model, ensuring that no fine details of the mold are lost in the manufacturing process. The prosthetist then lays up the fabrics deemed necessary for the patient's height, weight, and activity level; these are normally carbon and fiberglass fibers (shown in black, white, and gray). These fabrics are tied to a metal mounting plate positioned at the distal of the socket (which is at the top of the diagram) which is omitted from the diagram above for simplicity's sake. The mounting plate becomes an integral part of the socket and serves as the attachment point for the terminal device. After the fibers and mounting plate are in place, a second PVA vacuum bag is pulled over the part (shown in red). It is sealed at the bottom using electrical tape and a second vacuum port pulls the bag down around the part. The top of the bag is open, and resin (shown in green) is introduced through the top.

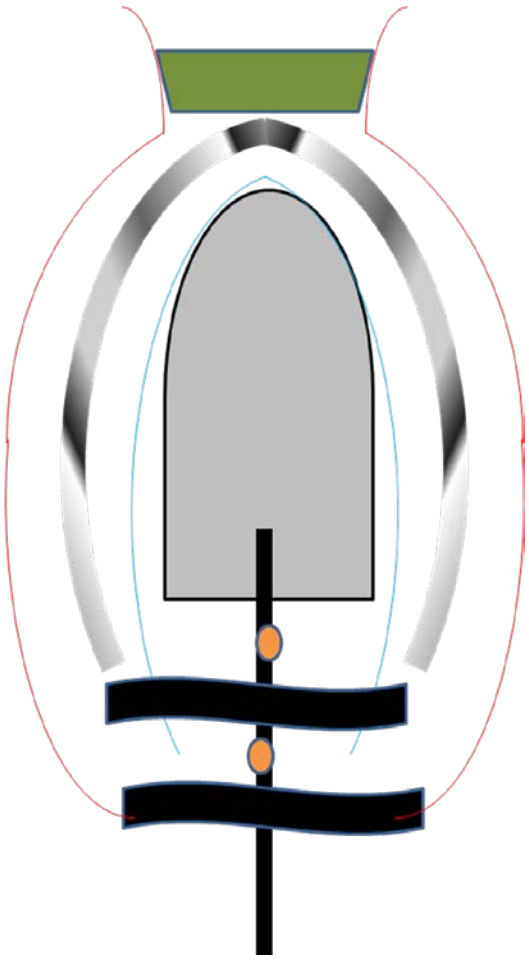

**Figure 1: Schematic of Socket Fabrication**

The resin is pulled into the fabrics by the vacuum force, and the prosthetist is also able to encourage it to move through the part by physical manipulation of the resin pot which forms at the distal end. After

the resin has fully wet the fabrics, and any excess has been squeezed out of the part, the resin's cure cycle can be initiated using a heat gun. Heat is applied to encourage the start of the cure, but is monitored such that the temperature of the part does not exceed the melting temperature of the vacuum bag.

## Vacuum Assisted Resin Transfer Molding (VARTM)

Vacuum Assisted Resin Transfer Molding (VARTM), as practiced in the more traditional composites field, will be described here, to highlight the differences between it and the process as applied to socket manufacturing.

The advantages offered by the VARTM process benefit not only the quality of the final part, but also the fabricators. VARTM process allows for minimum exposure of workers to the harmful chemicals in the resins, and also minimizes the environmental impact of fabrication. It further results in fabricated parts of extremely high quality at relatively low cost. This is generally due to the compaction forces applied to the parts by the vacuum force, which results in a small amount of voids, and a high amount of fibers relative to the resin. Voids are deleterious to mechanical strength by mechanisms similar to those found in metals; they act as stress risers which can initiate failure at loading levels lower than what the part may otherwise be able to withstand. High fiber content is advantageous because the mechanical properties of the fibers are much greater than those of the resin; all other factors being equal, the optimum resin content would be the minimum required to keep the part held together.

VARTM uses vacuum force to pull resin into the fiber structure of a part and the same vacuum force to compact the part, which results in a low resin content. This simple statement somewhat masks the difficulty this processing technique actually entails. The following will pursue a sequential (versus global) description of VARTM.

In the simplest case, reinforcing fabric is placed on a solid mold and a vacuum bag sealed around the edges of the mold. Resin is introduced on one side of the part and vacuum introduced on the other side of the part. The intent is that the vacuum pulls the resin into the vacuum bag, through the reinforcing fabric, and toward the vacuum line. The problem with this simple set-up is that the vacuum force will pull the vacuum bag tightly against the top of the part, forcing resin to travel only through the reinforcing fabric. This results in an extremely tortuous path, over which the resin cannot travel effectively. The path is also extremely long; it is essentially the width of the part. The result is a failed infusion, where the resin gels before it can travel through the entire part.

What is required, then, is a material which allows the resin to effectively pass through it. This material is known as resin distribution material, and is placed on top of the part. Resin distribution material prevents the bag from completely collapsing onto the part, and allows resin to travel over the part, then infusing down through the thickness of the part, a relatively short length. This then solves the problem observed above, and resin is capable of infusing the entire part. However, upon gelling, the resin which remains in the resin distribution material solidifies as well, and the distribution material remains bonded

to the final part. The result is the inclusion of the resin distribution material, which adds additional weight without adding much strength.

This can be further refined by including a peal-ply. The peal-ply is a thin layer which is placed in direct contact with the part, between the resin distribution material and the part. The peal-ply has small holes in it, to allow resin to move from the distribution material to the part. In addition, the peal-ply has been coated with a material which does not adhere to the resin (normally either nylon or silicone). The result is that after the resin gels, only small bridges of resin adhere the part to the resin distribution material, and thus the distribution material can be relatively easily broken free.

The final part which can be employed in VARTM processing is breather material. Breather material is used to allow the vacuum optimum access to the part by preventing the collapse of the vacuum bag at the edges of the part; this results in better compaction, faster infusion, and greater removal of voids, both from air entrained in the resin, and from volatiles evolved by the polymerization reactions undergone by the resin. The placement of breather, whether only near the vacuum source, or completely surrounding the part, is not strictly prescribed, and likely differs based on the part being fabricated.

After infusion, the cure cycle can be initiated.

## Socket Manufacturing versus Traditional VARTM

While on the surface socket manufacturing appears to follow the methods used in Vacuum Assisted Resin Transfer Molding (VARTM), there are differences that socket manufacturing exploits that simplify the process considerably. The major difference is the ease with which a prosthetist can manipulate the resin pot formed at the distal end during infusion. As mentioned above, physical manipulation of the resin pot can encourage resin infusion; this is done simply by pinching the outer vacuum bag by hand above the resin pot and squeezing the resin pot, forcing resin into the part. In traditional VARTM, the resin is not easily manipulated into the part. This is because it is generally separated from the part by a length of tubing; this is done to prevent the pot from attaching to the final part, which would then require considerable labor to remove. Additionally, the behavior of the PVA during infusion aids the manipulation of the resin into the socket. PVA is affected by moisture, becoming more compliant when moistened; it is common to moisten the vacuum bag prior to stretching it over the socket during fabrication. The PVA also becomes more compliant when in contact with the resin, lessening the force which is required to squeeze resin past the pot formed at the distal end and into the socket.

In terms of affecting resin infusion into the socket, the physical manipulation of resin plays a much more important role than the vacuum force used. This statement can be supported by the following two examples.

- First, when the vacuum bag is pulled over the positive model and secured in place, there is insufficient support to prevent the bag from collapsing toward the mounting pipe. Since the bag

is secured in place at the bottom, and stretched tightly at the top, this collapsing effect under vacuum pressure can cause the bag to stretch and pop. This has resulted in the use of very small vacuum pressures during socket manufacturing, when compared to more traditional VARTM processing. A picture of the bag collapsing at toward the mounting pipe is shown below.

**Figure 2: Illustration of the collapse of the vacuum bag**

- Secondly, when a similar method is attempted for flat panel fabrication, failed infusion results. Flat panel fabrication was pursued using a feed line to connect the resin pot to the part, with vacuum force alone used to draw resin into the part. Infusion was only able to proceed ~ 2 inches from the feed source, where infusion stalled until the resin gelled. This was done using two vacuum forces, one similar to those used for socket fabrication, and one more in line with those used in traditional VARTM processing. This result is not surprising when the mechanism of resin infusion in VARTM described above is considered. In VARTM processing, the 'resin distribution material' allows resin flow along the top of the part, after which infusion down through the part occurs.

The physical manipulation of the resin pot may be sufficient for getting resin into the socket without any vacuum applied, although this study did not attempt this. However, getting resin into the fibers is not the only purpose of the vacuum force; compaction is also required. Lower vacuum force can often result in the formation of resin rich pockets, often found at undercuts in the positive model. These form because the vacuum force is insufficient to force the fibers closely to the positive model at these relatively difficult geometric areas. A resin rich area will be substantially weaker than its surroundings, and may also provide an area for failure initiation. Examples of these undercuts were observed on below the knee (BK) sockets at areas that correspond to the patella tendon and behind the knee.

In order to avoid the formation of resin rich pockets, one recommendation is to use higher vacuum forces during socket fabrication. This will require minor modifications to the current methodology. The first modification is that a good seal must be formed at the inner vacuum bag, to prevent leaks in the vacuum force from the inner bag to the outer bag. For this purpose, a new product has been introduced into the prosthetics marketplace, which is a pre-sealed inner vacuum bag; the current program did not make extensive use of these inner vacuum bags, but these can be easily implemented. The second modification is to use a material like a breather to support the outer vacuum bag between the positive model and the point to which the vacuum bag is secured. By supporting this area, the vacuum bag will be prevented from stretching when vacuum force is applied, and the vacuum force can be increased. The third is to limit the extent to which physical manipulation is used to force resin into the fibers. The PVA bag becomes compliant when in contact with the resin and physically forcing the resin into the fabric by manipulation of the bag causes stretching of the bag. This will counteract the efforts of the vacuum force to consolidate the composite, leaving more resin in the part. The results of these changes will be lower void content and higher fiber to resin fraction, both of which will lead to greater strength to weight ratios. The upside of these modifications would be the elimination of resin rich pockets, which will reduce failure initiation points, and increase the strength to weight ratio.

# Flat Panel Testing

## Background

One of the primary goals of this program was to compare materials commonly available to prosthetists, in order to inform fabrication decisions. This task is considerably complicated by the purposes of the socket. The socket should securely attach the terminal device to the residual limb, transfer loads through the residual limb soft tissue, and be comfortable in all use scenarios. Attachment and suspension issues are outside the scope of this project. However, transferring loads and comfort are both tied to the mechanical performance of the socket and the materials used, to some extent. In order to transfer load effectively and remain comfortable, the mechanical property which needs to be optimized is poorly defined at this point, as the loads put on the socket are poorly defined. Also, since

the residual limb is able to withstand different loading states at different positions, the comfortable metric may vary depending on the position in the socket.

Given this uncertainty, four mechanical tests were selected. These were carried out by a certified test lab in accordance to ASTM standards for testing composite materials. I will briefly describe these tests here and what the results may indicate.

The first test which was performed on samples taken from flat panels was ASTM D 3039 Tensile Properties. This test determines the in-plane tensile properties, which include the Tensile Modulus and the Strain at Failure. When a material is subjected to tensile loads, it stretches and gets longer. The Tensile Modulus is a description of the how much a material will stretch when pulled for a given force. Higher Tensile Modulus indicates a smaller stretch for a given load.

The second test performed was ASTM D 695 Compressive Properties. This test determines the Compressive Modulus, which is similar to the Tensile Modulus described above; it represents how much a material will compress for a given force. The importance of this material property may be initially overestimated, because the compressive mode of loading does not occur over a large area of the socket. True compressive loading would have the loading applied in the same plane as the fiber orientation; this may occur to a small extent along the walls of the socket, but the majority of the load is expected to be at the distal end, where the fibers are actually oriented perpendicular to the load application.

The third test performed was ASTM D 790 Flexural Properties. This test determines the Flexural Modulus, which is similar to the two moduli described above; it represents how much a material will flex for a given force. This force, for composite materials, is applied perpendicular to the plane in which the fibers are oriented.

The last test performed was ASTM D 2344 Short-Beam Shear Strength. This test determines the strength between the layers of fibers when loaded in shear, which is defined as a force which causes the parallel layers to slide past each other. Caution must be used in interpreting this data; interlaminar failures can arise from shear failure and also from cyclic loadings, and the Short-Beam Shear Strength may not correspond directly to interlaminar failures from fatigue.

The loading of a material can be extremely complex. For example, consider the below figure.

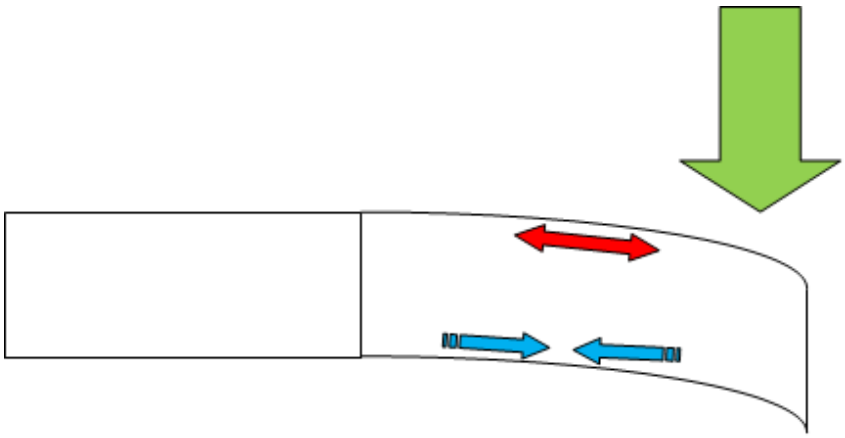

**Figure 3: Illustration of complex loading**

Consider a material, represented by the horizontal white box, which is subjected to a bending force, represented by the green arrow pointing down. The material will deform in the direction of the bending force, the amount of which will be determined by the flexural modulus. Also, when the material deforms, the material will experience both tension and compression forces, as it complies with the bending force. On the top of the material, a tension force will be observed, as the material stretches to accommodate the bending. This is represented by the red arrow. On the bottom of the material, a compression force will be observed, as the material is forced to bunch up; this is represented by the blue arrows. This simple example shows how one load can induce several others inside the material. Since the loads experienced by the socket are poorly understood at the present time, all the material properties described above are important, although we do anticipate that some loading moments will be more important than others.

ASTM Standards require flat samples, so traditional VARTM processing was used to fabricate flat samples. The important distinctions between VARTM and socket fabrication have been discussed. The VARTM processing used greater vacuum forces than socket fabrication generally does; this may have increased the material properties of the flat panels over those of the same materials fabricated using the techniques used for socket. However, as all of the flat panels were fabricated using the same VARTM processing, comparisons can be made from one sample to the next, which allows us to make recommendations.

The details of panel fabrication were as follows. Traditional VARTM processing methods were used. The materials available to prosthetists are generally available as woven tubes; the weave is a plain weave, meaning that the fiber bundles in one direction go over one of the fiber bundles in the other direction and then under one of these bundles, which can be referred to as a 1 x 1 weave. This tube can be stretched, reducing the diameter of the tube, to accommodate the dimensions of the residual limb. However, when this is done, the fiber orientation within the layer is altered. Fiber orientation is perhaps the most important variable in determining the mechanical properties of the fabricated part. Prosthetists neither strictly control nor monitor the fiber orientation during socket fabrication. For this

project, fiber orientation must be strictly controlled in order to make comparisons on a similar basis. It was determined that the most effective way of controlling the fiber orientation was to increase the diameter of the tube until the fibers were perpendicular; relative to the tube's main axis, this weave would be referred to as ± 45°. The test direction was the same as the tube's main axis, so that the fiber direction was also $\pm$ 45°. Each panel was formed from 5 layers of fabric; this was done partly because of thickness minimum requirements in the ASTM standards.

## Results and Discussion

There are a wide variety of materials available to prosthetists. Testing each combination would be prohibitively expensive for this project. The project was structured to compare the effect of a single variable, such as the reinforcements used, while other variables, such as the resin used, was kept constant.

In one series of experiments, the effect of reinforcement fabrics was studied. Several reinforcement fabrics are available to prosthetists. In order to compare them against each other, a 'baseline' resin was chosen, which would be used for all panels in this series. The 'Composite CMRK' resin from SPT was chosen for this. The reinforcements we chose to investigate were 1) carbon, $\pm$ 45 $^{o}$ weave, 12k tow size, 2) fiberglass, $\pm$ 45 $^{o}$ weave, 6K tow size, satin weave 3) light-weight carbon, $\pm$ 45 $^{o}$ weave, 6k tow size, 4) a hybrid of carbon and fiberglass, $\pm$ 45 $^{o}$ weave, 12k tow size, and 5) a second hybrid of carbon and fiberglass, $\pm$ 45 $^{o}$ weave, 6k tow size.

The 'baseline' reinforcement is the carbon fabric with 12k tow size; it was used for the majority of layers within the panels. The 'baseline' panel has five layers of the 'baseline' carbon, and is represented by the notation CCCCC. For each additional reinforcement under investigation, we made two panels; the first had the middle (of five) layers replaced with the new reinforcement, and is represented by the notation CC-R-CC. The second had the second and fourth layers replaced with the new reinforcement, and is represented by the notation C-R-C-R-C. The results of these tests are shown in the figures below; the data has been normalized to the 'baseline' system, which has 5 layers of carbon with 12k tow size. The raw data will be given in the Appendix.

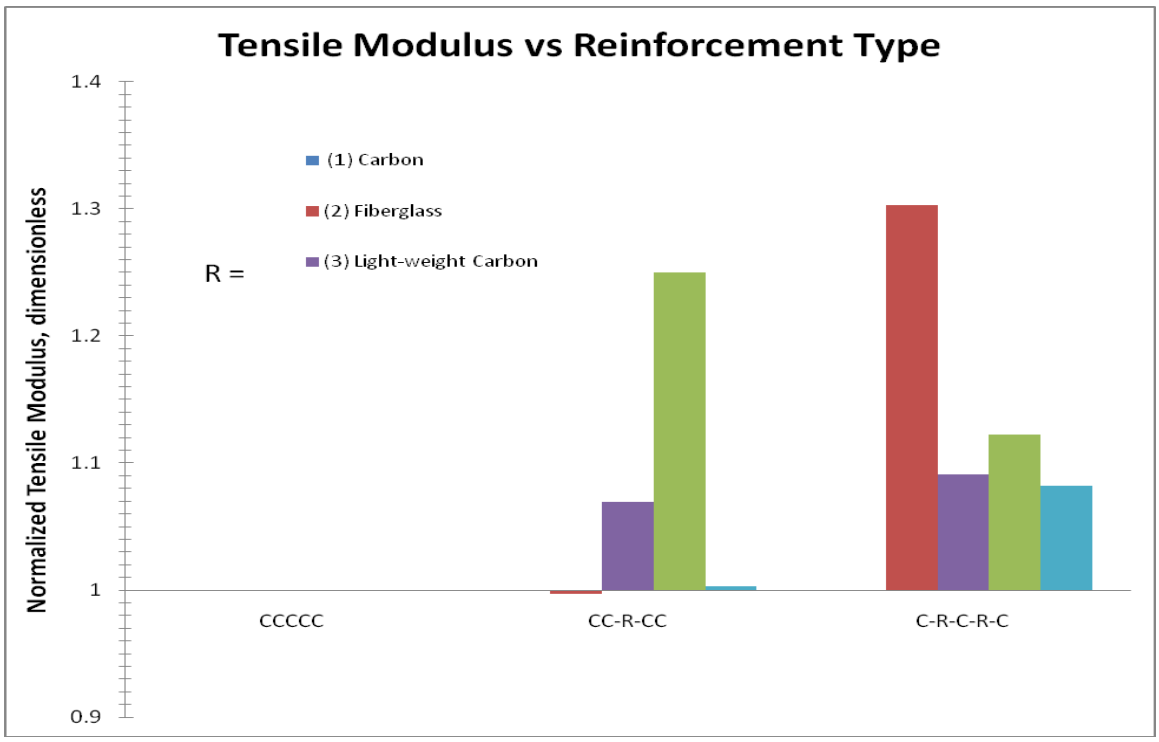


**Figure 4: Comparison of Tensile Modulus for varying reinforcements in CMRK resin**

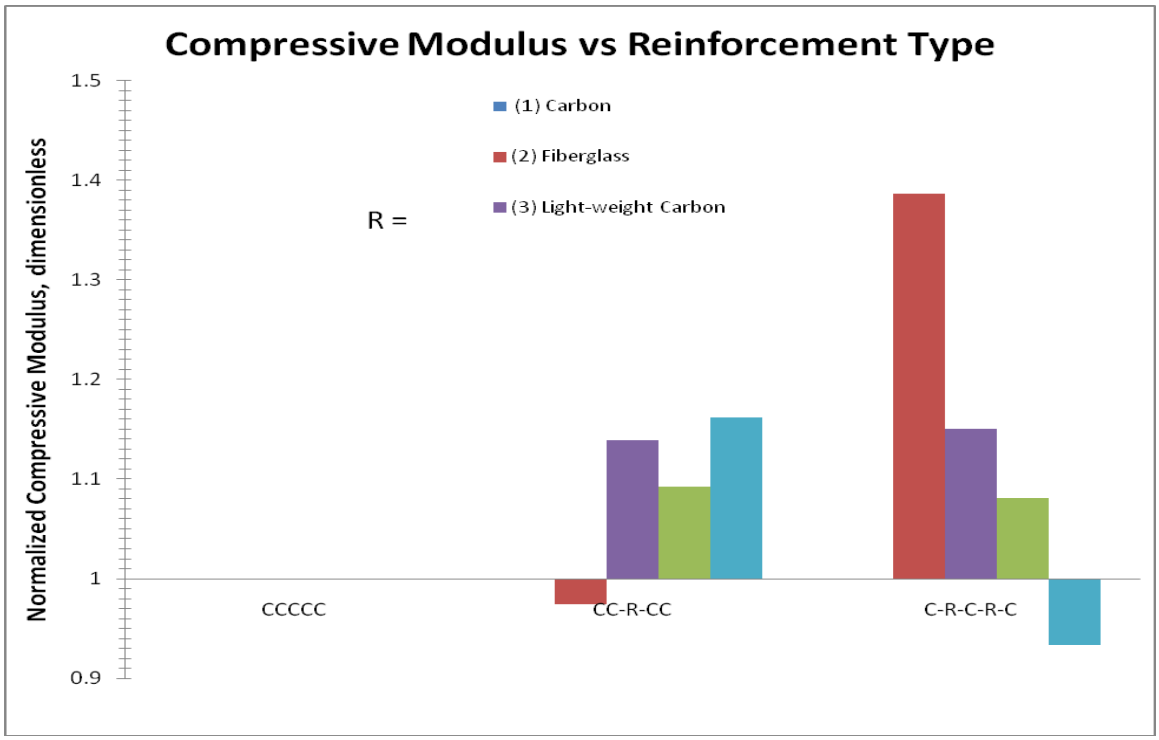


**Figure 5: Comparison of Compressive Modulus for varying reinforcements in CMRK resin**

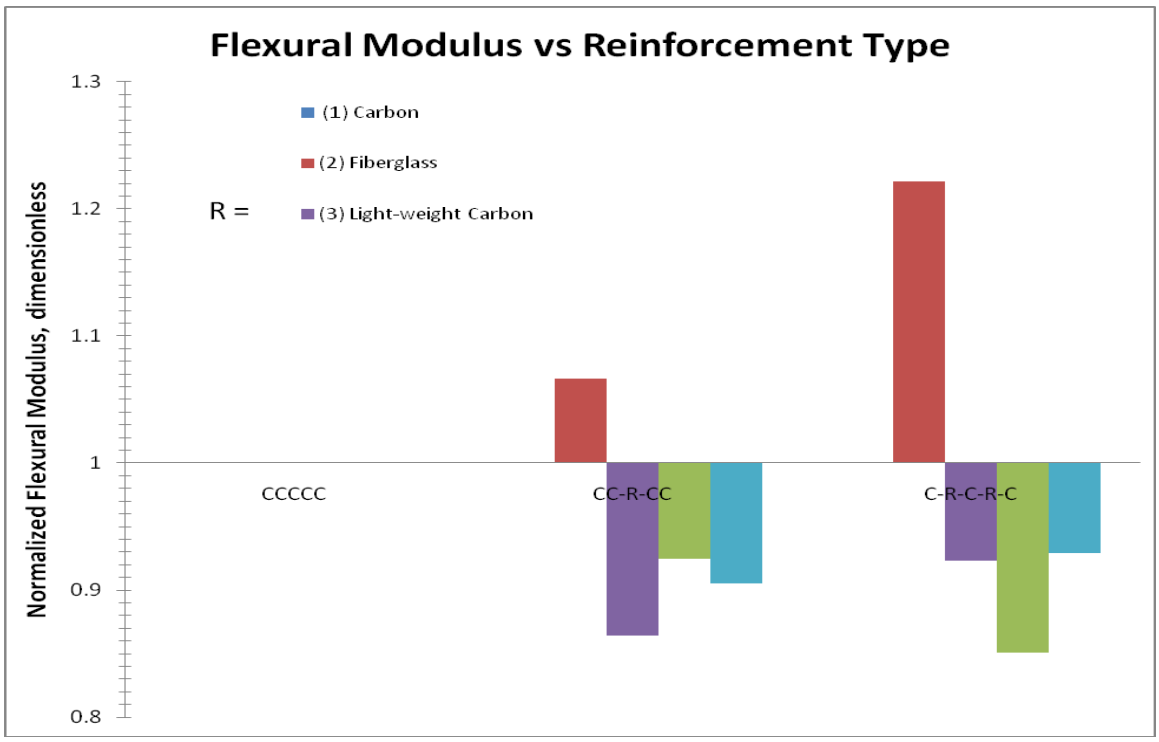


**Figure 6: Comparison of Flexural Modulus for varying reinforcements in CMRK resin**

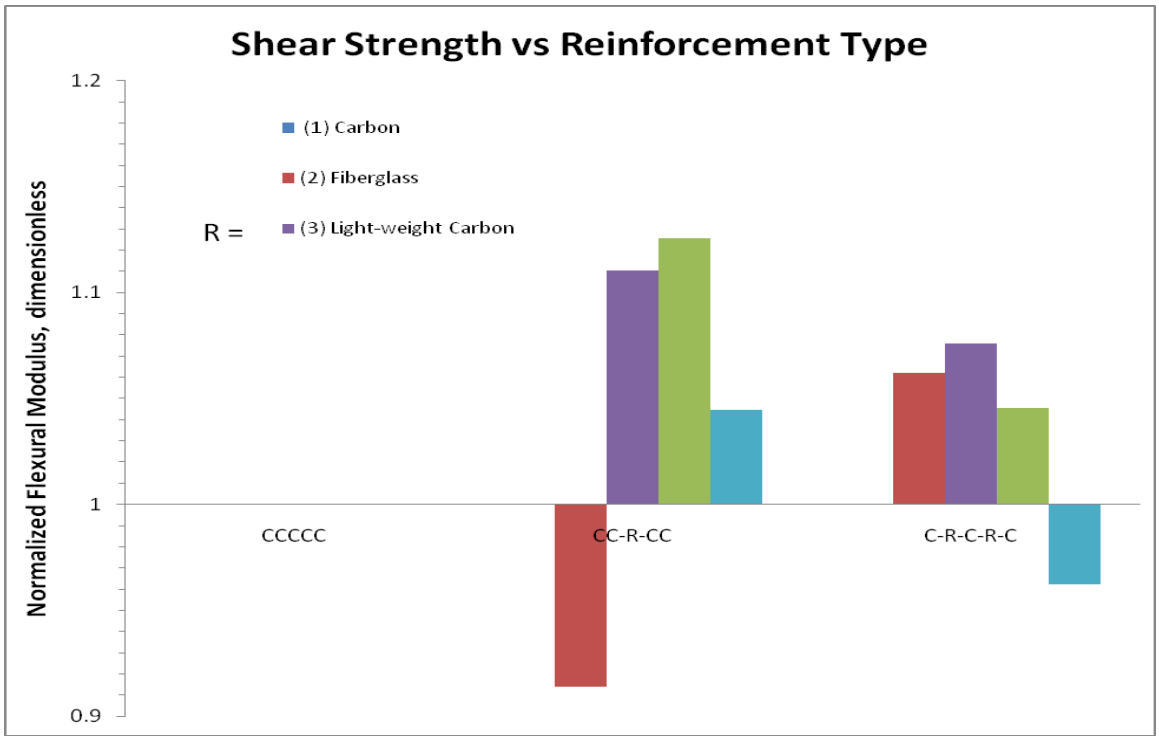


**Figure 7: Comparison of Shear Strength for varying reinforcements in CMRK resin**

The results are somewhat surprising. Compared to a pure carbon structure (the baseline at the left of each graph), many of the mechanical properties are increased when fiberglass is added to the structure. This can be easily observed in Figures 4 - 6 by watching the maroon line representing the fiberglass reinforcement. This fiberglass should have mechanical properties much less than the carbon used; the carbon filament's tensile strength is approximately 4,400 MPa, whereas the fiberglass would be 2,000 MPa, and the carbon's Young's Modulus is approximately 234 GPa, whereas the fiberglass would be 80 GPa. Where the five layer structure has two layers replaced with the weaker fiberglass, we find 30% increase in tensile modulus, 40% increase in compressive modulus, and 20% increase in flexural modulus. Although the carbon is lighter weight (density of carbon will be approximately 1.80 g/cm$^3$ versus the density of fiberglass of 2.55 g/cm$^3$), the cost is substantially more for the carbon fabric. Comparing the fabric on an area basis, the carbon fabric is approximately 25% more than the fiberglass fabric.

Another variable which we will be investigating is the resin used. Many resin systems are available to prosthetists. In order to compare them against each other, a baseline series of panels was chosen. For each resin investigated, three panels were made using the two most common reinforcements, the baseline carbon fabric (1) and fiberglass (2). The three panels were 1) five layers of baseline carbon fibers, represented by the blue line marked CCCCC, 2) the baseline carbon with the middle (of five) layer replaced with fiberglass, represented by the maroon line marked CC-FG-CC, and 3) the baseline carbon with the second and forth layers replaced with fiberglass, represented by the green line marked C-FG-C-FG-C. The resin systems investigated are 1) Composite CMRK resin from SPT, 2) Acrylic Flexible Resin from SPS, 3) 80:20 Acrylic Resin (80% rigid, 20% flexible) from SPS, 4) Epox-Acryl from SPS, 5) Advanced Dura-Limb Resin from SPT, 6) ER Resin from SPS, and 7) Ultra Performance Epoxy Resin from SPT. Another system was also investigated, which consisted of pre-promoted polyester resins which are sold as either 'rigid' or 'flexible.' We used three mixing ratios of rigid to flexible, essentially three more resin 'systems' to investigate. These would be labeled as 8) 100:0 Rigid:Flexible Polyester, 9) 75:25 Rigid:Flexible Polyester, and 10) 50:50 Rigid:Flexible Polyester. Also included in these charts is a comparison of CMRK based on the catalyst used to activate it; the 'baseline' catalyst loading is 2 weight percent of the resin, and the alternative loading level is 3 weight percent. The results of these tests are shown in the figures below; the data has been normalized to the 'baseline' system used previously (five layers of carbon with 12k tow size and CMRK resin). The raw data will be given in the Appendix.

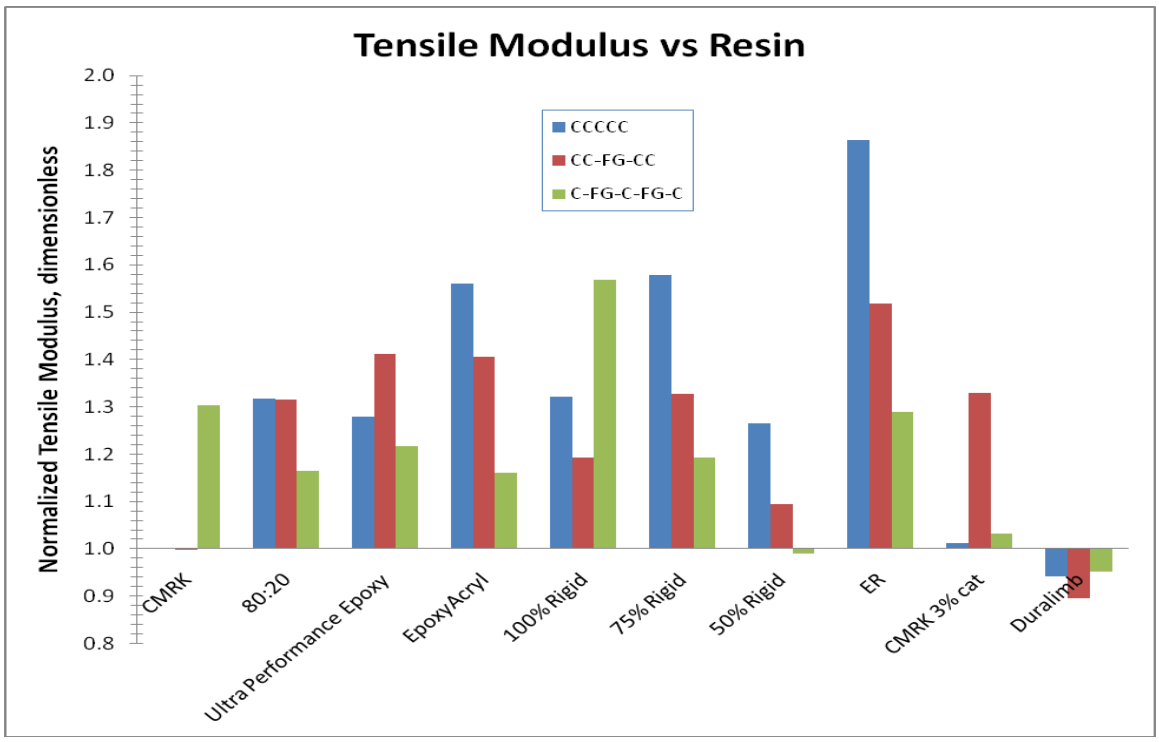


**Figure 8: Comparison of Tensile Modulus for varying resins**

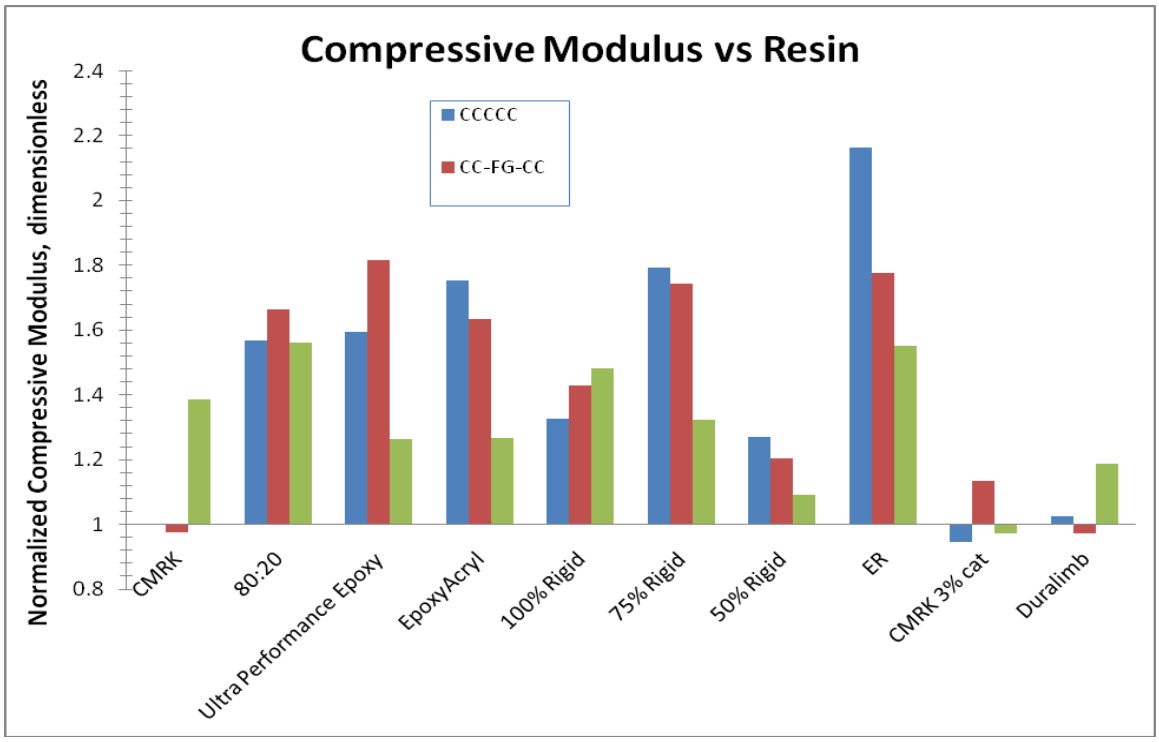


**Figure 9: Comparison of Compressive Modulus for varying resins**

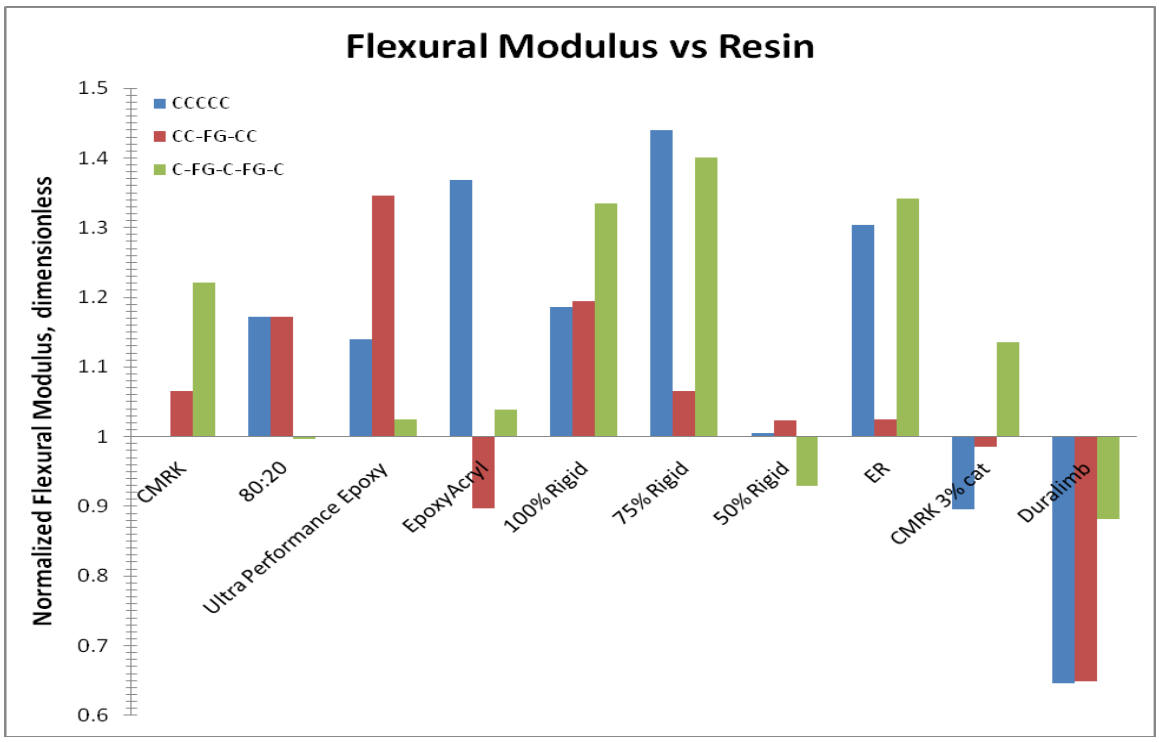


**Figure 10: Comparison of Flexural Modulus for varying resins**

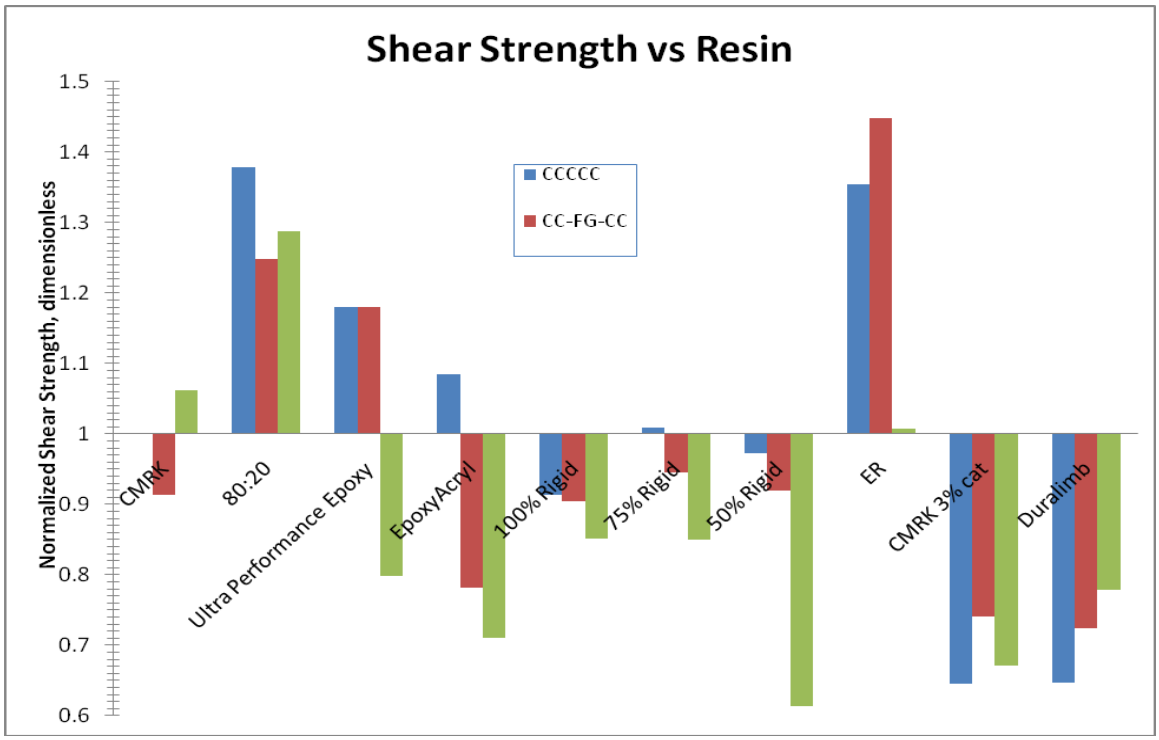


**Figure 11: Comparison of Shear Strength for varying resin**

Of note is the reproduction of the results from Figures 4-7 on the far left of the graph. Figures 4-7 have results for CMRK resin, and for the three structures shown in Figures 8-11, and so there is an overlap to the data displayed.

The surprising nature of the results observed in the CMRK resin discussed above, namely that replacing the carbon with the weaker fiberglass, does not appear to hold, in general, for the other resins studied. Rather, the panels made of all carbon (CCCCC, blue line) appear to have greater mechanical properties than the panels with one fiberglass layer (CC-FG-CC, maroon line), which appear to have greater mechanical properties than the panels with two fiberglass layers (C-FG-C-FG-C, green line). For the sake of clarity, error bars have been omitted from the graphs, but often, when the data is close, the difference between is statistically insignificant.

The series of resins representing a mixture of pre-promoted polyester resins yielded puzzling results. Often, the results of at least two of the three structures studied follow the pattern 75% rigid > 100% rigid > 50% rigid. This is a surprising result. It was expected that the mechanical properties would either increase or decrease with increasing rigid resin content, but this was not observed. Because of this, these resin systems were not considered for further study.

The comparison of different catalyst loading of the CMRK resin is also surprising. The chemistry of the system would suggest that the catalyst content would not affect the mechanical properties; however, the data contradicts this supposition for some of the mechanical tests, namely the flexural modulus and the shear strength. At this time, the reason for this is not known.

The choice of a resin is complicated, as may be clear by the figures above. A resin system rarely offers increased mechanical properties for all properties tested, and a clear priority of the mechanical properties does not exist at this time. The data does indicate that the Duralimb resin is not better than the baseline resin. Therefore, in selecting resin systems to be tested as fabricated into sockets, systems which showed relatively consistently higher mechanical performance relative to the baseline were given greater consideration, and systems where the structures tested (i.e., the various carbon and fiberglass panels fabricated) were relatively internally consistent were favored.

It was the original, perhaps naïve, hypothesis of the study that the flat panel results would inform the choice of sockets which would be tested. The data coupled with the complicated and unknown loading state of the socket makes choosing materials rather difficult, at best. The choice of which sockets to fabricate and test was therefore aligned to study clinical fabrication procedures rather than only focusing on the difference between materials.

# Socket Testing

## Background

Flat panel testing as described above may shed some light on what materials can form the best socket. However, as discussed above, the complex loading state of a socket makes selecting a basis for recommendation difficult. The solution is to test the materials used in the form in which they will be used. In order to do this, sockets were made using the methods described above and tested according to ISO 10328. The loading condition selected was, according to the ISO standard's terminology, P4 II, which is a testing condition related to the instant of maximum loading which occurs late in the stance phase of walking for an A80 patient (approximate patient weight, 80 kg or 175 lbs). The sockets were tested to a proof load of -1,811 N; the proof load is defined as the load representing an occasional sever event, which can be sustained by the socket and still allow it to function as intended. The sockets were then subsequently tested to an ultimate load; the ultimate load is defined as the load representing a gross single event, which can be sustained by the socket but which would render it unusable thereafter. The ultimate load prescribed by the ISO standard for the P4 loading level is -3,623 N. However, the sockets in this study were tested to their failure or -10,000 N; this was done so that the sockets could be compared one to the next based on their ultimate strength.

In order to make the comparison as valid as possible, the fabrication of the sockets was required to be as repeatable as possible, especially in the position of the attachment point. Four-hole attachment points were used. The positioning of the attachment point was accomplished as follows. A relatively simple transtibial socket was selected. A negative mold was formed of the rectified plaster mold. Two holes of slightly varying size were drilled through the negative mold, and pins were placed through the mold. Plaster was then used to make copies of the original plaster mold, and each subsequent copy had pin holes in identical spots. These pins were used to align the four-hole attachment plate, using a special 'key' which fit the two pins and the four-hole plate. Sockets were thus fabricated around these pins, with attachment points in the same position each time.

Sockets were fabricated using the methods described above. One important difference between clinical practice and the procedures described above should be noted. In clinical practice, sockets are generally formed using two infusions of resin. The first infusion includes all of the reinforcements positioned underneath the attachment point. The socket can then be tested by the patient for preliminary fit and measurements pertaining to the alignment of the terminal devices taken. It is only at this point that the prosthetist knows where the attachment point should be placed. The attachment point is secured to the first laminated structure and permanently incorporated into the socket when a second infusion of resin is introduced to fabrics tied to the attachment point. Except for one socket, all of the sockets below were fabricated in a single infusion. This difference has several major implications for the overall strength of the socket, which will be discussed later.

The ISO standard is intended to set the testing method for all prosthetic components used in lower limb prosthetic systems. However, the specific aspects of socket testing are not specifically addressed. In particular, the specific method of loading the composite socket through a plug simulating the residual limb is not specified, and is therefore open to rational choice. Previous studies have used a hard plaster plug to apply load to the socket, but it was fashioned such that a void was left at the distal end. This choice affected the test outcome and the observed failure modes. In the present study, we have chosen to use a plaster plug which extends fully to the distal end of the socket covered in a relatively thick viscoelastic liner identical to those worn by many amputees. The goal of this choice was to more closely approximate the hydrostatic-type loading anticipated from the combination of soft tissues and liners frequently observed in use.

## Results and Discussion

The first socket tested was fabricated from a single of infusion of CMRK resin. Two carbon layers were placed under the plate, and three were tied into the plate. This first socket was an approximation of what might be observed clinically, in terms of how many layers are used. The carbon braided tube was reflexed to form double layers, and the third 'single' layer was trimmed at the attachment plate. The ultimate strength of the socket was greater than the -10,000 N capability of the testing fixtures, and so failure was not observed. The maximum force subjected to this socket was -13,734.1 N, which is 279% more than the P4 loading level. The socket's ultimate strength indicates that it may be suitable for a P6 loading level, and likely beyond. Based upon the static strength testing, it seems unnecessary to use five total layers for any patient, but this does not take into account the fatigue strength of the socket.

The second and third sockets fabricated were also fabricated from a single infusion of CMRK resin; they each had two layers of carbon fabric under the plate. As before, the braided sleeve was relaxed to form double layers. Whereas the 'single' layer had been trimmed close to the attachment point on socket #1, socket #2 left 3 inches of the single layer to fold down over the distal end. This formed a socket with 4 layers tied into the attachment plate near the distal end, but only 3 of these layers extended beyond the attachment plate by more than 3 inches. Socket #3 had 4 layers tied into the attachment point. The purpose of comparing sockets # 1, 2, and 3 was to determine the added ultimate strength of reinforcing only the distal end by reflexing the end of a single layer. However, as socket #1, which had the fewest layers, did not fail below the testing equipment limit of -10,000 N, it was unreasonable to expect that either sockets #2 or #3 would fail, and thus they were not tested at all.

The fourth socket was fabricated from a single infusion of CMRK resin; two layers of fiberglass were placed under the attachment plate, and a single layer of fiberglass was tied into the attachment plate. The purpose of this socket was to explore the lower limit of socket strength, as this socket was envisioned to be the lowest strength socket which would ever be used clinically, and indeed is thinner than any socket I have observed. However, it was important to determine if the testing apparatus would be capable of applying loads which would fail any sockets. The ultimate strength of this socket was -8,197.7 N, which is 125% more than the P4 requirement of -3,623 N. The failure occurred at the

distal end, in the layers which were tied into the attachment plate. Note the appearance of large cracks and pulled fibers at the distal side of the attachment plate.

**Figure 12: Medial close up of the failure of Socket #4**

**Figure 13: Posterior close up of failure of Socket #4**

The fifth socket was fabricated using a single infusion of the CMRK resin. The reinforcement fabric used was the baseline carbon sleeve which has a tow size of 12k. Two layers were placed under the attachment plate, and a single layer was tied into the plate. It was also projected that this socket would be relatively weaker than socket #1, as there would be less carbon used in the fabrication. The socket's ultimate strength was -8,706.7 N, which is 140% more than the P4 loading required, and was indeed less than the ultimate strength of socket #1. The failure mode was again at the distal end where the attachment point was secured to the composite structure. The figure below shows a concentration of damage at the posterior near the attachment point.

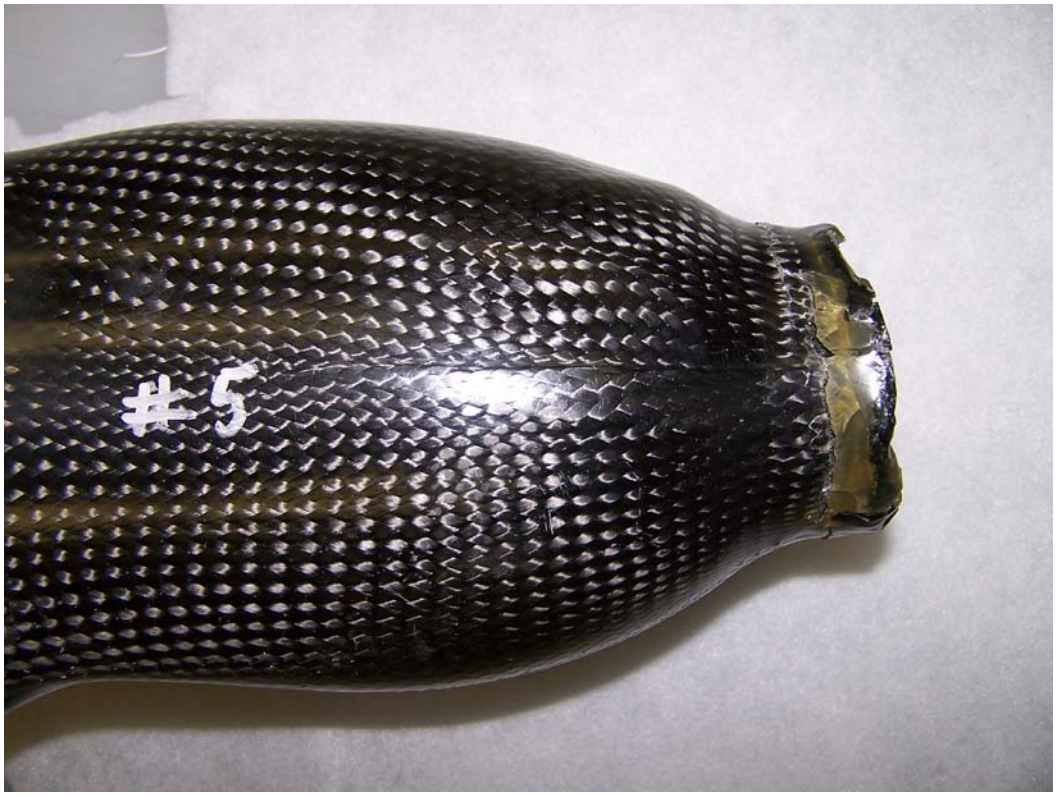


**Figure 14: Medial close up of the failure of Socket #5**

The series represented by sockets #4 and 5 explore the relative strength gained by using carbon over fiberglass. Their ultimate strength is very similar for the same number of layers arranged in the same configuration, and using the same resin. The carbon has only a slight advantage. However, the fiberglass fabric used has a much smaller tow size, and as a consequence, three fiberglass layers represent much less total material than three carbon layers. The advantage of the carbon over the fiberglass appears to be extremely small, with respect to the static strength.

The sixth socket was fabricated using a single infusion of the CMRK resin. The reinforcement fabric used was a lightweight carbon sleeve which has a tow size of 6k. Two layers were placed under the attachment plate and a single layer was tied into the plate. It was also projected that this socket would be relatively weaker than both socket #1 and socket #5, as there would be less carbon used in the fabrication. The socket's ultimate strength was -6,279.7 N, which is 70% more than the P4 loading required. The failure mode was again at the distal end where the attachment point was secured to the composite structure. Note the concentration of damage at the posterior.

**Figure 15: Medial close up of the failure of Socket #6**

The seventh socket was fabricated using a single infusion of CMRK resin. The reinforcement fabric was the baseline carbon (12k tow size). Two layers were placed under the attachment plate and a single layer was tied into the plate, except this time three inches were reflexed to give additional reinforcement to the distal end of the socket. The intent was to show whether, statically speaking, reinforcing the distal end of the socket would yield the equivalent strength of an entire layer. The socket's ultimate strength was above the testing fixture limit of -10,000 N, which means its strength is at least 176% more than the P4 loading required; it is impossible to estimate how much loading this socket could withstand prior to failing. The strength increase over a socket which does not have the additional three inches of fabric reinforcing the distal end was at least -1,364.6 N, which is by itself 37% of the total loading required by the P4 requirement.

The eighth socket was fabricated using a single infusion of CMRK resin. The reinforcement fabric was the baseline carbon (12k tow size). Two layers were placed under the attachment plate and two layers were tied into the plate. This socket, in addition to sockets #5 and #7, were meant to explore the strength gained by reinforcing only the distal end versus the strength gained by an entire additional layer. The eight socket's ultimate strength was above the testing fixture limit of -10,000N, which means that its strength is at least 176% more than the P4 loading requirement. It is impossible to estimate how much loading this socket could withstand prior to failing, and how much stronger this socket may be than socket #7.

The series represented by sockets #4, 7, and 8 explores an important concept in the fabrication of sockets. Socket #4 had only one layer tied into the reinforcement plate, socket #7 had one complete layer and one partial layer (three inches past the attachment plate), and socket #8 had two complete layers. The partial layer adds tremendous static strength to the socket, by itself accounting for at least 37% of the P4 loading level requirement. It is not clear at this time how much an additional layer adds, but it is also at least 37% of the P4 loading level. The selective reinforcement of the distal end addresses the failure mode observed by reinforcing the attachment point, and the entire layer may not be required. However, it is important to remember that this result is only indicated by the static results; the fatigue strength of the socket may be greatly increased by an entire layer over a partial layer.

The ninth socket was fabricated using a double infusion of the CMRK resin. Two layers of carbon were placed under the attachment plate and infused in the first infusion. And additional layer of carbon was tied into the attachment plate and infused in a second infusion. The ultimate strength was -8,682.2 N, which is 140 % of more than the P4 loading required and statistically indistinguishable from socket #5. The failure mode was again at the distal end where the attachment point was secured to the composite structure. Note the concentration of damage at the distal end.

**Figure 16: Lateral close up of failure of Socket #9**

The series represented by sockets #4 and #9 explores the effect on the static strength of a single infusion versus a double infusion fabrication mode. At the interface between two infusions, the bond

between the layers will be much weaker than the bond formed between the same layers done in a single infusion. In the traditional composites community, this process is described as secondary bonding, and the procedures for forming an optimum interface are well defined and followed. These procedures generally include roughing and cleaning the surface. Roughing the surface using sanding or a similar physical technique gives the resin from the subsequent infusion more physical area to bond to, as well as potentially giving asperities to distribute loading onto. Cleaning the surface removes small particulates which can weaken the bond formed by the second infusion. When considering secondary bonding encountered in socket fabrication, it is pertinent to note that the failures which are observed are frequently interlaminar failures around the brim of the socket. It is likely that these interlaminar failures are occurring at this secondarily bonded interface between a first and second infusion; to combat this, it is suggested that greater care be taken to the preparation of the surface of the initial infusion, especially in the area within 3-5 inches of the brim. This area should be roughed and cleaned as carefully as possible, using a relatively coarse grained sandpaper, and acetone or water for cleaning. The ninth socket was fabricated with careful attention paid to the preparation of the interface. The static results show that the ultimate strength is essentially the same for sockets fabricated with either one or two infusions, as expected. However, the fatigue behavior between these two sockets is likely vastly different.

The tenth socket was fabricated using a single infusion of CMRK resin. The reinforcing fabric used was the baseline carbon (12k tow). One layer was placed under the attachment plate and two layers were tied into the plate. The socket's ultimate strength was above the testing fixture limit of -10,000 N, which means that its strength is at least 176% more than the P4 loading requirement. It is impossible to estimate how much loading this socket could withstand prior to failing.

The series represented by sockets #4 and #10 explores the effect on the static ultimate strength of sockets which have similar total amounts of carbon, but only vary on the relative placement of the attachment plate. By putting an additional layer tied into the attachment plate, the ultimate strength of socket #10 is increased over socket #4 (by an unknown amount greater than 23%), even though the inner socket, underneath the attachment plate, is thinner. The additional tied into the plate addresses the failure mechanism observed in other sockets, which will be discussed below Nominally speaking, by addressing one failure mechanism, the possibility for another failure mechanism becomes more probable. However, even with this increased probability, and with the inner socket relatively weaker, the ultimate strength of the socket is still higher than the testing fixture limit. This seems to indicate that the inner socket can be fabricated by as little as a single layer. This may not be feasible in a double infusion fabrication methodology, and again, the fatigue behavior may indicate differently, but the data in the present study indicates that thinner inner sockets deserve consideration.

The eleventh socket was fabricated using a single infusion of the 80:20 Acrylic Resin (80% rigid, 20% flexible) from SPS. The reinforcement fabric was the baseline carbon (12k tow). Two layers were placed under the attachment plate and a single layer was tied into the plate. The socket's ultimate strength was above the testing fixture limit of -10,000 N, which means that its strength is at least 176% more

than the P4 loading requirement. It is impossible to estimate how much loading this socket could withstand prior to failing.

The twelfth socket was fabricated using a single infusion of the ER Resin from SPS. The reinforcement fabric was the baseline carbon (12k tow). Two layers were placed under the attachment plate and a single layer was tied into the plate. The socket's ultimate strength was above the testing fixture limit of -10,000 N, which means that its strength is at least 176% more than the P4 loading requirement. It is impossible to estimate how much loading this socket could withstand prior to failing.

The series represented by sockets #4, #11, and #12 explores the effect of the resin on the static ultimate strength of the sockets which have identical amounts of carbon. When the 80:20 resin or the ER resin is used instead of the CMRK resin, we find that the ultimate strength of socket is increased (by an unknown amount greater than 23%). The static data indicate that the CMRK resin is considerably weaker at the attachment plate. This is intimately related to the failure mechanism, which is discussed below. It is also important to note that the fatigue behavior of these resins may be vastly different.

## Static Failure Mechanism

The dominant failure mechanism appears at the distal end, and damage is always accumulated at the posterior. A schematic of the test is shown below.

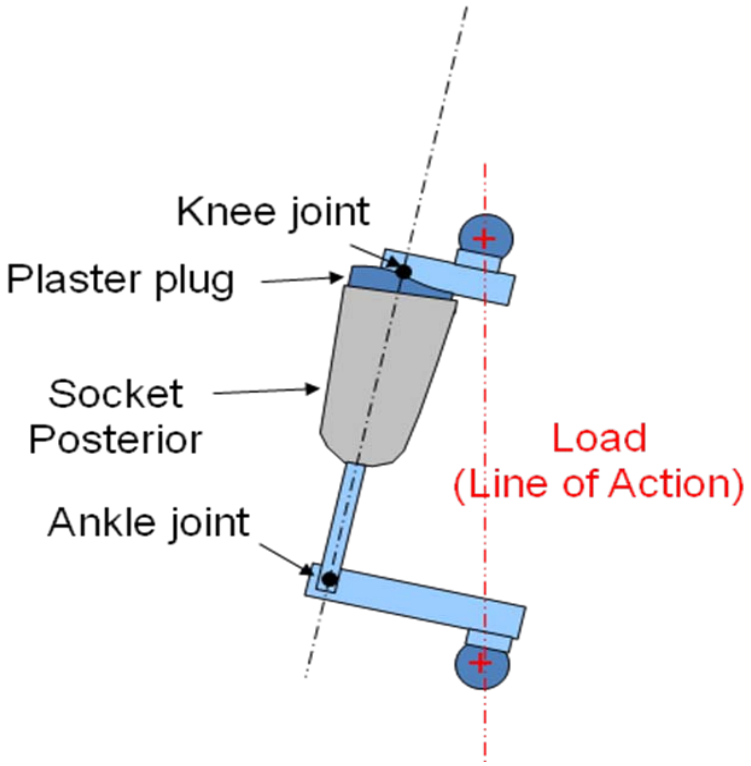


**Figure 17: Socket Test Fixture Schematic**

The compressive force exerted on the socket while off-axis results in both a compressive force and a bending moment which can be visualized as shown below. The green arrows indicate the induced compressive force and bending moment, the red arrow indicates the induced tensile stress, and the blue indicates the induced compressive stress. Considering the schematic above, the tensile force will be on the posterior of the socket, and the compressive force will be observed at the anterior.

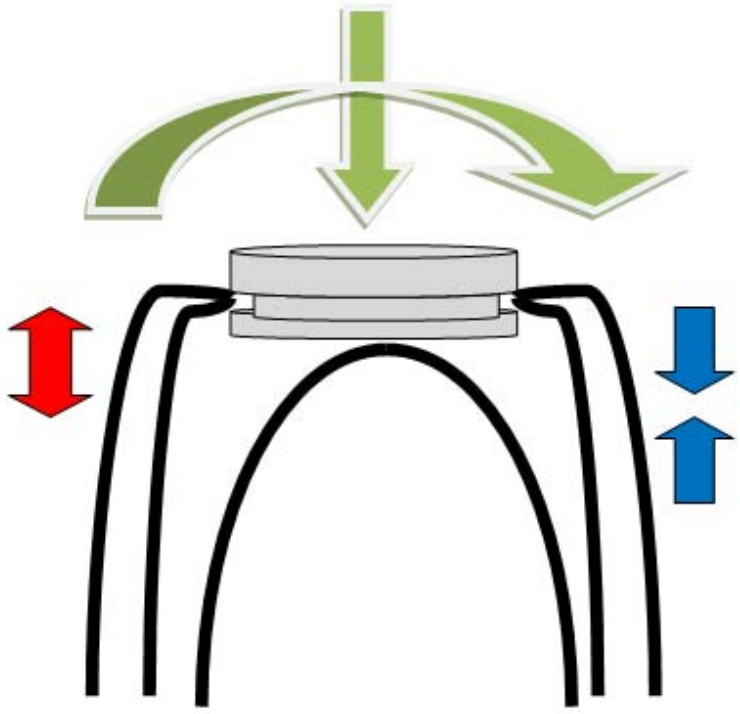

**Figure 18: Induced forces at attachment plate**

The compressive force and the bending moment can both be responsible for failures in sockets tested by the ISO standard in the II configuration. In previous socket testing efforts (Current et al, Static Structural Testing of transtibial composite sockets, Prosthetics and Orthotics International, 23, p 113, 1999), the distal end of the socket was unsupported from the interior, and the compressive force resulted in some failures. In the present work, the socket was supported by a full-length plaster plug covered in a thick viscoelastic liner, and the bending moment appears to be responsible for the observed failures. Neither an unsupported socket nor a rigidly supported socket perfectly mirrors the properties of the residual limb, so at best, both situations are approximations of use conditions. Further evaluation of the optimum method for testing sockets is certainly warranted. We concluded that a completely unsupported socket held the potential for introducing failure modes which would not

be observed in use, and instead chose the system described. It is possible that compressive failures may have been observed with the sockets when another choice for socket loading method was used.

The bending moment at the attachment plate will result in tension on one side of the socket and compression on the opposite side. The failure pictures above seem to indicate matrix failure on the tension side (which is the posterior side, see Figure 17). At this point, the fiber orientation is likely to be, relative to the main axis of the socket, relatively low compared to the rest of the socket. This is a consequence of pulling the braided sleeve into the smallest possible diameter. The below figure illustrates the situation. The grey cylinder in the background represents the attachment plate. The black lines, both solid and dashed, represent the fibers in the reinforcing fabric.

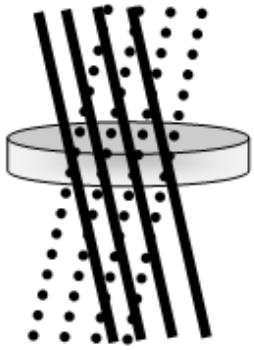

**Figure 19: Schematic of fiber angle at the attachment plate**

As mentioned in the introduction to this report, fiber angle is perhaps the most the most important factor in determining the mechanical properties of a composite part. Composite parts, by their very nature, will have different properties when tested in different directions, because the fibers are placed in some directions, but not others. Coupled with that the fact that the fibers are the dominant mechanical constituent, it becomes important to understand how fiber orientation is affecting the observed failure mechanism. Preliminary measurements show that the fibers are approximately $\pm$ 30° to the socket's main axis for the carbon cloth, and $\pm$ 20° for the fiberglass.

In order to quantify the effect of fiber orientation on the mechanical properties of the fabricated parts, the following series of experiments were performed. Flat panels were fabricated exactly as described above. Five layers were used, and the baseline carbon (12k tow size) was used for the majority of layers, and as before, the fiber orientation was monitored and set at $\pm$ 45°. CMRK resin was used for all panels. However, for the middle layer, an 'oriented' layer was used, where the fabric was rotated such that, relative to the test direction, the fibers were set at 0° / 90°. Both carbon and fiberglass was used for these 'oriented' layers, and much as before, in some panels the middle of the five layers was replaced (and is represented by CC-R-CC) and in other panels the second and fourth layers were replaced (and is

represented by C-R-C-R-C). The same mechanical tests as discussed above were performed, but for the sake of simplicity, the presentation here will be limited to only the tensile and compressive tests.

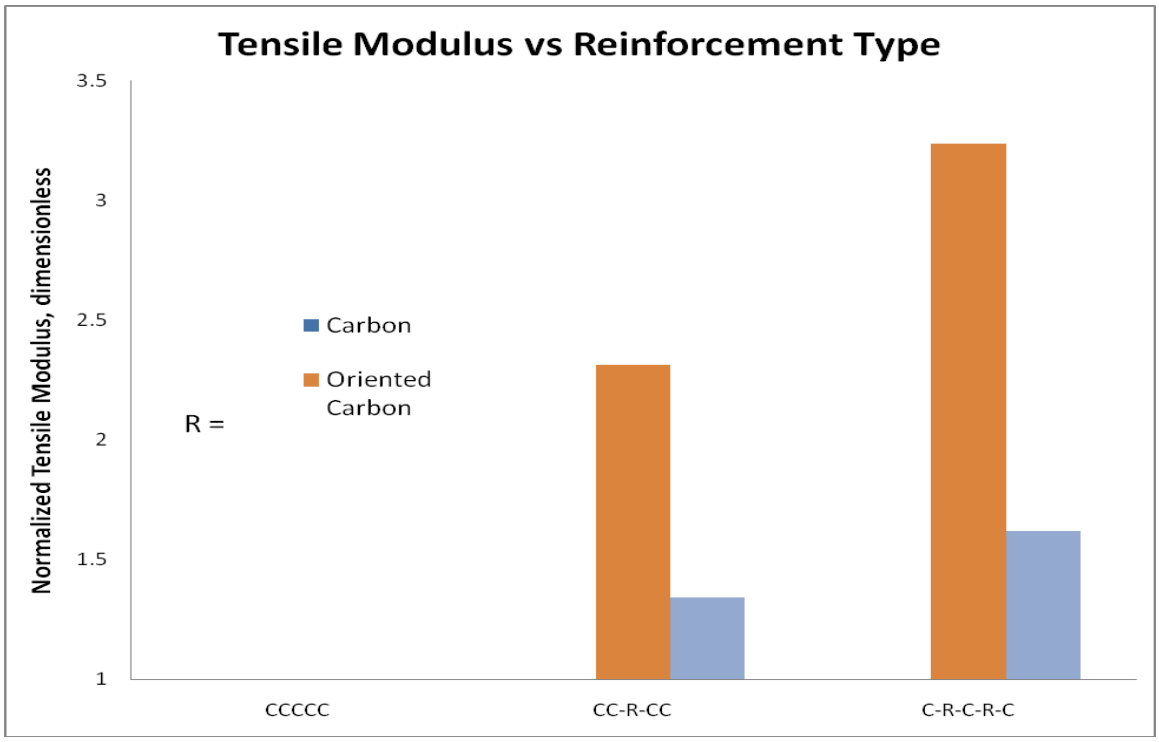


**Figure 20: Comparison of Tensile Modulus for oriented layers in CMRK resin**

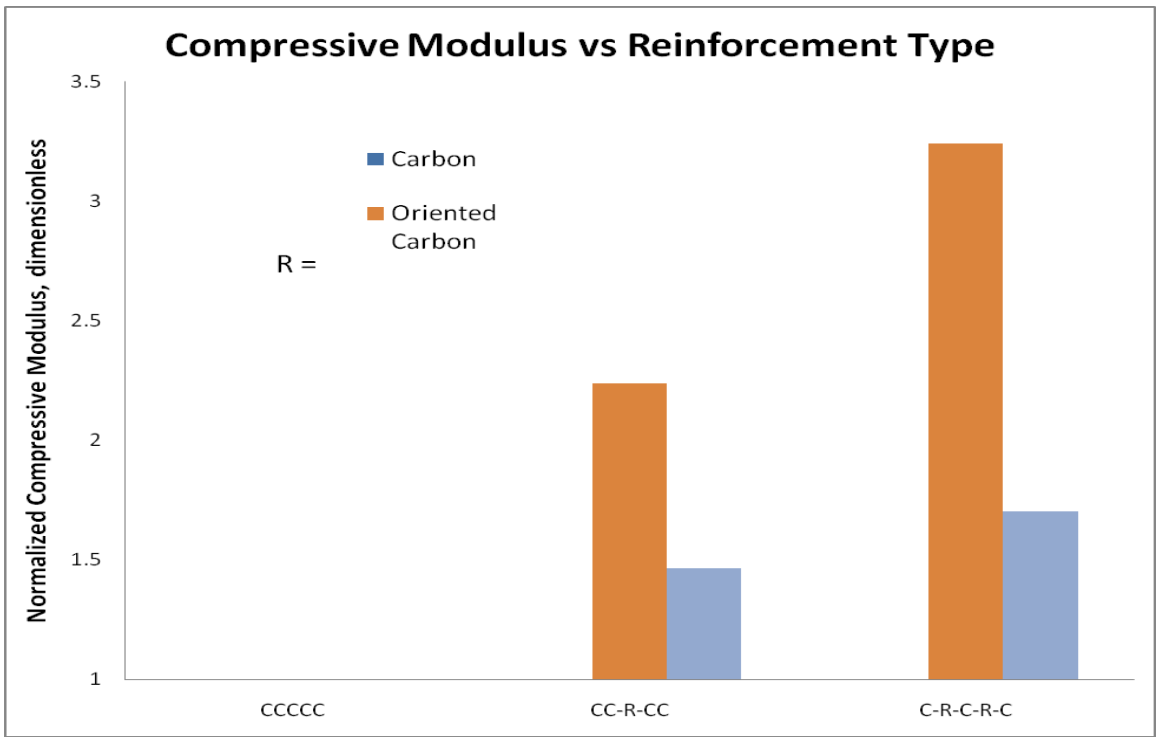


**Figure 21: Comparison of Compressive Modulus for oriented layers in CMRK resin**

One important thing to note is that, when the default layers from this study, which are oriented ± 45° from the test axis, are tested along that test axis (0°), all of the fibers get a chance to contribute to the mechanical strength. However, when a layer is rotated to 0° / 90°, only those fibers which are oriented at 0° really get to contribute to the mechanical properties; essentially, the effectiveness of the fibers oriented at 90° to the test direction is zero. This essentially means that half of the fibers in the fabric oriented at 0° / 90° are not participating in the mechanical test. With that in mind, we can see that the oriented layers dramatically increase the mechanical properties of the fabricated part. With one oriented carbon layer, the tensile modulus is increased 131% and the compressive modulus increased 124%. With two oriented layers, the tensile modulus is increased 234% and the compressive modulus is increased 224%. Even when replacing the much stronger carbon with fiberglass (carbon filament's tensile strength is approximately 4,400 MPa, the fiberglass would be 2,000 MPa), one layer of the oriented fiberglass increases the tensile modulus 34%, and two layers of oriented fiberglass increases the tensile modulus 62%. This occurs despite the fact that only half of the fibers in the oriented layer are truly participating in the mechanical evaluation.

The above discussions on the importance of fiber orientation and the forces induced at the attachment plate help to explain the global results of the socket testing. The socket testing shows an accumulation of damage to the composite structure at the distal end, posterior. According to the schematic, this area should experience an induced tensile loading. In this study, failure is only observed in sockets where only a single layer is tied into the attachment plate. Apparently, one layer of reinforcing fabric is

insufficient to carry the induced tensile forces. However, when just 3 inches of additional fabric were reflexed over the socket, the ultimate strength increased (by an unknown amount). Also, when the resin used exhibited larger tensile strengths, the socket's ultimate strength increased. See Figure 8, and notice that the 80:20 resin and ER resin (for a five layer carbon panel) exhibit tensile modulus increases of 32% and 86%, respectively, over the CMRK resin. This explains why sockets #11 & #12 exhibited higher ultimate strengths, despite only having one layer of carbon tied into the plate.

If this theory regarding the failure mechanism is correct, reinforcement of the distal end, posterior is warranted. In order to reinforce this area, low-angle fibers should be added to help distribute the load. The optimum solution, which will yield the greatest increase in strength for the smallest increase in weight, is to add fibers which are parallel to the main axis of the socket. One possibility is to use a unidirectional fabric and cut strips of the material to align the fibers to the 0° axis. A more easily implemented solution would be to use a bi-directional tape (for example, the tape available from US Composites, http://www.shopmaninc.com/carbonpage.html, Catalog Number FG-CF5704). Wrapping this tape around the attachment point will put fibers in the most critical direction (0° to the socket's main axis) relatively easily. As the stresses should be localized at the attachment point, a three or four inch width tape should be sufficient. It is projected that the addition of a bi-directional tape could add as much strength as an additional layer over the entire socket. Carbon tapes which are available in prosthetic catalogs cannot be easily used to add fibers to the 0° direction; rather, using them near the attachment plate will add fibers in the 90° direction, where they will have only a marginal impact on the ultimate strength. The practice of reflexing an additional three inches at the distal end will also result in adding low-angle fibers to the critical point, and is also easily implemented.

# Acknowledgements

This work was supported by contract numberN00014-06-0045/DO4 from the Office of Naval Research.

The work of D. Stefan Dancila, PhD, Samer A Tawfik, PhD, and Robert S Kistenberg, MPH, CP, FAAOP, is gratefully acknowledged. This team was responsible for devising a method of producing identical sockets and rapidly testing sockets according to the ISO standard. Their input on the fabrication and testing methods, as well as expertise in the prosthetics field, was invaluable.

The technical input of Charles Rowe and Ryan Frankart is also gratefully acknowledged.

# Appendix

## Data

| | Tensile | | | | Compression | |
|---|---|---|---|---|---|---|
| Panel # | Mpsi | SD | % | SD | Mpsi | SD |
| 1 | 1.4 | 0.1 | 8.258 | 3.70828397 | 1.4282 | 0.121147431 |
| 2 | 1.4 | 0.1 | 12.634 | 4.808557996 | 1.392 | 0.140700036 |
| 3 | 1.8 | 0.1 | 4.314 | 1.503456019 | 1.98 | 0.146623668 |
| 4 | 1.7 | 0.074966659 | 9.812 | 1.407789047 | 1.5602 | 0.175832875 |
| 5 | 1.6 | 0.105735519 | 9.472 | 3.312909597 | 1.5432 | 0.091390371 |
| 6 | 1.5 | 0.121942609 | 12.982 | 1.818617607 | 1.6268 | 0.163014417 |
| 7 | 1.5 | 0.184580606 | 6.804 | 2.826389924 | 1.6432 | 0.207587813 |
| 8 | 1.4 | 0.049497475 | 9.704 | 1.120571283 | 1.6594 | 0.14655818 |
| 9 | 1.5 | 0.12980755 | 6.988 | 1.277603225 | 1.3326 | 0.157094876 |
| 10 | 3.2 | 0.128179562 | 1.722 | 0.18403804 | 3.1952 | 0.463217767 |
| 11 | 4.5 | 0.158335088 | 1.468 | 0.149063745 | 4.6316 | 0.624918635 |
| 12 | 1.9 | 0.110090872 | 2.134 | 0.228648201 | 2.0938 | 0.265655228 |
| 13 | 2.2 | 0.080808415 | 2.16 | 0.225499446 | 2.4334 | 0.14194823 |
| 17 | 1.8 | 0.136491758 | 9.548 | 2.250037777 | 2.2412 | 0.369236645 |
| 18 | 1.8 | 0.032710854 | 9.466 | 1.880765801 | 2.3764 | 0.393832198 |
| 19 | 1.6 | 0.065802736 | 12.542 | 0.476308723 | 2.2308 | 0.463572756 |
| 20 | 1.8 | 0.161152102 | 7.102 | 0.886323869 | 2.2782 | 0.49896062 |
| 21 | 2.0 | 0.273623829 | 6.438 | 1.4590305 | 2.5936 | 0.411779431 |
| 22 | 1.7 | 0.314054135 | 6.5 | 3.765149399 | 1.806 | 0.345461286 |
| 23 | 2.2 | 0.094180677 | 2.99 | 1.039350759 | 2.5024 | 0.220361748 |
| 24 | 1.9 | 0.160062488 | 5.378 | 0.869120245 | 2.332 | 0.368558001 |
| 25 | 1.6 | 0.092032603 | 6.754 | 1.531267449 | 1.809 | 0.211979952 |
| 26 | 1.8 | 0.084083292 | 5.982 | 0.894606059 | 1.892 | 0.103336828 |
| 27 | 1.7 | 0.047644517 | 8.06 | 2.152208168 | 2.0406 | 0.33350907 |
| 28 | 2.2 | 0.22367387 | 4.424 | 1.601961298 | 2.1154 | 0.303635143 |
| 29 | 2.2 | 0.080124902 | 3.354 | 0.877114588 | 2.5588 | 0.341734107 |
| 30 | 1.8 | 0.152315462 | 4.552 | 1.197380474 | 2.4888 | 0.374655442 |
| 31 | 1.7 | 0.132211951 | 7.198 | 3.634978679 | 1.8896 | 0.336647887 |
| 32 | 1.8 | 0.067305275 | 4.18 | 1.559759597 | 1.8154 | 0.450845095 |
| 33 | 1.5 | 0.048785244 | 6.612 | 2.058074343 | 1.7202 | 0.308815803 |
| 34 | 1.4 | 0.081055537 | 9.004 | 2.032579642 | 1.557 | 0.225438462 |
| 35 | 2.6 | 0.053103672 | 2.152 | 0.539323651 | 3.0878 | 0.747406984 |
| 36 | 2.1 | 0.109224539 | 5.54 | 1.852174398 | 2.5372 | 0.301949002 |
| 37 | 1.8 | 0.096591925 | 4.992 | 1.688807271 | 2.2174 | 0.456393799 |
| 38 | 1.4 | 0.054954527 | 2.284 | 0.962460389 | 1.3506 | 0.206286936 |
| 39 | 1.8 | 0.292950508 | 4.472 | 2.368009713 | 1.6182 | 0.229733977 |
| 40 | 1.4 | 0.021213203 | 4.948 | 1.15124715 | 1.3876 | 0.261143256 |
| 41 | 1.3 | 0.058566202 | 7.712 | 2.883282851 | 1.4636 | 0.313334167 |
| 42 | 1.2 | 0.172046505 | 6.792 | 1.059207251 | 1.3892 | 0.250843975 |
| 43 | 1.3 | 0.061237244 | 8.346 | 1.326661223 | 1.6942 | 0.199300527 |

| | Flexural | | Shear | |
|---|---|---|---|---|
| Panel # | Mpsi | SD | psi | SD |
| 1 | 1.828614 | 0.202945428 | 3656.0961 | 197.7072325 |
| 2 | 1.949458 | 0.251633107 | 3341.6796 | 269.6116624 |
| 3 | 2.23389 | 0.365770616 | 3883.7365 | 367.1909947 |
| 4 | 1.69117 | 0.23008516 | 4115.4841 | 429.5655511 |
| 5 | 1.555946 | 0.14514413 | 3821.9321 | 283.6094429 |
| 6 | 1.580098 | 0.275132383 | 4059.8556 | 298.9202953 |
| 7 | 1.688568 | 0.169109684 | 3933.4615 | 366.8933058 |
| 8 | 1.655362 | 0.157731409 | 3819.9207 | 307.244868 |
| 9 | 1.69919 | 0.165949859 | 3518.4018 | 262.2747106 |
| 10 | 1.61865 | 0.177571804 | 3829.1877 | 400.9529088 |
| 11 | 3.182102 | 0.320463226 | 4815.278 | 114.3278476 |
| 12 | 2.019526 | 0.76613703 | 4025.8615 | 291.7120766 |
| 13 | 2.234632 | 0.152536362 | 4087.4367 | 169.9750527 |
| 17 | 2.142624 | 0.16665705 | 5038.7414 | 259.4332888 |
| 18 | 2.14228 | 0.357621398 | 4563.4776 | 206.4676617 |
| 19 | 1.821922 | 0.189534644 | 4707.5166 | 187.4143058 |
| 20 | 2.084236 | 0.327920788 | 4317.1336 | 215.5071093 |
| 21 | 2.460624 | 0.12214256 | 4313.5553 | 83.90292864 |
| 22 | 1.873444 | 0.338316691 | 2919.2403 | 338.0316295 |
| 23 | 2.502852 | 0.375735511 | 3963.6994 | 112.0171229 |
| 24 | 1.640364 | 0.350998703 | 2860.4624 | 534.5004187 |
| 25 | 1.900314 | 0.158105103 | 2599.166 | 293.5619444 |
| 26 | 2.168076 | 0.198615808 | 3339.203 | 179.4212081 |
| 27 | 2.1837 | 0.316863391 | 3307.8746 | 149.7476531 |
| 28 | 2.439356 | 0.331812029 | 3112.8396 | 218.0825312 |
| 29 | 2.632124 | 0.150026733 | 3691.0598 | 288.4515014 |
| 30 | 1.949 | 0.132570271 | 3457.4612 | 220.2011871 |
| 31 | 2.559888 | 0.383744237 | 3108.8706 | 176.8511506 |
| 32 | 1.837534 | 0.312344962 | 3553.0204 | 221.2372373 |
| 33 | 1.871284 | 0.184405713 | 3359.6768 | 209.8681673 |
| 34 | 1.699666 | 0.46457883 | 2241.2764 | 151.9551166 |
| 35 | 2.38422 | 0.269369037 | 4951.1797 | 472.5539492 |
| 36 | 1.874486 | 0.215618636 | 5293.3918 | 533.1663766 |
| 37 | 2.45328 | 0.128156227 | 3682.1763 | 239.4799076 |
| 38 | 1.637372 | 0.245082941 | 2359.7198 | 168.9885306 |
| 39 | 1.802434 | 0.264272235 | 2707.5839 | 117.5597958 |
| 40 | 2.076156 | 0.524687133 | 2454.6186 | 128.8449549 |
| 41 | 1.182526 | 0.134624942 | 2364.853 | 143.123788 |
| 42 | 1.187488 | 0.173489453 | 2650.2543 | 179.7465826 |
| 43 | 1.613234 | 0.181516677 | 2849.6252 | 156.789895 |

| Panel # | Resin Name | Reinforcement | Description | Description |
|---|---|---|---|---|
| 1 | CMRK | Carbon | CCCCC | 45 only |
| 2 | CMRK | Fiberglass | CC-R-CC | 45 only |
| 3 | CMRK | Fiberglass | C-R-C-R-C | 45 only |
| 4 | CMRK | HCF8 | CC-R-CC | 45 only |
| 5 | CMRK | HCF8 | C-R-C-R-C | 45 only |
| 6 | CMRK | LCB6 | CC-R-CC | 45 only |
| 7 | CMRK | LCB6 | C-R-C-R-C | 45 only |
| 8 | CMRK | LCF6 | CC-R-CC | 45 only |
| 9 | CMRK | LCF6 | C-R-C-R-C | 45 only |
| 10 | CMRK | Oriented Carbon | CC-R-CC | 90 layers |
| 11 | CMRK | Oriented Carbon | C-R-C-R-C | 90 layers |
| 12 | CMRK | Oriented FG | CC-R-CC | 90 layers |
| 13 | CMRK | Oriented FG | C-R-C-R-C | 90 layers |
| 17 | 80:20 | Carbon | CCCCC | 45 only |
| 18 | 80:20 | Fiberglass | CC-R-CC | 45 only |
| 19 | 80:20 | Fiberglass | C-R-C-R-C | 45 only |
| 20 | Ultra Performance Epoxy | Carbon | CCCCC | 45 only |
| 21 | Ultra Performance Epoxy | Fiberglass | CC-R-CC | 45 only |
| 22 | Ultra Performance Epoxy | Fiberglass | C-R-C-R-C | 45 only |
| 23 | EpoxyAcryl | Carbon | CCCCC | 45 only |
| 24 | EpoxyAcryl | Fiberglass | CC-R-CC | 45 only |
| 25 | EpoxyAcryl | Fiberglass | C-R-C-R-C | 45 only |
| 26 | 100% Rigid | Carbon | CCCCC | 45 only |
| 27 | 100% Rigid | Fiberglass | CC-R-CC | 45 only |
| 28 | 100% Rigid | Fiberglass | C-R-C-R-C | 45 only |
| 29 | 75% Rigid | Carbon | CCCCC | 45 only |
| 30 | 75% Rigid | Fiberglass | CC-R-CC | 45 only |
| 31 | 75% Rigid | Fiberglass | C-R-C-R-C | 45 only |
| 32 | 50% Rigid | Carbon | CCCCC | 45 only |
| 33 | 50% Rigid | Fiberglass | CC-R-CC | 45 only |
| 34 | 50% Rigid | Fiberglass | C-R-C-R-C | 45 only |
| 35 | ER | Carbon | CCCCC | 45 only |
| 36 | ER | Fiberglass | CC-R-CC | 45 only |
| 37 | ER | Fiberglass | C-R-C-R-C | 45 only |
| 38 | CMRK 3% cat | Carbon | CCCCC | 45 only |
| 39 | CMRK 3% cat | Fiberglass | CC-R-CC | 45 only |
| 40 | CMRK 3% cat | Fiberglass | C-R-C-R-C | 45 only |
| 41 | Duralimb | Carbon | CCCCC | 45 only |
| 42 | Duralimb | Fiberglass | CC-R-CC | 45 only |
| 43 | Duralimb | Fiberglass | C-R-C-R-C | 45 only |

| Panel # | Catalyst amount |
|---|---|
| 1 | 2% |
| 2 | 2% |
| 3 | 2% |
| 4 | 2% |
| 5 | 2% |
| 6 | 2% |
| 7 | 2% |
| 8 | 2% |
| 9 | 2% |
| 10 | 2% |
| 11 | 2% |
| 12 | 2% |
| 13 | 2% |
| 17 | 2% |
| 18 | 2% |
| 19 | 2% |
| 20 | 2% |
| 21 | 2% |
| 22 | 2% |
| 23 | 2% |
| 24 | 2% |
| 25 | 2% |
| 26 | 2% |
| 27 | 2% |
| 28 | 2% |
| 29 | 2% |
| 30 | 2% |
| 31 | 2% |
| 32 | 2% |
| 33 | 2% |
| 34 | 2% |
| 35 | 2% |
| 36 | 2% |
| 37 | 2% |
| 38 | 3% |
| 39 | 3% |
| 40 | 3% |
| 41 | 2% |
| 42 | 2% |
| 43 | 2% |

## Socket Testing Report

# MECHANICAL TESTING OF PROSTHETIC COMPOSITE TRANS-TIBIAL SOCKETS

## Final Report

DLLC-SCRA-RPT-001

Submitted to the
Applied Research and Development Institute (ARDI)
91 Technology Drive, Suite 200
Clemson Research Park
Anderson, SC 29625

Attn: Dr. Christopher W. Norfolk, Program Manager

April 27, 2009

**DANCILA LLC**
*Research, Development, and Technological Innovation*

The present Final Report is issued by *DANCILA LLC*, a limited liability company located at 1505 Versailles Ct., Marietta GA 30066-7828 U.S.A. ("*DLLC*") to the Applied Research and Development Institute, having its principal place of business located at 91 Technology Drive, Suite 200, Clemson Research Park, Anderson, SC 29625 ("ARDI"), for research activities rendered by *DLLC* to ARDI, under the Firm Fixed Price ("FFP") research agreement DLLC-SCRA-AGR-001.1 of November 28, 2008, incorporated herein by reference.



*1505 Versailles Ct., Marietta, GA 30066*
*(678) 525 2724*
*www.dancila.com*

# Table of Contents





1505 Versailles Ct., Marietta, GA 30066
(678) 525 2724
www.dancila.com

## Executive Summary

Quasi-static mechanical testing of a set of ten trans-tibial composite sockets was successfully performed generally following the guidelines provided by the ISO 10328 standard in order to determine their strength. All sockets exceeded the ultimate load requirements imposed by the standard for the corresponding loading level and loading configuration (P4 II). Extended load range testing showed that only 4 of the 10 sockets failed at load levels under -10,000 N.

All observed failures occurred at the distal end of the composite socket, in the region where the four screw plate is incorporated into the socket. This appears to be the weak aspect of the socket design, due to both the stress concentrations introduced and due to the stiffness and material characteristics mismatch, which lead to failure initiation and to a progression of the failure surface in the weak interface between the composite material and the four screw plate.

Significant variability in the manufactured socket configurations was observed. This is attributed to, and inherent in the manufacturing technology used, which is typical in the field of prosthetics. In particular it is very difficult when using this manufacturing technology to precisely and in a repeatable/reproducible manner position the reinforcement layers. It is also difficult to precisely control the fiber volume fraction and/or to avoid the formation of resin rich pockets. While a developed method of positioning of the four-screw plate in a repeatable and reproducible manner across sockets was effective, further improvements and refinements are needed. A source of particular variability is the folding of the reinforcement fiber layers over the four-screw plate ring and their fixation, both of which are viewed as playing a significant role in the overall strength of the socket.

The response observed reflects both differences in material properties (matrix resin system, reinforcement fiber type, tow size, sock size, etc.) and variability in manufacturing among composite sockets. It is not possible to differentiate between the two effects in the results.

Acoustic emission was successfully used to monitor the initiation and progression of damage during testing.



1505 Versailles Ct., Marietta, GA 30066
(678) 525 2724
www.dancila.com

## 1. Introduction

Modern composite materials capitalize upon the outstanding specific strength and stiffness of high performance fibers and upon the enhanced mechanical properties of modern resin systems. In addition to structural weight savings, composite materials make possible the tailoring of structural elastic deformation and failure modes through the use of their intrinsic anisotropy.

The use of composite materials has expanded far beyond the original aerospace focus to numerous other fields, including prosthetics. Residual limb prosthetic sockets, including trans-tibial sockets, are among the numerous composite material applications in this field. The application goals for composite material use in prosthetic sockets include weight savings and improved strength.

Given their essential function in supporting patient locomotion and the potential consequences of their failure during use, mechanical testing of composite sockets to ensure strength, stiffness, and fatigue life is necessary.

Testing standards have been developed for this purpose. The international standard ISO 10328 "Prosthetics – Structural Testing of Lower Limb Prostheses – Requirements and Test Methods," (Ref. 1) is a relevant example. While it is recognized that actual in-service loading of lower limb prostheses is complex and affected by significant variability among patients and across the usage spectrum, standardized testing is based upon a choice of a few conservative combinations of loading configurations and loading levels that could be replicated with relative ease and accuracy throughout the community of practice.

ISO 10328 addresses the overall mechanical testing of lower limb prostheses. However, the specific aspects of socket (and in particular of composite socket) mechanical testing are not specifically addressed.

To date testing standards for composite sockets have not been developed. Published investigations regarding mechanical testing of composite sockets reveal variability in the applied testing methods, testing fixture designs, composite socket load application, number of specimens for each socket configuration and loading mode combination, etc. (Refs. 2-4). One consequence of this variability is that the results of various investigations are neither highly reliable nor directly comparable.

Reference 1 provides for lower limb prostheses testing using the application of a pair of equal and opposite forces acting along the same given line of action, a load application configuration that can be easily implemented using a universal tension-compression materials testing machine. The levels of applied load and the position and orientation of the line of action of the force with respect to the reference coordinate system of the prosthetic limb are



1505 Versailles Ct., Marietta, GA 30066
(678) 525 2724
www.dancila.com

prescribed based upon several parameters, including the body weight range of the target patients for which the prosthesis is designed and the specific stance phase of gait considered.

Published investigations regarding the mechanical response of composite sockets generally follow the guidelines of Ref. 1 from which they derive the characteristics of the loading level and the position and the orientation of the loading line of action.

One aspect that is not specified, and therefore is open for rational choice, is the specific method of loading of the composite socket through the plug simulating the residual limb.

In the published literature a plaster plug is used to partially fill and transmit mechanical loading to the inner proximal region of the socket, while the distal part of the socket is left unloaded/unsupported from the interior of the socket. As a consequence, the distal socket region is only loaded from the outside by the distal lower limb prosthetic hardware, and the reported failure modes observed are clearly reflecting this choice of loading configuration.

An argument can be made that the above loading configuration choice is not an accurate reflection of actual in-use loading of the prosthetic socket by a residual limb, and that the combination of soft tissue of the residual limb and gel liner effects result in a composite socket loading that can be more closely characterized as hydrostatic. Consequently, for the present investigation a composite socket inner loading method that uses a full length residual limb plaster plug covered by a relatively thick elastomeric liner has been selected with the aim of more closely approximating a hydrostatic-type loading.

One of the main goals of the present investigations was to compare under quasi-static loading the mechanical strength of composite sockets manufactured from various material systems.

One other main goal of the present investigation was to explore the use of acoustic emission as a tool for detecting the initiation and progression of damage during load application.

## 2. Prosthetic Composite Trans-Tibial Socket Set

A set of 10 composite trans-tibial sockets selected out of a set of 12 manufactured at the Applied Research and Development Institute (ARDI) has been tested. Based upon initial testing results the other two sockets have been deemed overly stiff and strong to generate any useful testing results within the testing parameters selected for the set. Composite sockets 1 and 4-12 were tested.

All sockets have been manufactured based upon the residual limb model of a 175 lb body weight (approx. 80 kg body mass) patient.



1505 Versailles Ct., Marietta, GA 30066
(678) 525 2724
www.dancila.com

Identical plaster molds of the residual limb were used for manufacturing each socket. Each plaster mold identically encased a ½" utility-grade steel pipe shank extending out of the plaster mold at the proximal end. Each steel pipe shank had a small machined flat surface extending over a substantial portion of its exposed length, to be used as an angular degree of freedom positioning key during all phases of manufacturing and testing.

Composite socket load application from the distal end was accomplished via a four screw plate incorporated into each socket. With the goal of manufacturing nominally identical composite sockets, provisions were made for the identical positioning of the machined aluminum alloy distal four-screw plate in each socket. For this purpose each plaster plug identically encased at its distal end two parallel steel pins of different diameter, protruding from the plaster mold to serve as a position key and to allow the sliding positioning of the four screw plate at the appropriate stage of the manufacturing process. The steel pins were accessible at the completion of the manufacturing process and were removed in preparation for socket testing.

Relatively thick (9 mm class) elastomeric liners were used to cover each plaster mold, and the composite sockets were laminated over the combined plaster mold and elastomeric liner model.

In brief, a room temperature Vacuum Assisted Resin Transfer Molding (VARTM) composite socket manufacturing process, following standard practice in the field of prosthetics, was used. Dry woven yarn tubular sections were successively draped in layers over the mold, the machined aluminum distal four-screw plate was slide-guided into position at a selected stage, and one or more of the subsequent woven layers were tied into a groove of the plate. Subsequent vacuum application was used to consolidate the woven fiber layers, and vacuum assisted resin infusion followed by curing completed the manufacturing process.

The proximal end of the cured composite socket was trimmed off to a typical socket trim line, thereby removing any constraining effect that the trimmed off part may have had upon the relative movement of the plaster plug during load application.

A number of material systems (fiber and resin combinations) of interest for prosthetic composite socket manufacturing was investigated by ARDI via a room temperature coupon level quasi-static mechanical testing program, and a selection of material systems of interest was made. Each of the ten sockets tested in this investigation implemented a different selected material system.

Accelerated ageing of the composite sockets using autoclave heating was performed in order to ensure that the resin curing process was complete at the time of testing.



1505 Versailles Ct., Marietta, GA 30066
(678) 525 2724
www.dancila.com

## 3. Mechanical Testing

As stated, one of the goals of the mechanical testing performed in this investigation was to compare the relative strength of the ten composite sockets under quasi-static mechanical loading following guidelines of the ISO 10328.

The definition of the reference coordinate system for a residual limb/lower limb prosthesis is provided in Section 6 of Ref. 1.

The definition of load levels and load application line offsets is provided in Sections 7 and 8 of Ref. 1.

The loading level of Ref. 1 corresponding to lower limb prosthetic devices for a patient with a body weight of 175 lbs (approx. 80 kg. body mass) is identified as test loading level P4.

A late stance phase of gait was selected for this investigation. This corresponds to test loading condition II of Ref. 1.

Table 6 of Ref. 1 (pg. 16) provided the required P4 II values of load application point offsets:

$o_T$= -44 mm
$f_T$= 51 mm
$o_B$= -22 mm
$f_B$= 124 mm

Table 8 of Ref 1 (pg. 17) provided the required P4 II values of loading:

Stabilizing force $F_{stab}$= -50 N
Settling force $F_{set}$ = -828 N
Proof test force $F_{sp}$ = -1,811 N
Ultimate static test force $F_{su,\ upper\ level}$ = -3,623 N

The negative sign is used in this document to comply with the standard sign convention that compressive loading is negative.

Load application is to be performed in load control mode at a rate of -100 N/s. The load application method needs to ensure the application of only the prescribed force and no moments.

The proximal steel pipe shank extending from each plaster mold was used to accurately position and support a proximal test fixture steel plate used for load application during testing.



1505 Versailles Ct., Marietta, GA 30066
(678) 525 2724
www.dancila.com

A solid steel shank terminated with a thick steel flange was used to attach to the four screw plate at the distal end of the composite socket. A thick steel plate end fixture was designed to ride on the solid steel shank and to allow a precise positioning in both axial and angular directions.

Both the proximal and the distal end plate fixtures had longitudinal channel slots machined to allow the precise positioning and bolt/nut locking of a spherical joint component.

Given the interest in comparing the relative strength of the ten sockets of this investigation it was decided to perform testing, if necessary, beyond the ultimate static test force level $F_{su\ upper\ level}$ = -3,623 N prescribed by Ref. 1. A minimum force level of -10 kN was used in designing and sizing the test fixtures, and in programming the testing machine procedure, the data acquisition, and the acoustic emission hardware and software.

An MTS tension-compression servo-hydraulic testing machine was used for this investigation. The testing machine is controlled through the MTS TestStar and TestWareSX software via an MTS digital controller. Test procedures, data acquisition, and parametric signal output were programmed.

Testing of the first socket was exploratory and was performed in displacement control mode at 1 mm/s in order to explore the full load vs. displacement response.

For all subsequent composite sockets loading was performed in load control mode at -100 N/s. Unloading was performed at 300 N/s. Generally following the guidelines of Sections 15 and 16 of Ref. 1:

First, a conditioning stage ramp loading at -100 N/s from -50 N to -828 N, followed by a hold for 30 s, and concluded with ramp unloading at 300 N/s to -50 N was applied.

Second, a proof loading stage with ramp loading at -100 N/s from -50 N to -1,811 N , followed by a hold for 30 s, and concluded with a ramp unloading at 300 N/s to -50 N was applied.

Finally, an ultimate loading stage with ramp loading at -100 N/s from – 50 N to -3,623 N, followed by a hold for 3 s, followed by a further ramp loading at – 100 N/s to -10,000 N was applied. If /when socket failure occurred testing was terminated, otherwise unloading at a rate of 300 N/s to -50 N concluded the stage.

For all tests performed load application point displacement vs. load data was acquired. The testing machine was also programmed to output an analog signal proportional to applied load, to be sensed by the acoustic emission equipment and to allow correlation between acoustic emission measurements and the corresponding applied load level.



1505 Versailles Ct., Marietta, GA 30066
(678) 525 2724
www.dancila.com

A Physical Acoustics PC-based acoustic emission equipment was used for acoustic emission measurements.

A set of high performance steel test fixtures was designed for load application at the prescribed location and with the prescribed orientation with respect to the composite socket. The design ensured the application of zero moments through the inclusion in the load path of a spherical joint at the proximal and the distal load application points.

Figure 1 shows a composite socket during testing. Details of the proximal and the distal test fixture hardware are shown in Figs. 2 and 3. Figure 4 shows a typical placement of the acoustic emission sensor on the composite socket during testing.

## 4. Results

### a. Trans-Tibial Composite Socket Testing Results

Testing results for each composite trans-tibial socket are presented in the following.

#### i. Trans-Tibial Composite Socket #1

Trans-tibial composite socket #1was tested under stroke control at a rate of 1 mm/s.

The load application point displacement and the cumulative acoustic emission counts measured are shown in Fig. 5 as a function of applied load.

The trans-tibial composite socket withstood a load of up to -13, 734 N without failure, at which load level the test was interrupted out of concern for overloading and potential damage of the test fixtures. Acoustic emission was acquired throughout the test. However, the load level signal output from the testing machine to the acoustic emission equipment saturated at -10 V at -10,000 N, as programmed, which prevents further correlation of acoustic emission with the corresponding load level. Consequently, Fig. 5 only shows the acoustic emission acquired down to -10,000 N.

From Fig. 5 it can be seen that acoustic emission, indicative of damage initiation and progression, occurs throughout the loading process and at an increasing rate with increasing load level. However, the first indication of damage in the load vs. displacement response appears as a notch beyond -6,000 N, and corresponds to an observed plastic deformation (occurrence of a plastic hinge) in the steel tube shank embedded in the plaster mold, followed by a cracking of the plaster mold. The steel tube shank is part of the load path for load application.



1505 Versailles Ct., Marietta, GA 30066
(678) 525 2724
www.dancila.com

Beyond this load level further bending of the steel pipe and further cracking of the plaster mold occur, possibly combined with further damage initiation and progression in the composite socket. However, it is not possible to differentiate the acoustic emission acquired by source, and hence it is not possible to ascertain the level of damage induced in the composite socket.

The composite socket preserved its load carrying capability up to -13, 734 N without any damage noticeable by visual inspection.

### ii. Trans-Tibial Composite Socket #4

Trans-tibial composite socket #4 was tested under load control at a loading rate of -100 N/s.

The results of the conditioning stage loading are shown in Fig. 6.

The results of the proof loading stage are shown in Fig. 7.

The results of the ultimate loading stage are shown in Fig. 8.

The measured strength of composite socket #4 exceeds the ISO 10328 requirement of $F_{su\ upper\ level}$ = -3,623 N prescribed by Ref. 1.

Acoustic emission data indicates that damage initiation and progression occurs during all loading stages. For each new loading stage, acoustic emission only resumes at load levels beyond the peak of previous loading, a well known acoustic emission effect.

During the ultimate loading stage and at a load level beyond the ultimate load $F_{su\ upper\ level}$ = -3,623 N prescribed by Ref. 1 plastic deformation of the steel pipe shank occurs at the exit point from the plaster mold, resulting in the formation of a plastic hinge and the occurrence of a crack splitting of the plaster mold (Fig. 9). As a result, the end of the screw that forms the proximal end spherical joint contacts the plaster mold and changes the subsequent load application to the plaster mold and implicitly to the composite socket. An estimate of -5,000 N for the load level at which the plastic hinge and plaster cracking occur can be obtained from the first notch in the displacement vs. load curve of Fig. 8.

Composite socket #4 failed at a load level of -8,197.7 N. The failure mode consists in fracture of the composite material in the region of the distal end that embeds the four screw plate, followed by a clean separation of the four screw plate (Figs. 10-11).



1505 Versailles Ct., Marietta, GA 30066
(678) 525 2724
www.dancila.com

### iii. Trans-Tibial Composite Socket #5

Trans-tibial composite socket #5 was tested under load control at a loading rate of -100 N/s.

To prevent the formation of a plastic hinge the proximal steel tube shank has been internally reinforced through the tight fit insertion of a 5/8" solid steel bolt, rendering the cross section effectively solid.

The results of the conditioning stage loading are shown in Fig. 12.

The results of the proof loading stage are shown in Fig. 13.

The results of the ultimate loading stage are shown in Fig. 14.

The measured strength of composite socket #5 exceeds the ISO 10328 requirement of $F_{su\ upper\ level}$ = -3,623 N prescribed by Ref. 1.

Acoustic emission data indicates that damage initiation and progression occurs during all loading stages. For each new loading stage, acoustic emission only substantially resumes at load levels beyond the peak of previous loading, a well known acoustic emission effect.

During the ultimate loading stage and at a load level beyond the ultimate load $F_{su\ upper\ level}$ = -3,623 N prescribed by Ref. 1 plaster mold split cracking occurs at an estimated load level of -5,000 N and can be recognized from the notch in the load application point displacement vs. load curve of Fig. 14.

Composite socket #5 failed at a load level of -8,706.7 N. The failure mode consists in fracture of the composite material in the region of the distal end that embeds the four screw plate, followed by a clean separation of the four screw plate (Fig. 15).

### iv. Trans-Tibial Composite Socket #6

Trans-tibial composite socket #6 was tested under load control at a loading rate of -100 N/s.

To prevent the formation of a plastic hinge the proximal steel tube shank has been internally reinforced through the tight fit insertion of a 5/8" solid steel bolt, rendering the cross section effectively solid.

The results of the conditioning stage loading are shown in Fig. 16.

The results of the proof loading stage are shown in Fig. 17.



1505 Versailles Ct., Marietta, GA 30066
(678) 525 2724
www.dancila.com

The results of the ultimate loading stage are shown in Fig. 18.

During the proof loading phase the locking bolt for the distal steel plate suddenly failed, leading to an unloading followed by reloading of the composite socket with a small load overshoot. However, even with the fixture plate sudden slip the permanent load application point displacement was only less than 3 mm, a value lower than the 5 mm limit imposed by Ref. 1.

The test fixture plates were modified to allow larger size locking bolts, which resolved the issue for all subsequent testing performed.

The measured strength of composite socket #6 exceeds the ISO 10328 requirement of $F_{su\ upper\ level}$ = -3,623 N prescribed by Ref. 1.

Acoustic emission data indicates that damage initiation and progression occurs during all loading stages. For each new loading stage, acoustic emission only substantially resumes at load levels beyond the peak of previous loading, a well known acoustic emission effect.

During the ultimate loading stage and at a load level beyond the ultimate load $F_{su\ upper\ level}$ = -3,623 N prescribed by Ref. 1 plaster mold split cracking occurs at an estimated load level of -4,500 N and can be recognized from the small notch in the load application point displacement vs. load curve of Fig. 18.

Composite socket #6 failed at a load level of -6,279.7 N. The failure mode consists in fracture of the composite material in the region of the distal end that embeds the four screw plate, followed by a clean separation of the four screw plate (Fig. 19).

### v. Trans-Tibial Composite Socket #7

Trans-tibial composite socket #7 was tested under load control at a loading rate of -100 N/s.

To prevent the formation of a plastic hinge the proximal steel tube shank has been internally reinforced through the tight fit insertion of a 5/8” solid steel bolt, rendering the cross section effectively solid.

The results of the conditioning stage loading are shown in Fig. 20.

The results of the proof loading stage are shown in Fig. 21.

The results of the ultimate loading stage are shown in Fig. 22.



1505 Versailles Ct., Marietta, GA 30066
(678) 525 2724
www.dancila.com

The measured strength of composite socket #7 exceeds the ISO 10328 requirement of $F_{su\ upper\ level}$ = -3,623 N prescribed by Ref. 1.

Acoustic emission data indicates that damage initiation and progression occurs during all loading stages. For each new loading stage, acoustic emission only substantially resumes at load levels beyond the peak of previous loading, a well known acoustic emission effect.

During the ultimate loading stage and at a load level beyond the ultimate load $F_{su\ upper\ level}$ = -3,623 N prescribed by Ref. 1 plaster mold split cracking occurs at an estimated load level of -6,000 N and can be recognized from the notch in the load application point displacement vs. load curve of Fig. 22.

Composite socket #7 did not fail. Figure 23 shows a close-up view of the distal end of the socket after testing.

### vi. Trans-Tibial Composite Socket #8

Trans-tibial composite socket #8 was tested under load control at a loading rate of -100 N/s.

To prevent the formation of a plastic hinge the proximal steel tube shank has been internally reinforced through the tight fit insertion of a 5/8" solid steel bolt, rendering the cross section effectively solid.

The results of the conditioning stage loading are shown in Fig. 24.

The results of the proof loading stage are shown in Fig. 25.

The results of the ultimate loading stage are shown in Fig. 26.

The measured strength of composite socket #8 exceeds the ISO 10328 requirement of $F_{su\ upper\ level}$ = -3,623 N prescribed by Ref. 1.

Acoustic emission data indicates that damage initiation and progression occurs during all loading stages. For each new loading stage, acoustic emission only substantially resumes at load levels beyond the peak of previous loading, a well known acoustic emission effect.

During the ultimate loading stage and at a load level beyond the ultimate load $F_{su\ upper\ level}$ = -3,623 N prescribed by Ref. 1 plaster mold split cracking occurs at an estimated load level of -6,000 N and can be recognized from the notch in the load application point displacement vs. load curve of Fig. 26.



1505 Versailles Ct., Marietta, GA 30066
(678) 525 2724
www.dancila.com

Composite socket #8 did not fail. Figure 27 shows a close-up view of the distal end of the socket after testing.

### vii. Trans-Tibial Composite Socket #9

Trans-tibial composite socket #9 was tested under load control at a loading rate of -100 N/s.

To prevent the formation of a plastic hinge the proximal steel tube shank has been internally reinforced through the tight fit insertion of a 5/8" solid steel bolt, rendering the cross section effectively solid.

The results of the conditioning stage loading are shown in Fig. 28.

The results of the proof loading stage are shown in Fig. 29.

The results of the ultimate loading stage are shown in Fig. 30.

The measured strength of composite socket #9 exceeds the ISO 10328 requirement of $F_{su\ upper\ level}$ = -3,623 N prescribed by Ref. 1.

Acoustic emission data indicates that damage initiation and progression occurs during all loading stages. For each new loading stage, acoustic emission only substantially resumes at load levels beyond the peak of previous loading, a well known acoustic emission effect.

During the ultimate loading stage and at a load level beyond the ultimate load $F_{su\ upper\ level}$ = -3,623 N prescribed by Ref. 1 plaster mold split cracking occurs at an estimated load level of -7,000 N and can be recognized from the notch in the load application point displacement vs. load curve of Fig. 30.

Composite socket #9 failed at a load level of -8,682.2 N. The failure mode consists in fracture of the composite material in the region of the distal end that embeds the four screw plate, followed by a clean separation of the four screw plate (Fig. 31).

### viii. Trans-Tibial Composite Socket #10

Trans-tibial composite socket #10 was tested under load control at a loading rate of -100 N/s.

To prevent the formation of a plastic hinge the proximal steel tube shank has been internally reinforced through the tight fit insertion of a 5/8" solid steel bolt, rendering the cross section effectively solid.



1505 Versailles Ct., Marietta, GA 30066
(678) 525 2724
www.dancila.com

The results of the conditioning stage loading are shown in Fig. 32.

The results of the proof loading stage are shown in Fig. 33.

The results of the ultimate loading stage are shown in Fig. 34.

The measured strength of composite socket #10 exceeds the ISO 10328 requirement of $F_{su\ upper\ level}$ = -3,623 N prescribed by Ref. 1.

Acoustic emission data indicates that damage initiation and progression occurs during all loading stages. For each new loading stage, acoustic emission only substantially resumes at load levels beyond the peak of previous loading, a well known acoustic emission effect.

During the ultimate loading stage and at a load level beyond the ultimate load $F_{su\ upper\ level}$ = -3,623 N prescribed by Ref. 1 plaster mold split cracking occurs at an estimated load level of -7,000 N and can be recognized from the notch in the load application point displacement vs. load curve of Fig. 34.

Composite socket #10 did not fail. A close-up view of the composite socket distal end is shown in Fig. 35.

### ix. Trans-Tibial Composite Socket #11

Trans-tibial composite socket #11 was tested under load control at a loading rate of -100 N/s.

To prevent the formation of a plastic hinge the proximal steel tube shank has been internally reinforced through the tight fit insertion of a 5/8” solid steel bolt, rendering the cross section effectively solid.

The results of the conditioning stage loading are shown in Fig. 36.

The results of the proof loading stage are shown in Fig. 37.

The results of the ultimate loading stage are shown in Fig. 38.

The measured strength of composite socket #11 exceeds the ISO 10328 requirement of $F_{su\ upper\ level}$ = -3,623 N prescribed by Ref. 1.

Acoustic emission data indicates that damage initiation and progression occurs during all loading stages. For each new loading stage, acoustic emission only substantially resumes at load levels beyond the peak of previous loading, a well known acoustic emission effect.



1505 Versailles Ct., Marietta, GA 30066
(678) 525 2724
www.dancila.com

During the ultimate loading stage and at a load level beyond the ultimate load $F_{su\ upper\ level}$ = -3,623 N prescribed by Ref. 1 plaster mold split cracking occurs at an estimated load level of -8,000 N and can be recognized from the notch in the load application point displacement vs. load curve of Fig. 34.

Composite socket #11 did not fail. A close-up view of the composite socket distal end is shown in Fig. 39.

### x. Trans-Tibial Composite Socket #12

Trans-tibial composite socket #12 was tested under load control at a loading rate of -100 N/s.

To prevent the formation of a plastic hinge the proximal steel tube shank has been internally reinforced through the tight fit insertion of a 5/8" solid steel bolt, rendering the cross section effectively solid.

The results of the conditioning stage loading are shown in Fig. 40.

The results of the proof loading stage are shown in Fig. 41.

The results of the ultimate loading stage are shown in Fig. 42.

The measured strength of composite socket #12 exceeds the ISO 10328 requirement of $F_{su\ upper\ level}$ = -3,623 N prescribed by Ref. 1.

Acoustic emission data indicates that damage initiation and progression occurs only above 4000 N, during the ultimate loading stage.

During the ultimate loading stage and at a load level beyond the ultimate load $F_{su\ upper\ level}$ = -3,623 N prescribed by Ref. 1 plaster mold split cracking occurs at an estimated load level of -8,000 N and can be recognized from the notch in the load application point displacement vs. load curve of Fig. 42.

Composite socket #12 did not fail. A close-up view of the composite socket distal end is shown in Fig. 43.



1505 Versailles Ct., Marietta, GA 30066
(678) 525 2724
www.dancila.com

## b. Summary of Testing Results

A summary of socket testing results is shown in Table I below.

**Table I. Summary of testing results**

| Socket No. | Conditioning Loading | | Proof Loading | | Ultimate Loading | | Socket Failure |
|---|---|---|---|---|---|---|---|
| | Min Load, N | Acoustic Emission Counts | Min Load, N | Acoustic Emission Counts | Min Load, N | Acoustic Emission Counts | |
| 1 | | | | | -13,734.1 | 72,762 | No |
| 4 | -921.1 | 1,564 | -1,876.3 | 1,741 | -8,197.7 | 53,209 | Yes |
| 5 | -901.2 | 217 | -1,870.2 | 2,234 | -8,706.7 | 53,209 | Yes |
| 6 | -884.3 | 3,276 | -2,064.9 | 13,876 | -6,279.7 | 31,056 | Yes |
| 7 | -893.5 | 160 | -1,854.9 | 1,350 | -10,071.3 | 9,719 | No |
| 8 | -892.0 | 9 | -1,861.0 | 4,427 | -10,141.8 | 60,257 | No |
| 9 | -879.7 | 8 | -1,856.4 | 1,112 | -8,682.2 | 99,402 | Yes |
| 10 | -870.5 | 193 | -1,861.0 | 5,487 | -10,069.7 | 95,034 | No |
| 11 | -872.1 | 70 | -1,850.3 | 2,516 | -10,048.3 | 222,720 | No |
| 12 | -890.5 | 1 | -1,845.7 | 2 | -10,048.3 | 107,208 | No |

## 5. Discussion

The results of the quasi-static testing performed show that all sockets exceeded the strength requirements specified by the ISO 10328 standard for the corresponding loading level and loading condition (P4 II).

Extended load level testing showed that only 4 of the 10 sockets failed under -10,000 N.

All observed failures occurred at the distal end of the composite socket, in the region where the four screw plate is incorporated into the socket. This appears to be the weak aspect of the socket design, due to both the stress concentrations introduced and due to the stiffness and material characteristics mismatch, which lead to failure initiation and to a progression of the failure surface in the weak interface between the composite material and the four screw plate.

Significant variability in the manufactured socket configurations was observed. This is attributed to, and inherent in the manufacturing technology used, which is typical in the field of prosthetics. In particular it is very difficult when using this manufacturing technology to precisely and in a repeatable/reproducible manner position the reinforcement layers. It is also difficult to precisely control the fiber volume fraction and/or to avoid the formation of resin rich pockets. While the developed method of positioning of the four-screw plate in a



1505 Versailles Ct., Marietta, GA 30066
(678) 525 2724
www.dancila.com

repeatable and reproducible manner across sockets was effective, further improvements and refinements are needed. A source of particular variability is the folding of the reinforcement fiber layers over the four-screw plate ring and their fixation, both of which are viewed as playing a significant role in the overall strength of the socket.

The response observed reflects both differences in material properties (matrix resin system, reinforcement fiber type, tow size, sock size, etc.) and variability in manufacturing among composite sockets. It is not possible to differentiate between the two effects in the results.

## 6. Conclusions

Quasi-static mechanical testing of a set of ten trans-tibial composite sockets was successfully performed following the guidelines of ISO 10328 to characterize their strength. All sockets exceeded the ultimate load level required by the ISO standard, and only four failed below -10,000 N.

Acoustic emission was instrumental in monitoring the onset and progression of damage. All observed failures involved clean separation of the four-screw metal plate from the composite socket. This appears to be the weak design feature of the socket configurations investigated.

It is necessary to perform more extensive testing using several test articles for each configuration in order to statistically characterize the measured response (average, standard deviation, etc.).

The socket loading method is likely to have a very significant influence upon test results. It is therefore necessary to study the effect of proximal socket loading and support configuration upon testing results.

The outcome of the mechanical testing is significantly influenced by both the characteristics of the material system used in each socket as well as by the variability in individual socket configuration due to the manufacturing technology used. Therefore it is not possible at this stage to draw definitive conclusions with regards to source of the observed behavior.

## 7. Recommendations for Future Work

It is recommended to extend the present study by testing at least three (preferably five or more) sockets for each configuration, thereby providing a basis for a statistical characterization of the results obtained.

It is also recommended to extend the scope of the present study to include fatigue response.



1505 Versailles Ct., Marietta, GA 30066
(678) 525 2724
www.dancila.com

## References

1. "ISO 10328: Prosthetics – Structural Testing of Lower Limb Prostheses – Requirements and Test Methods," International Standards Organization ISO 10328:2006(E).
2. Current, T. A., Kogler, G. F., and Barth, D. G., "Static Structural Testing of Trans-Tibial Composite Sockets," *Prosthetics and Orthotics International*, Vol. 23, No. 2, pp. 113-122, August 1999.
3. Neo, L. D., Lee, P. V. S., and Goh, J. C. H., "Principal Structural Testing of Trans-Tibial Prosthetic Assemblies: Specimen Preparation," *Prosthetics and Orthotics International*, Vol. 24, No. 3, pp. 241-245, December 2000.
4. Graebner, R. H., and Current, T. A., "Relative Strength of Pylon-to-Socket Attachment Systems Used in Trans-Tibial Composite Sockets," *Journal of Prosthetics & Orthotics*, Vol. 19, No. 3, pp. 67-74, July 2007.



1505 Versailles Ct., Marietta, GA 30066
(678) 525 2724
www.dancila.com

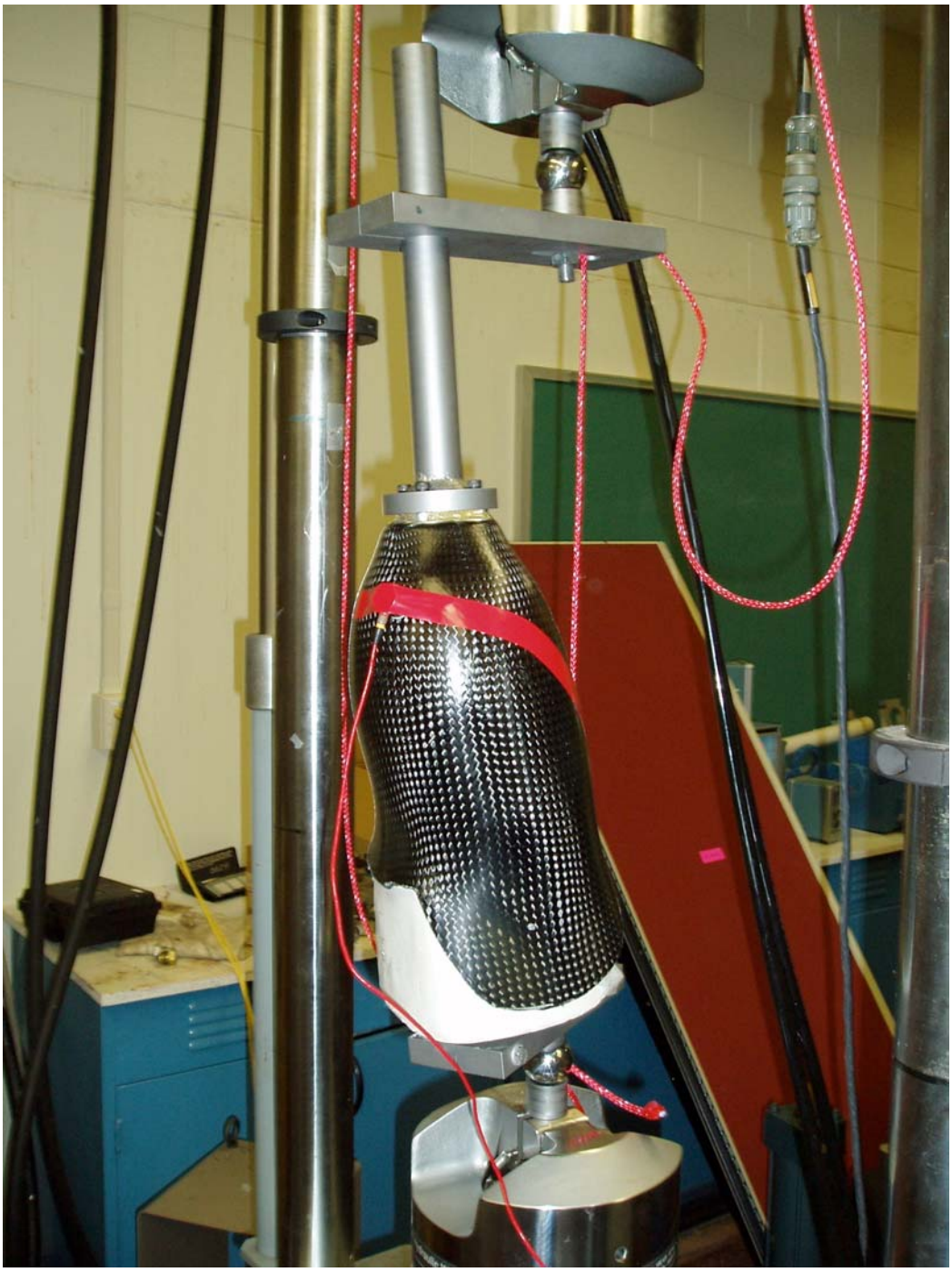

**Figure 1. Trans-tibial composite socket ready for testing.**



1505 Versailles Ct., Marietta, GA 30066
(678) 525 2724
www.dancila.com

**Figure 2. Distal end load fixture detail.**



1505 Versailles Ct., Marietta, GA 30066
(678) 525 2724
www.dancila.com

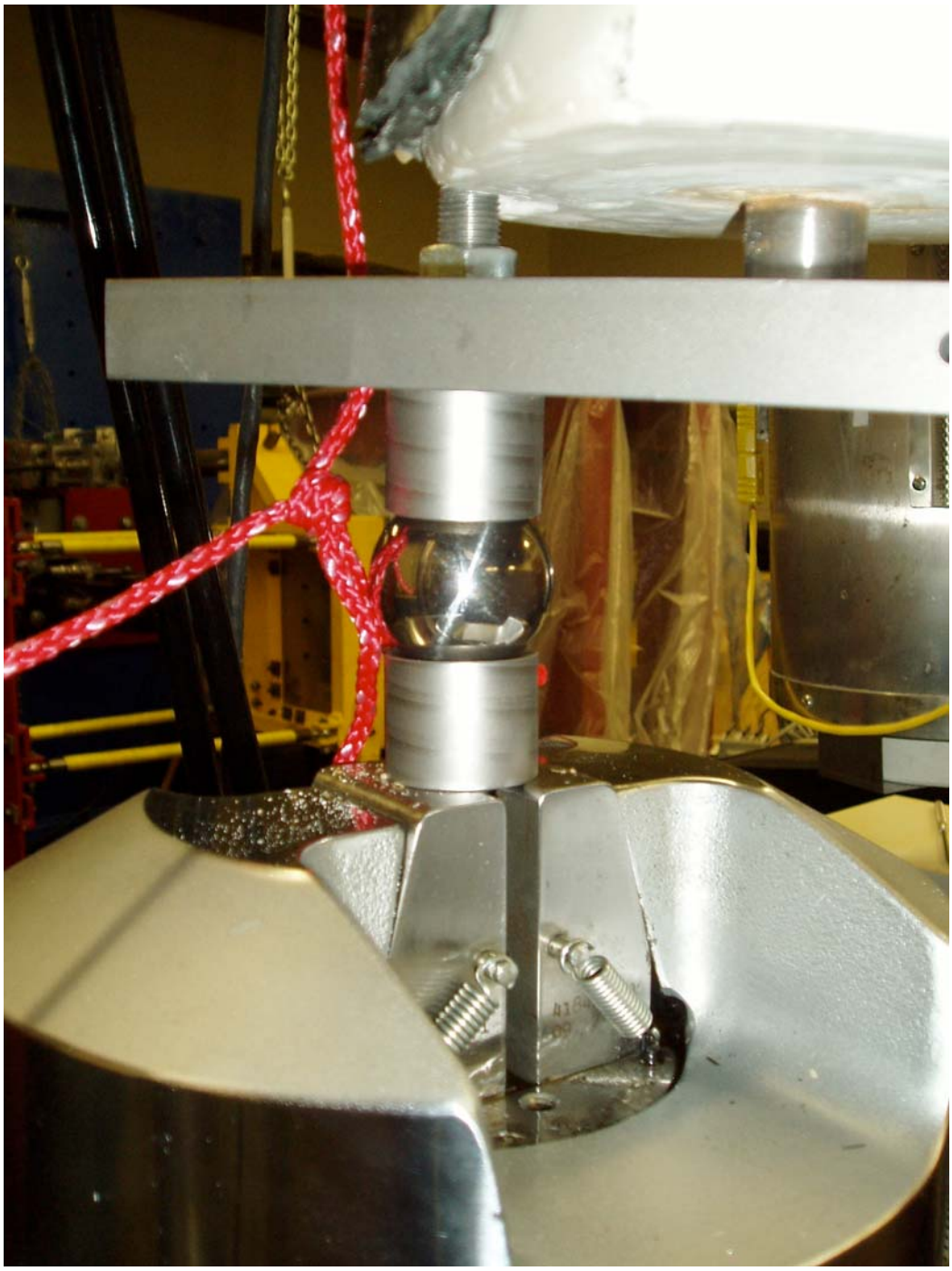

**Figure 3. Proximal end load fixture detail.**



1505 Versailles Ct., Marietta, GA 30066
(678) 525 2724
www.dancila.com

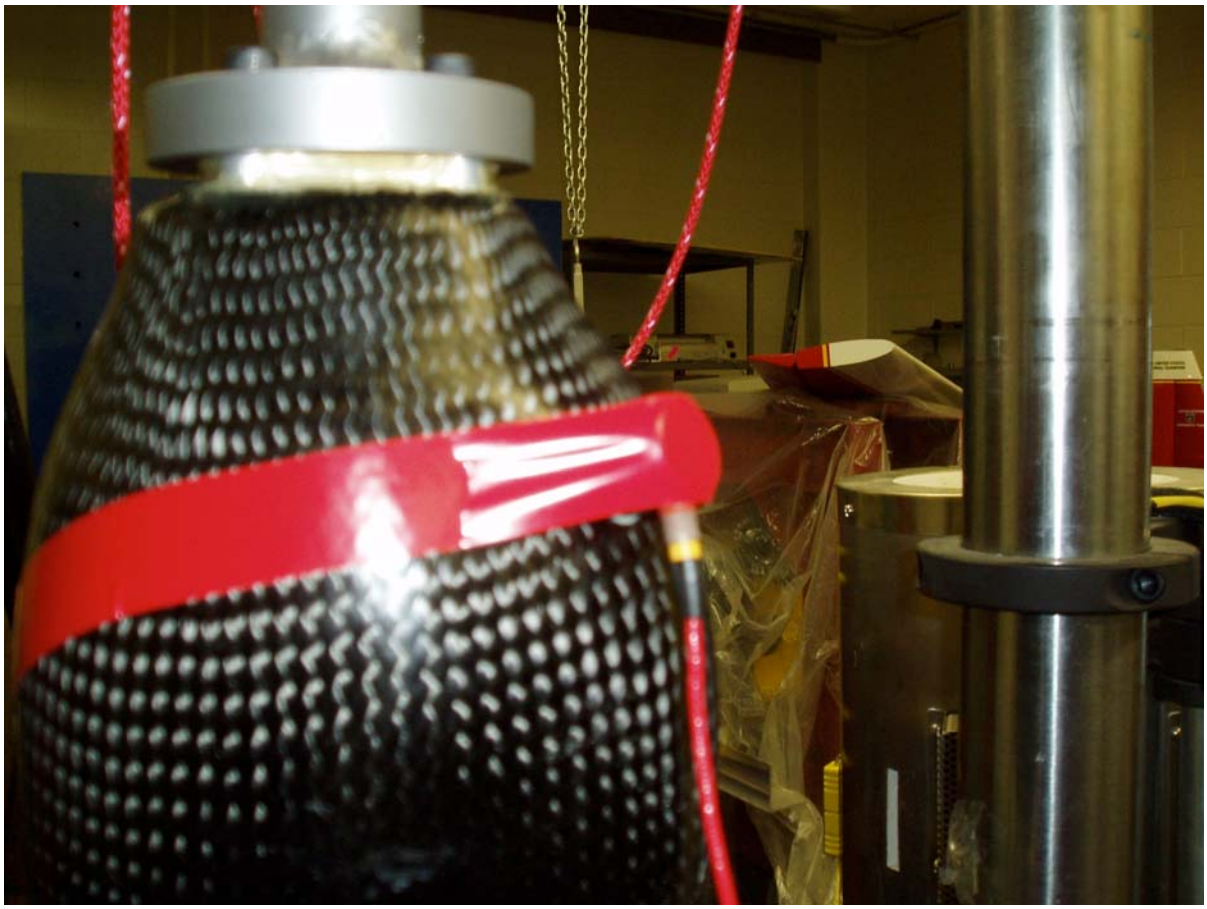

**Figure 4. Acoustic emission sensor placement.**



1505 Versailles Ct., Marietta, GA 30066
(678) 525 2724
www.dancila.com

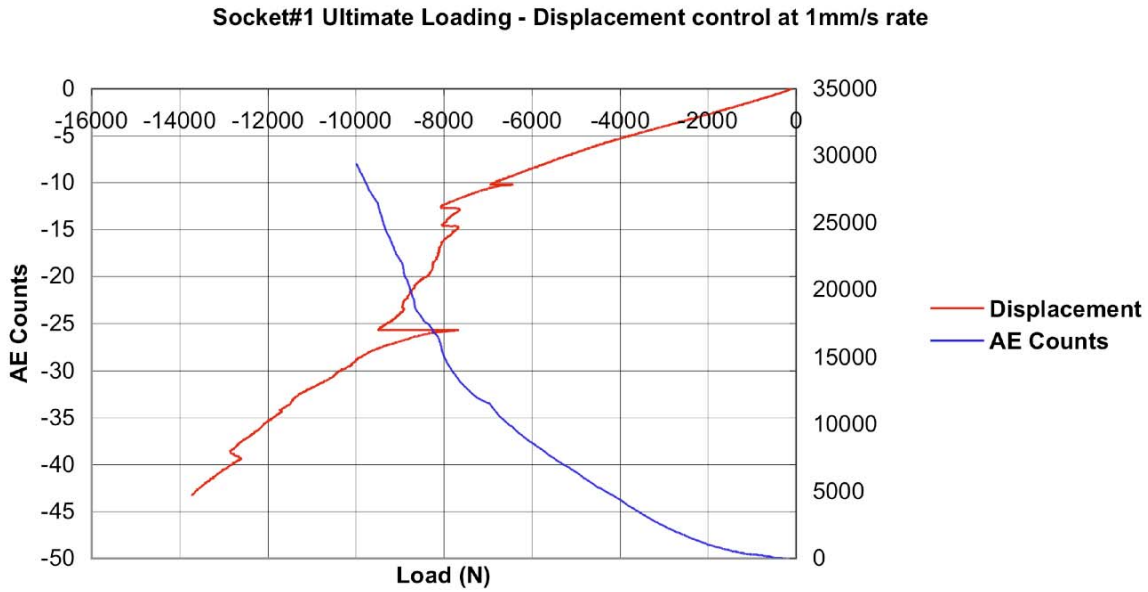


**Figure 5. Stroke and cumulative acoustic emission counts vs. applied load for socket #1.**

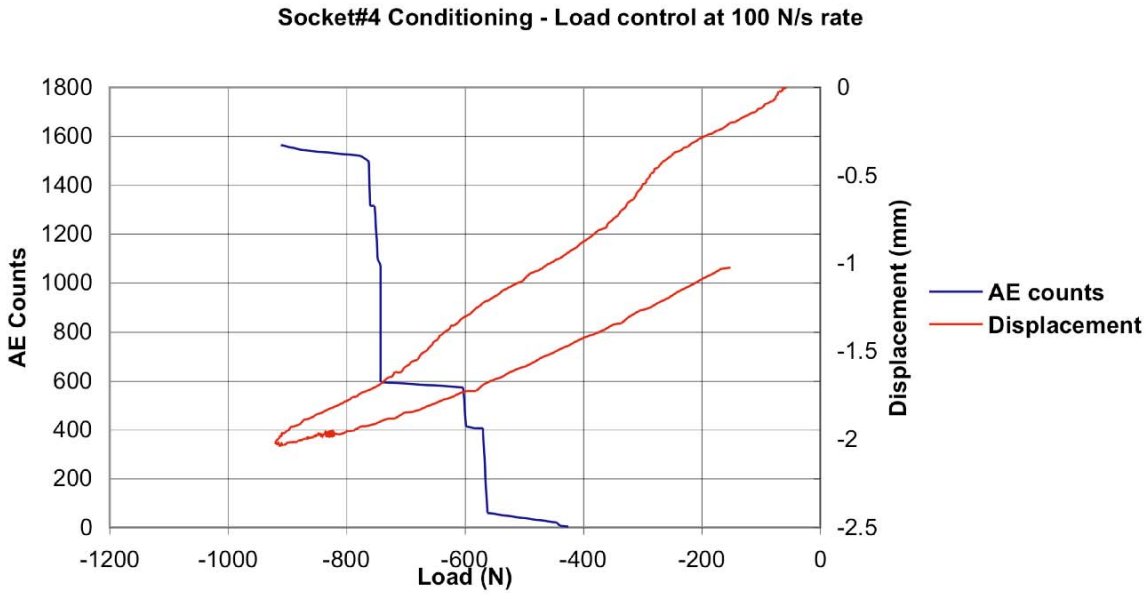


**Figure 6. Conditioning loading stage - Stroke and cumulative acoustic emission counts vs. applied load for socket #4.**



1505 Versailles Ct., Marietta, GA 30066
(678) 525 2724
www.dancila.com

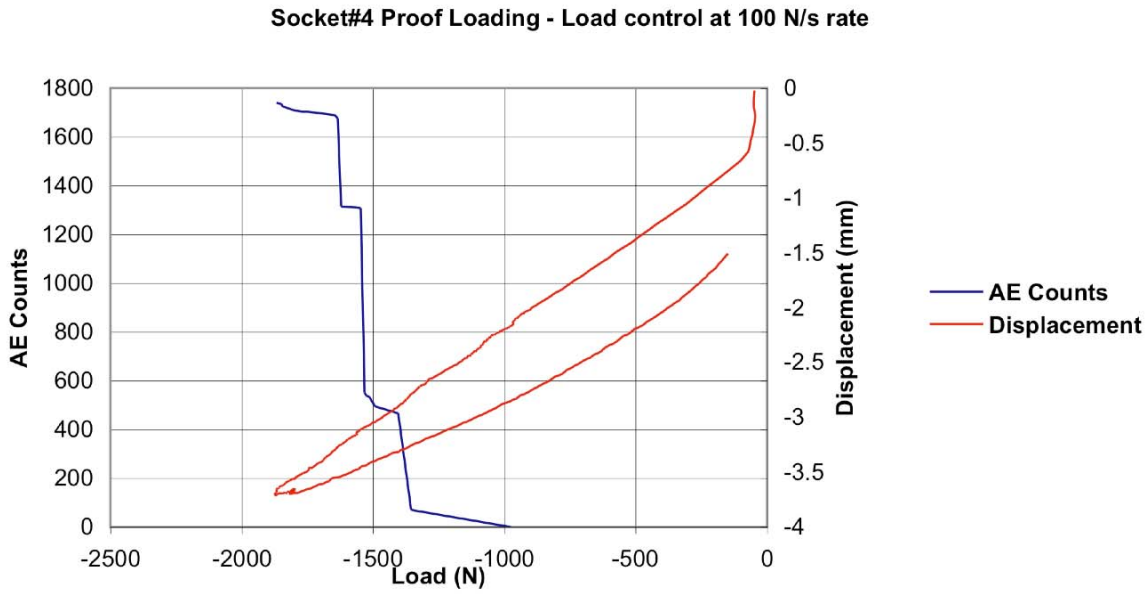


**Figure 7. Proof loading stage - Stroke and cumulative acoustic emission counts vs. applied load for socket #4.**

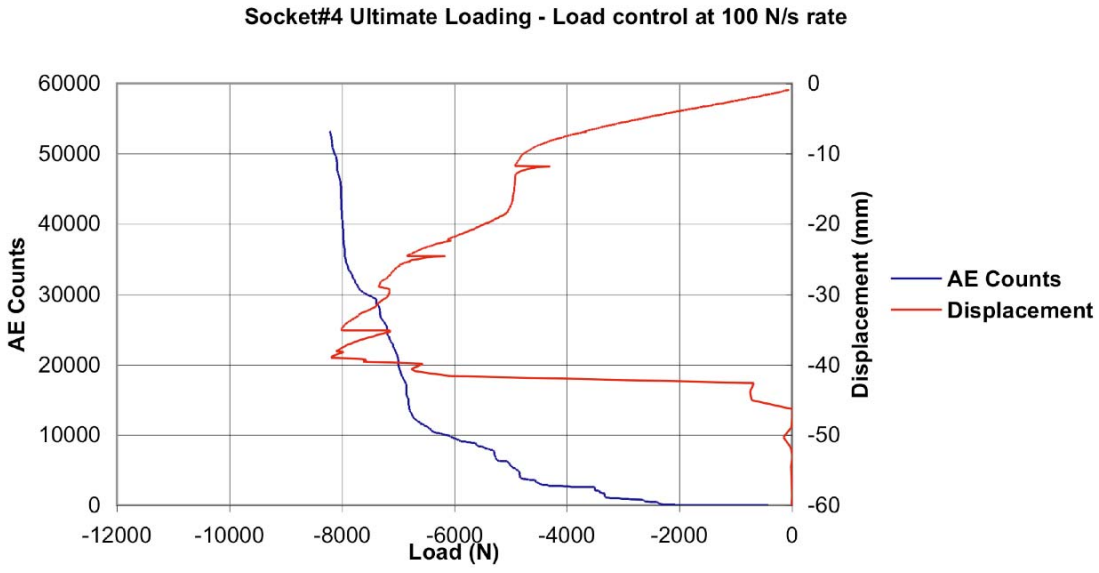


**Figure 8. Ultimate loading stage - Stroke and cumulative acoustic emission counts vs. applied load for socket #4.**



1505 Versailles Ct., Marietta, GA 30066
(678) 525 2724
www.dancila.com

**Figure 9. Steel shank plastic deformation and plaster mold cracking for socket #4.**



1505 Versailles Ct., Marietta, GA 30066
(678) 525 2724
www.dancila.com

**Figure 10. Failure region close-up view for socket #4.**



1505 Versailles Ct., Marietta, GA 30066
(678) 525 2724
www.dancila.com

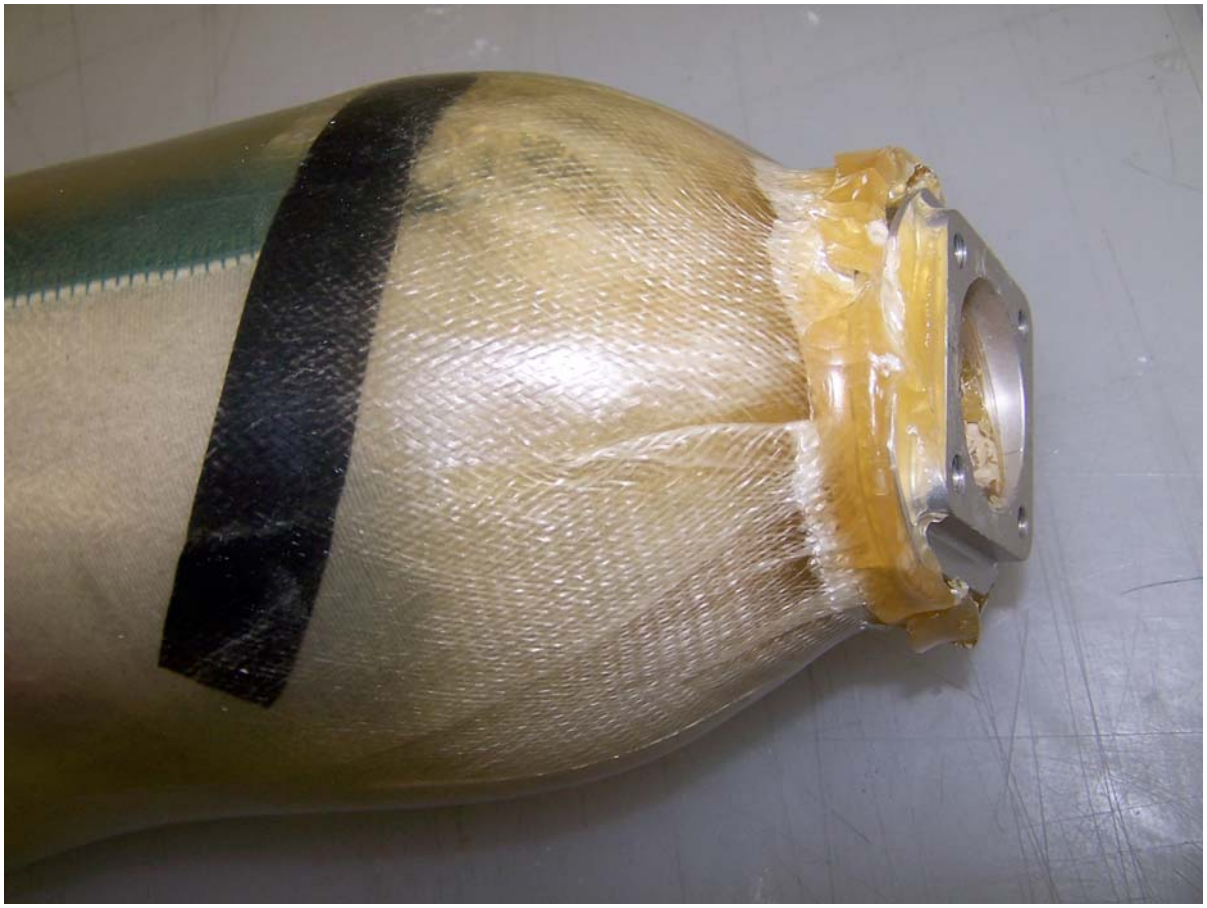

**Figure 11. Failure region close-up view for socket #4.**



1505 Versailles Ct., Marietta, GA 30066
(678) 525 2724
www.dancila.com

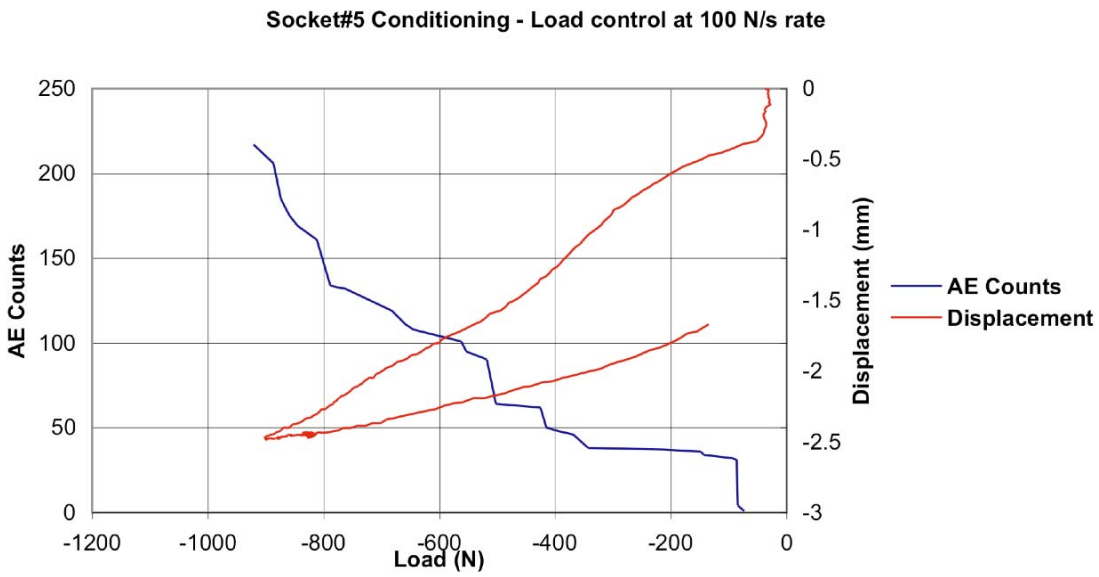


**Figure 12. Conditioning loading stage - Stroke and cumulative acoustic emission counts vs. applied load for socket #5.**

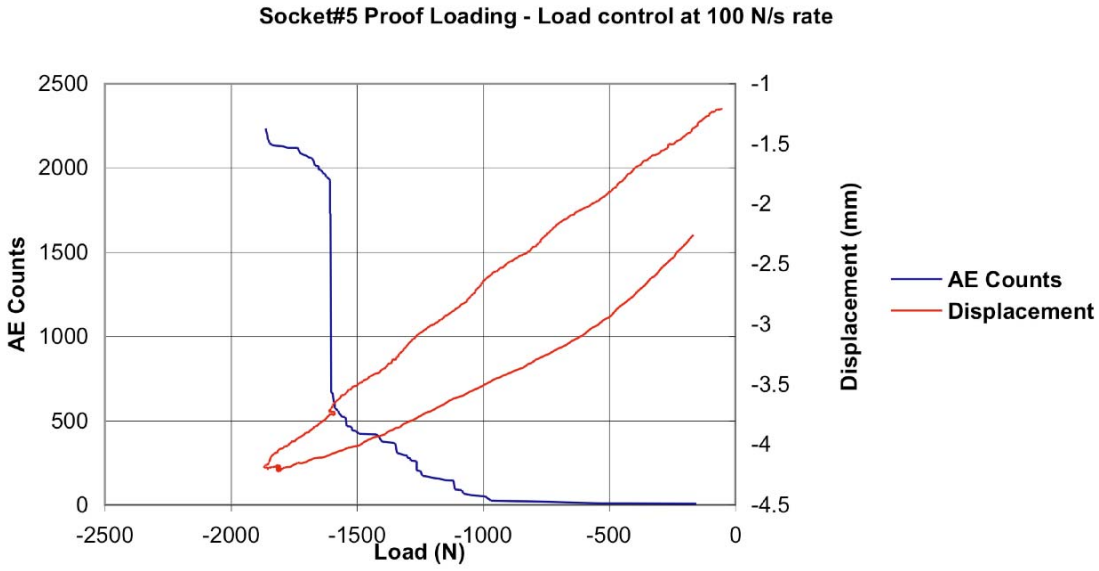


**Figure 13. Proof loading stage - Stroke and cumulative acoustic emission counts vs. applied load for socket #5.**



1505 Versailles Ct., Marietta, GA 30066
(678) 525 2724
www.dancila.com

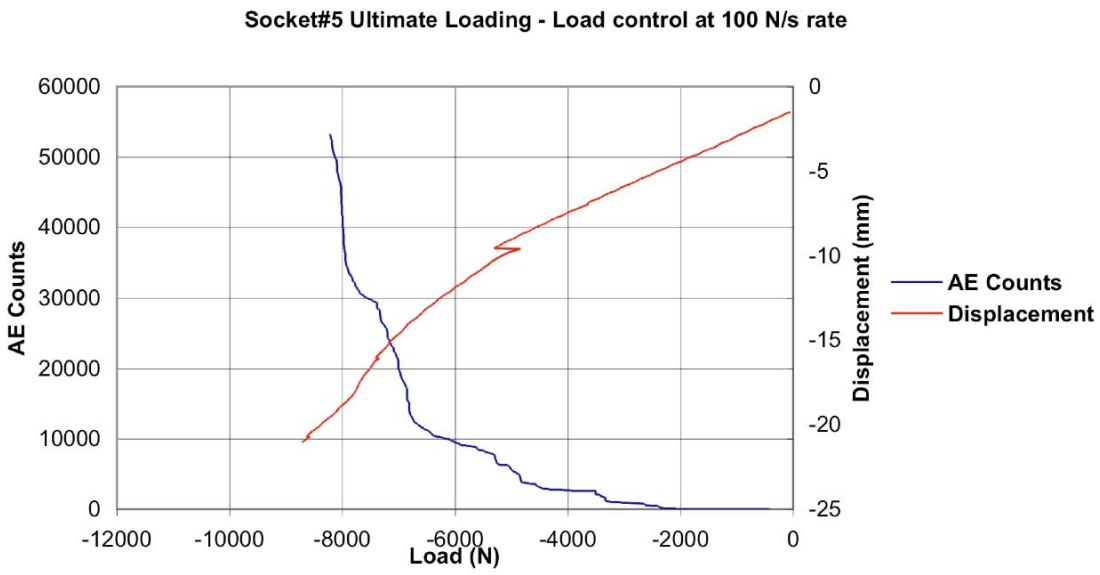


**Figure 14. Ultimate loading stage - Stroke and cumulative acoustic emission counts vs. applied load for socket #5.**



1505 Versailles Ct., Marietta, GA 30066
(678) 525 2724
www.dancila.com

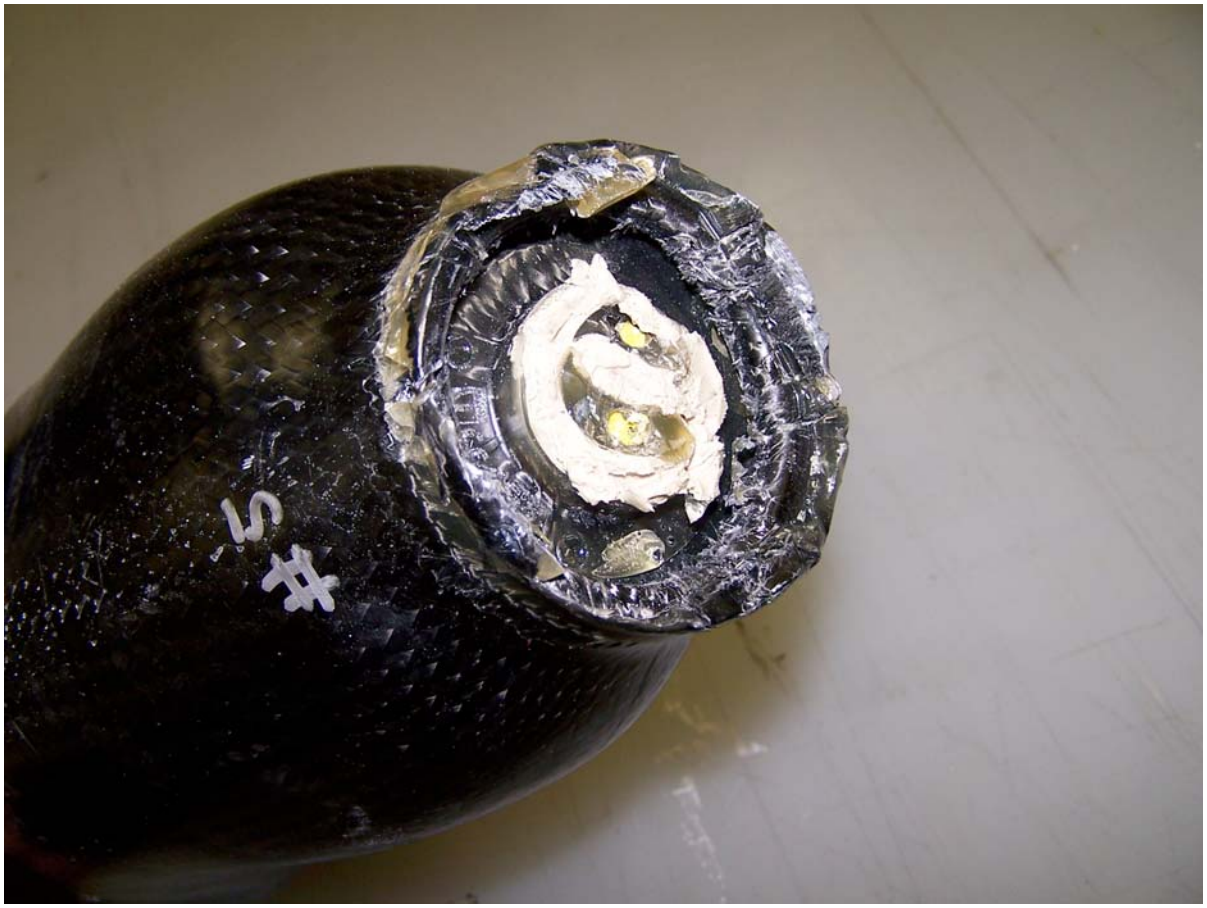


**Figure 15. Failure region close-up view for socket #5.**



1505 Versailles Ct., Marietta, GA 30066
(678) 525 2724
www.dancila.com

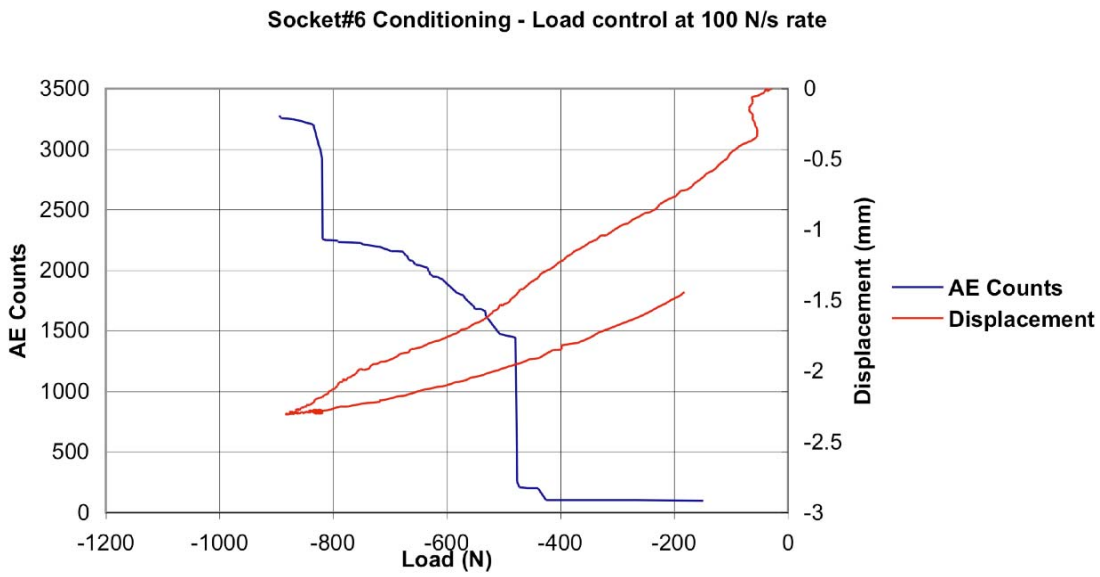


**Figure 16. Conditioning loading stage - Stroke and cumulative acoustic emission counts vs. applied load for socket #6.**

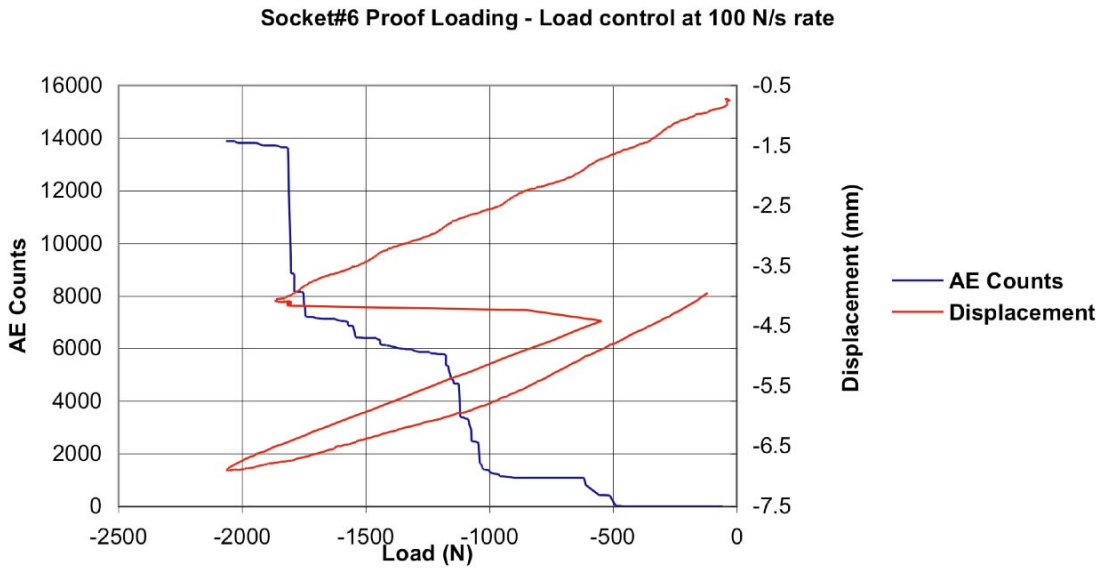


**Figure 17. Proof loading stage - Stroke and cumulative acoustic emission counts vs. applied load for socket #6.**



1505 Versailles Ct., Marietta, GA 30066
(678) 525 2724
www.dancila.com

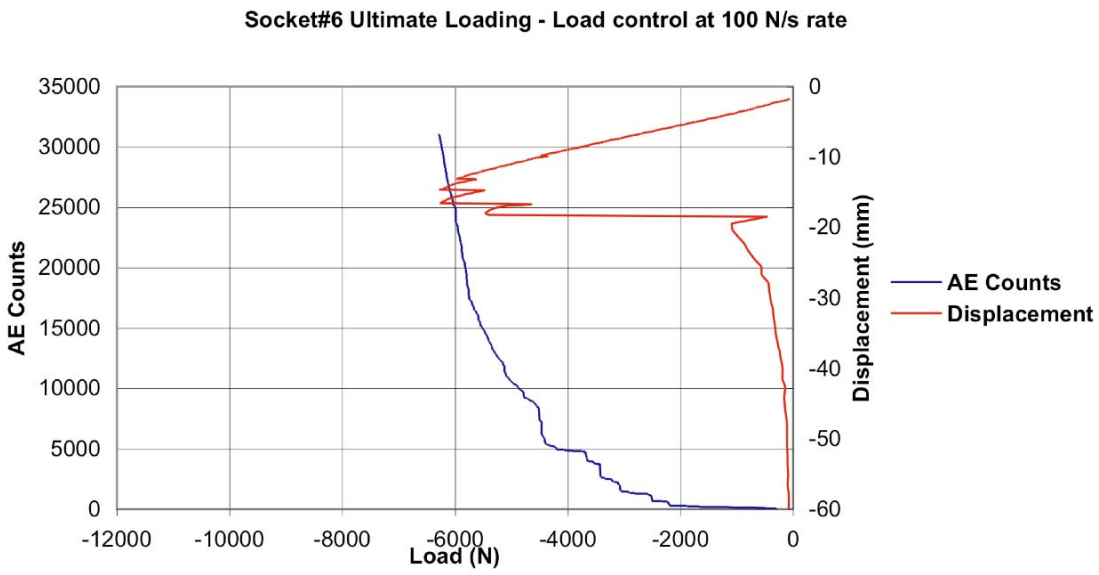


**Figure 18. Ultimate loading stage - Stroke and cumulative acoustic emission counts vs. applied load for socket #6.**



1505 Versailles Ct., Marietta, GA 30066
(678) 525 2724
www.dancila.com

**Figure 19. Failure region close-up view for socket #6.**



1505 Versailles Ct., Marietta, GA 30066
(678) 525 2724
www.dancila.com

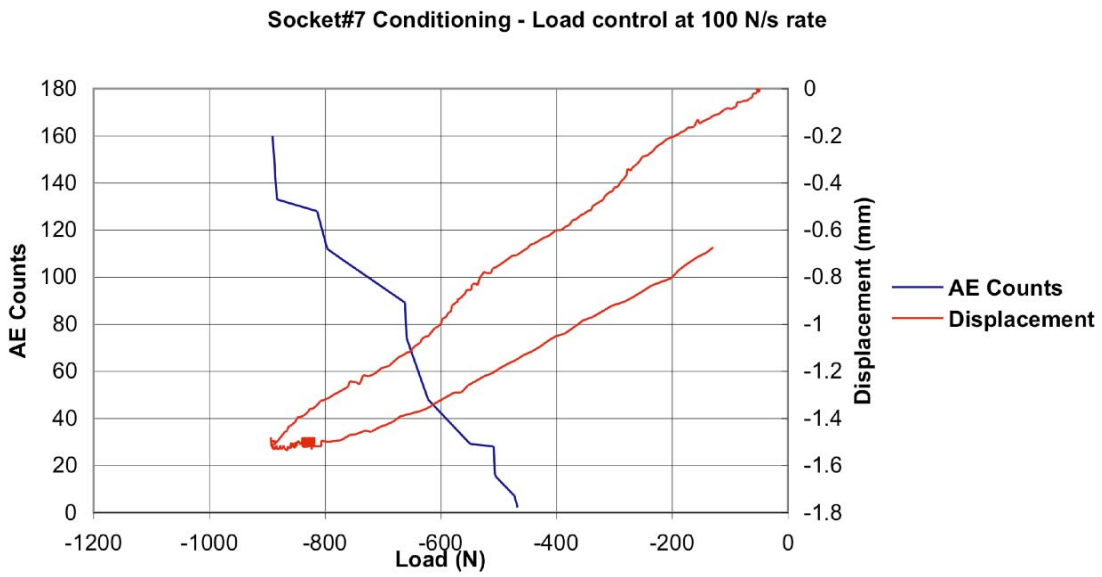


**Figure 20. Conditioning loading stage - Stroke and cumulative acoustic emission counts vs. applied load for socket #7.**

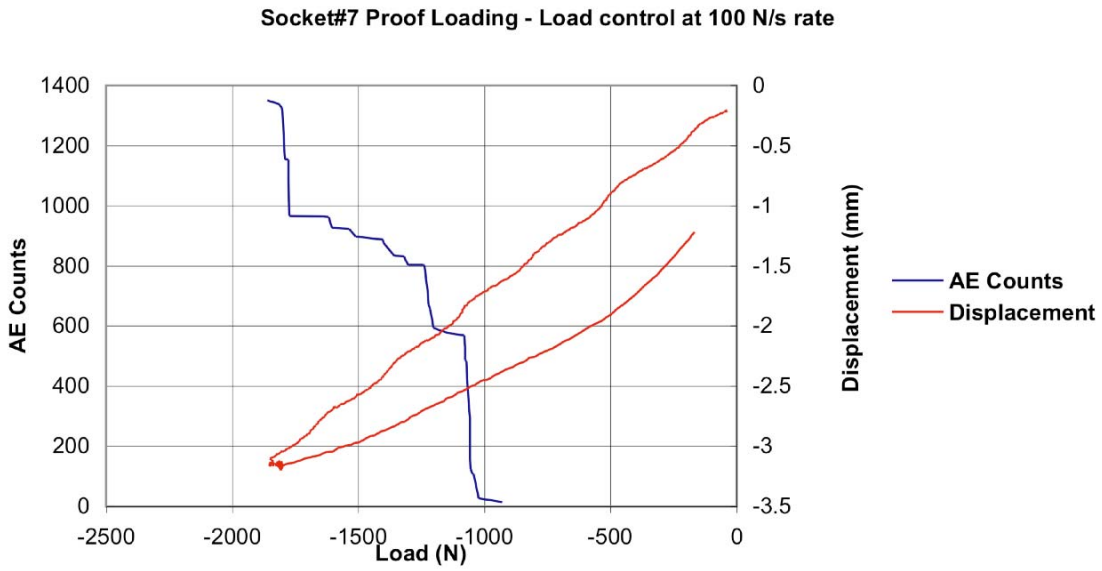


**Figure 21. Proof loading stage - Stroke and cumulative acoustic emission counts vs. applied load for socket #7.**



1505 Versailles Ct., Marietta, GA 30066
(678) 525 2724
www.dancila.com

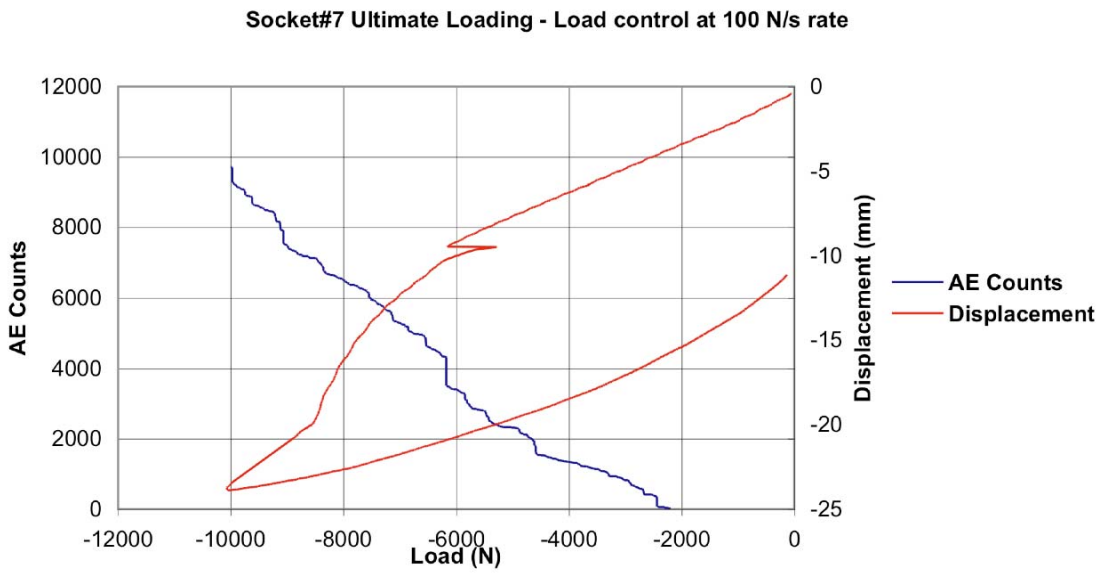


**Figure 22. Ultimate loading stage - Stroke and cumulative acoustic emission counts vs. applied load for socket #7.**



1505 Versailles Ct., Marietta, GA 30066
(678) 525 2724
www.dancila.com

**Figure 23. Distal region close-up view for socket #7.**



1505 Versailles Ct., Marietta, GA 30066
(678) 525 2724
www.dancila.com

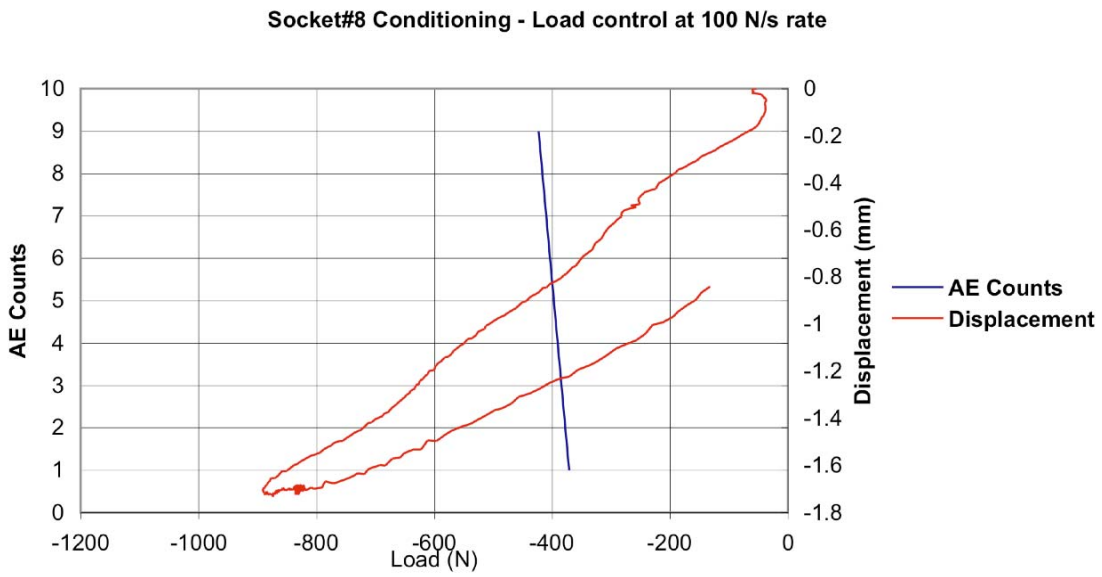


**Figure 24. Conditioning loading stage - Stroke and cumulative acoustic emission counts vs. applied load for socket #8.**

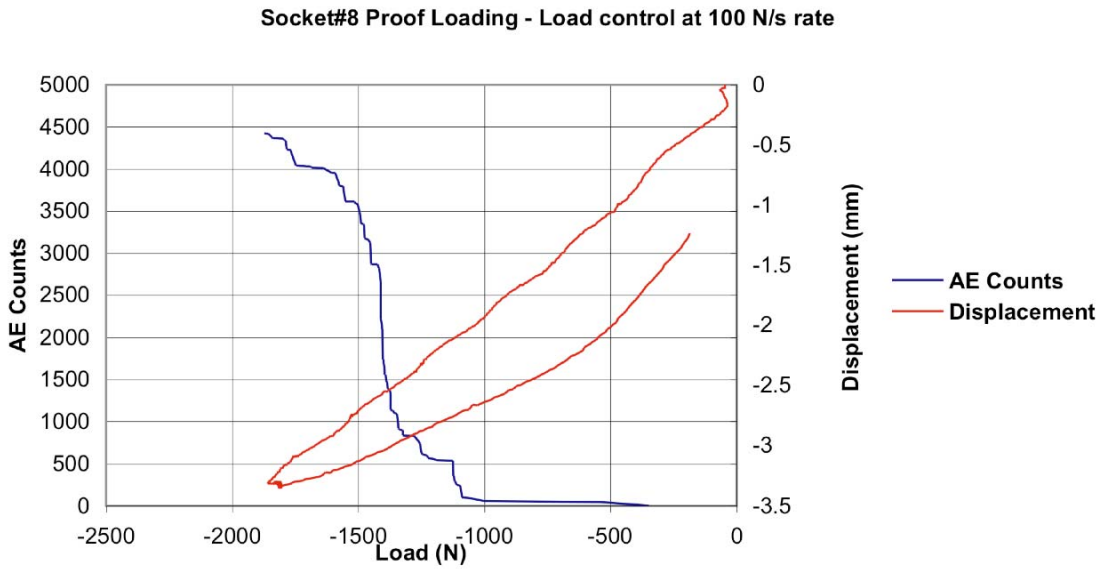


**Figure 25. Proof loading stage - Stroke and cumulative acoustic emission counts vs. applied load for socket #8.**



1505 Versailles Ct., Marietta, GA 30066
(678) 525 2724
www.dancila.com

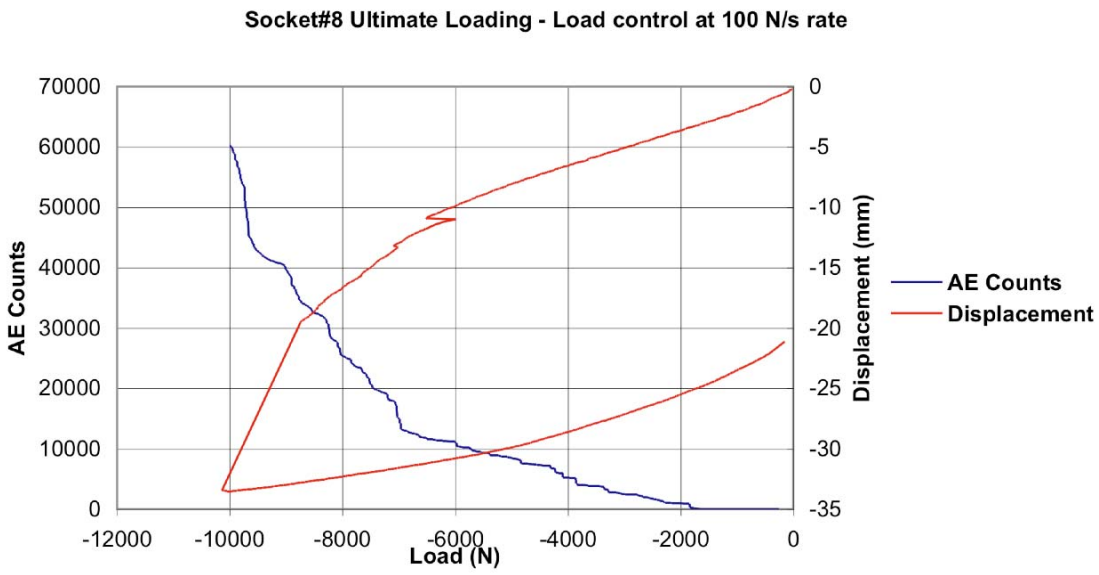


**Figure 26. Ultimate loading stage - Stroke and cumulative acoustic emission counts vs. applied load for socket #8.**



1505 Versailles Ct., Marietta, GA 30066
(678) 525 2724
www.dancila.com

**Figure 27. Distal region close-up view for socket #8.**



1505 Versailles Ct., Marietta, GA 30066
(678) 525 2724
www.dancila.com

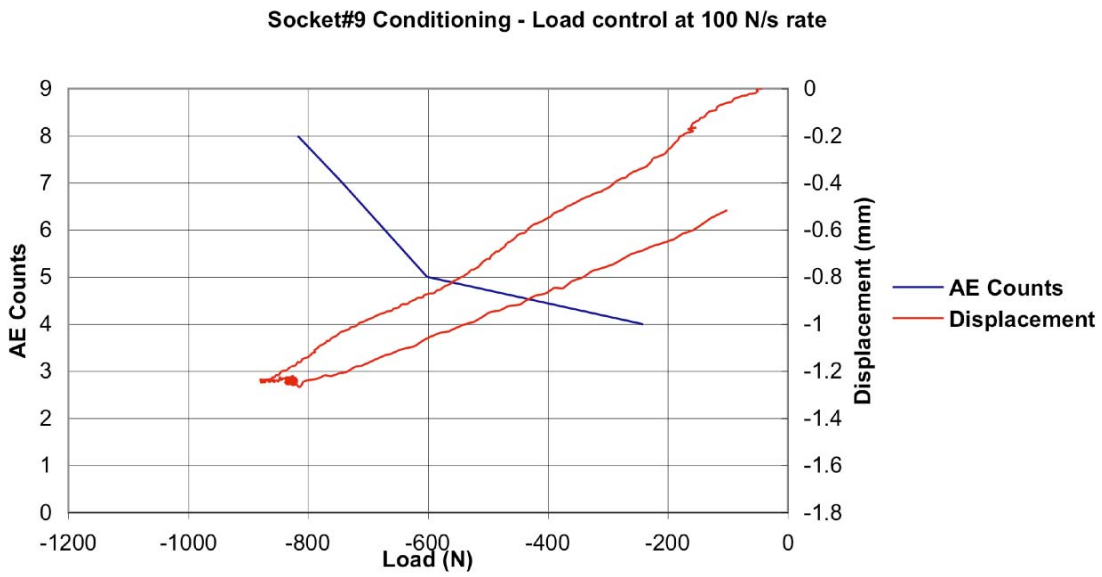


**Figure 28. Conditioning loading stage - Stroke and cumulative acoustic emission counts vs. applied load for socket #9.**

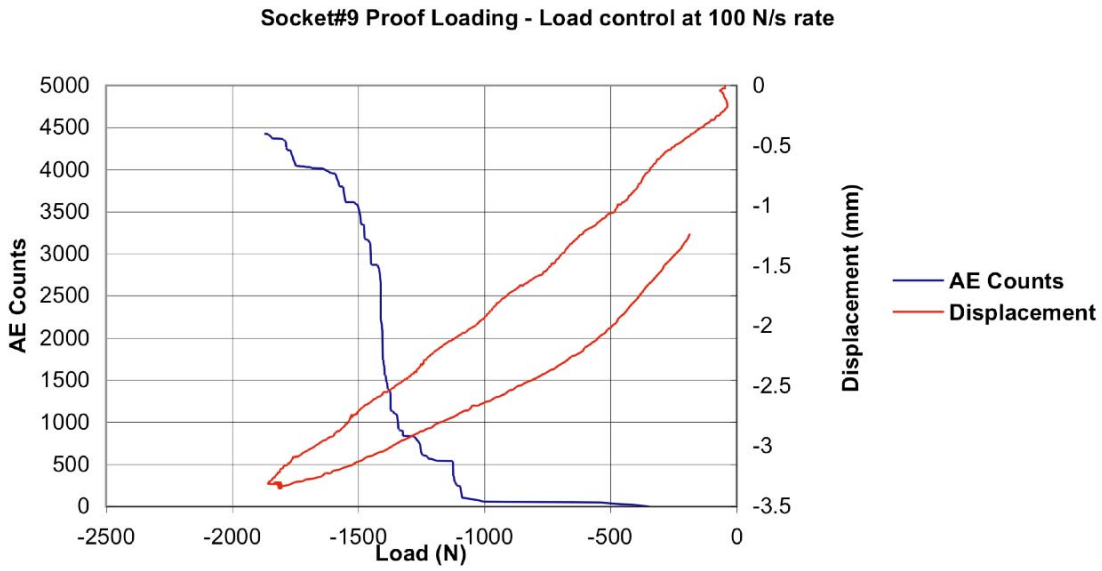


**Figure 29. Proof loading stage - Stroke and cumulative acoustic emission counts vs. applied load for socket #9.**



1505 Versailles Ct., Marietta, GA 30066
(678) 525 2724
www.dancila.com

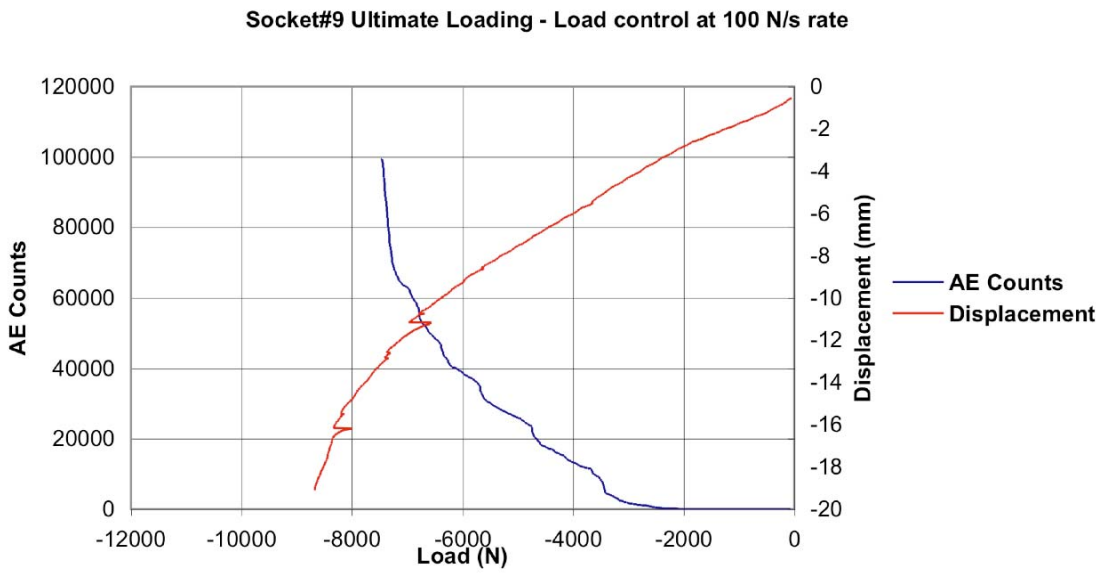


**Figure 30. Ultimate loading stage - Stroke and cumulative acoustic emission counts vs. applied load for socket #9.**



1505 Versailles Ct., Marietta, GA 30066
(678) 525 2724
www.dancila.com

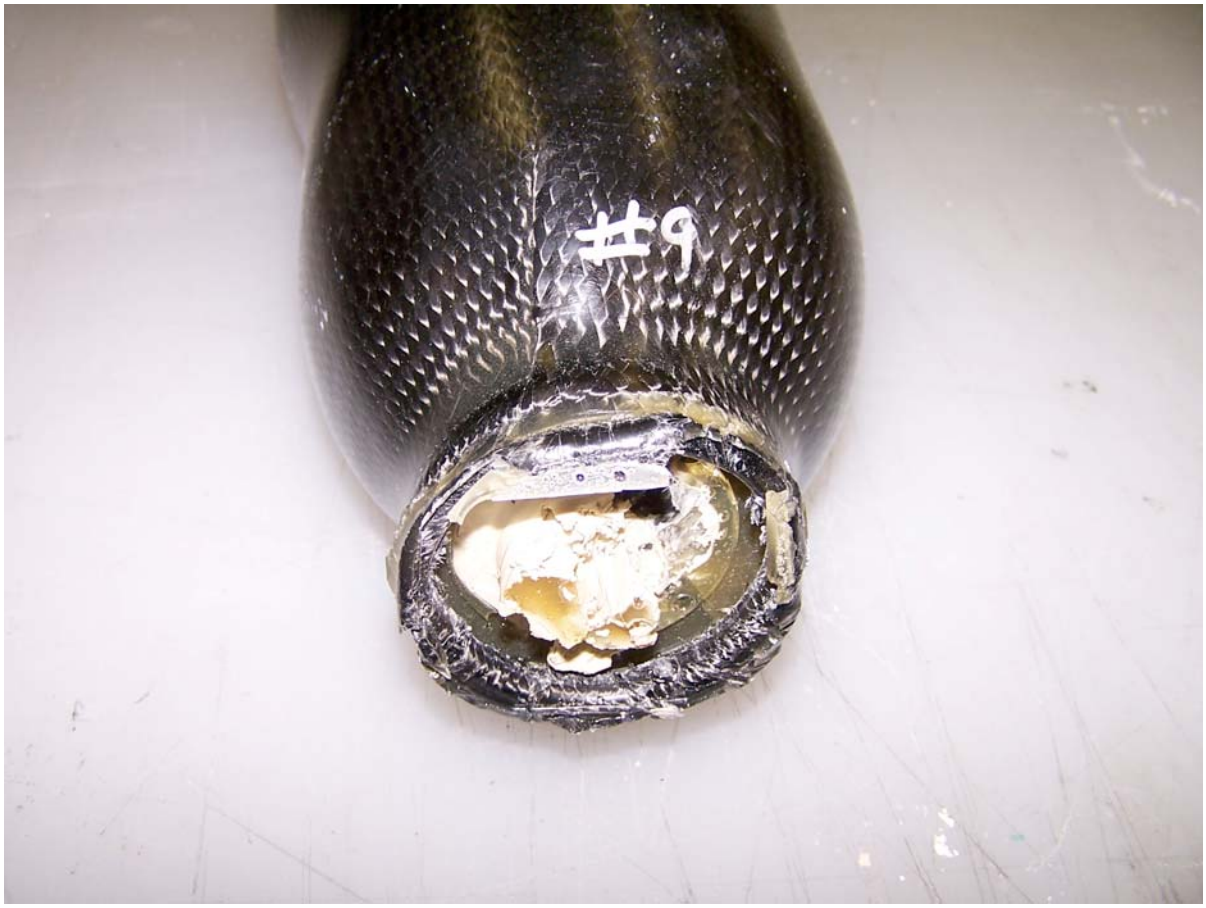


**Figure 31. Failure region close-up view for socket #9.**



1505 Versailles Ct., Marietta, GA 30066
(678) 525 2724
www.dancila.com

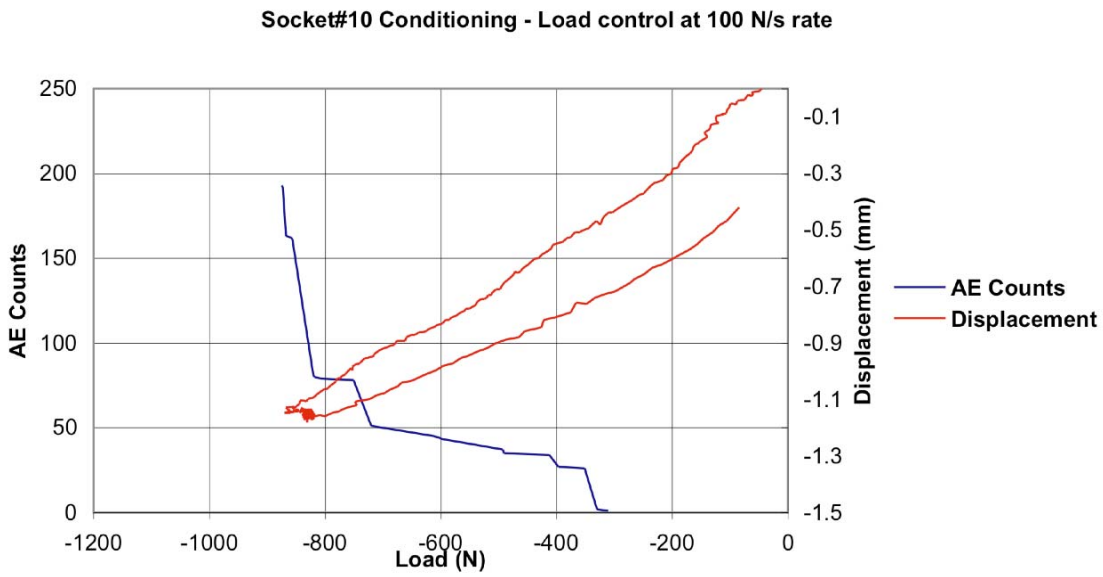


**Figure 32. Conditioning loading stage - Stroke and cumulative acoustic emission counts vs. applied load for socket #10.**

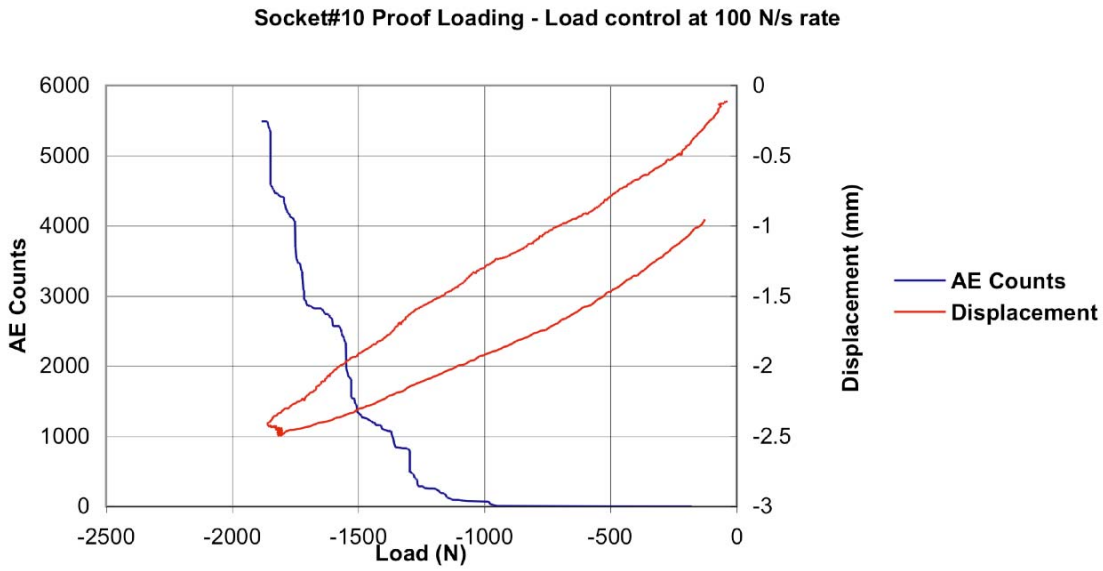


**Figure 33. Proof loading stage - Stroke and cumulative acoustic emission counts vs. applied load for socket #10.**



1505 Versailles Ct., Marietta, GA 30066
(678) 525 2724
www.dancila.com

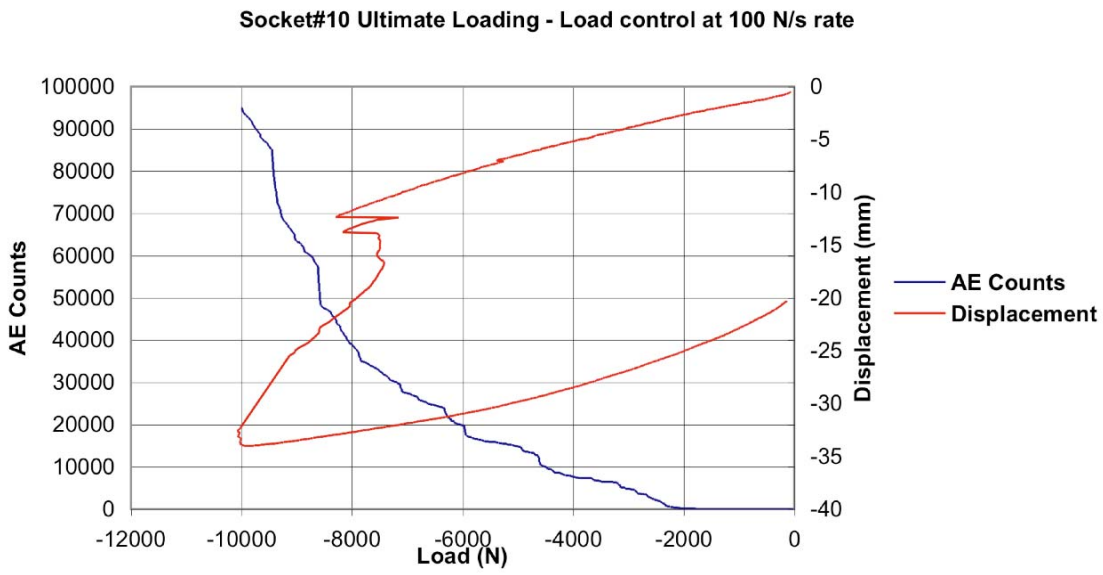


**Figure 34. Ultimate loading stage - Stroke and cumulative acoustic emission counts vs. applied load for socket #10.**



1505 Versailles Ct., Marietta, GA 30066
(678) 525 2724
www.dancila.com

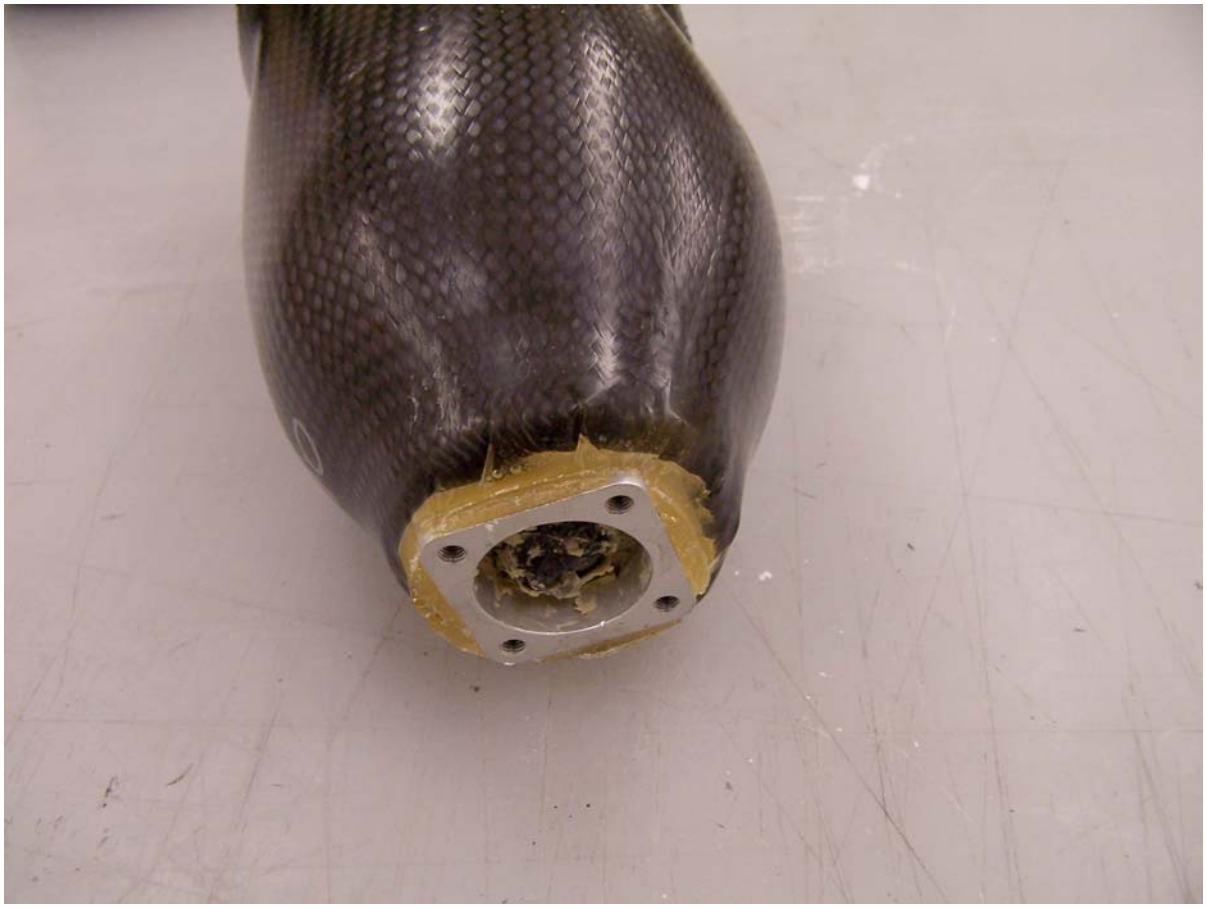

**Figure 35. Distal end close-up view for socket #10.**



1505 Versailles Ct., Marietta, GA 30066
(678) 525 2724
www.dancila.com

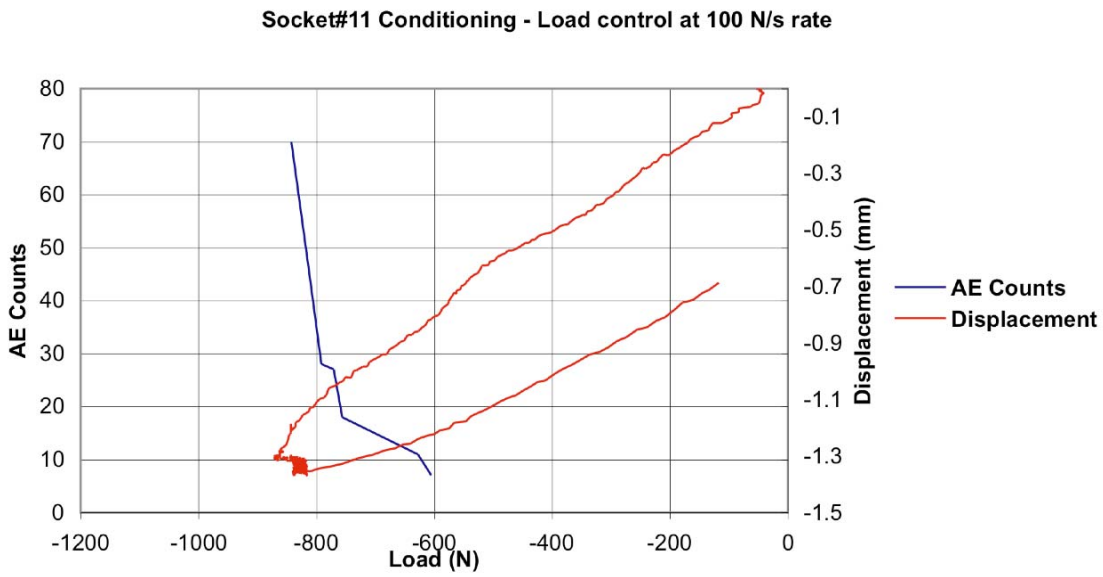


**Figure 36. Conditioning loading stage - Stroke and cumulative acoustic emission counts vs. applied load for socket #11.**

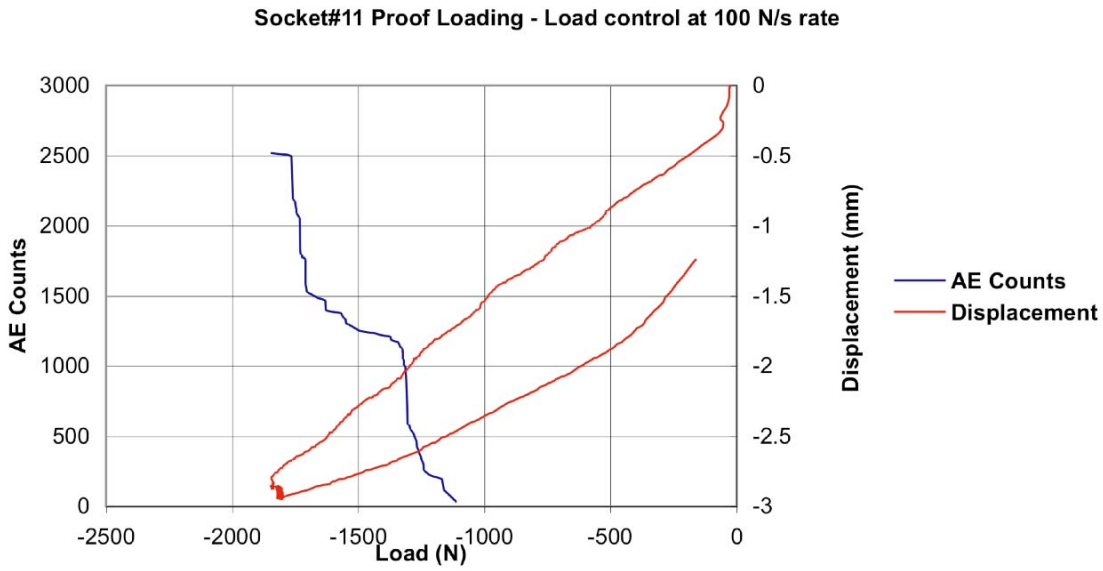


**Figure 37. Proof loading stage - Stroke and cumulative acoustic emission counts vs. applied load for socket #11.**



1505 Versailles Ct., Marietta, GA 30066
(678) 525 2724
www.dancila.com

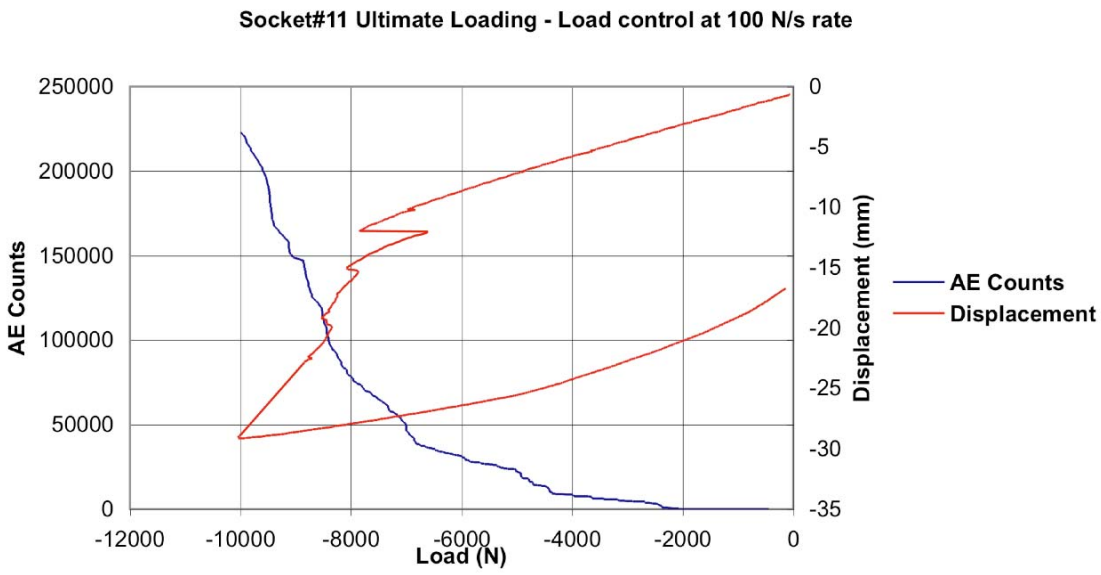


**Figure 38. Ultimate loading stage - Stroke and cumulative acoustic emission counts vs. applied load for socket #11.**



1505 Versailles Ct., Marietta, GA 30066
(678) 525 2724
www.dancila.com


**Figure 39. Distal end close-up view for socket #11.**



1505 Versailles Ct., Marietta, GA 30066
(678) 525 2724
www.dancila.com

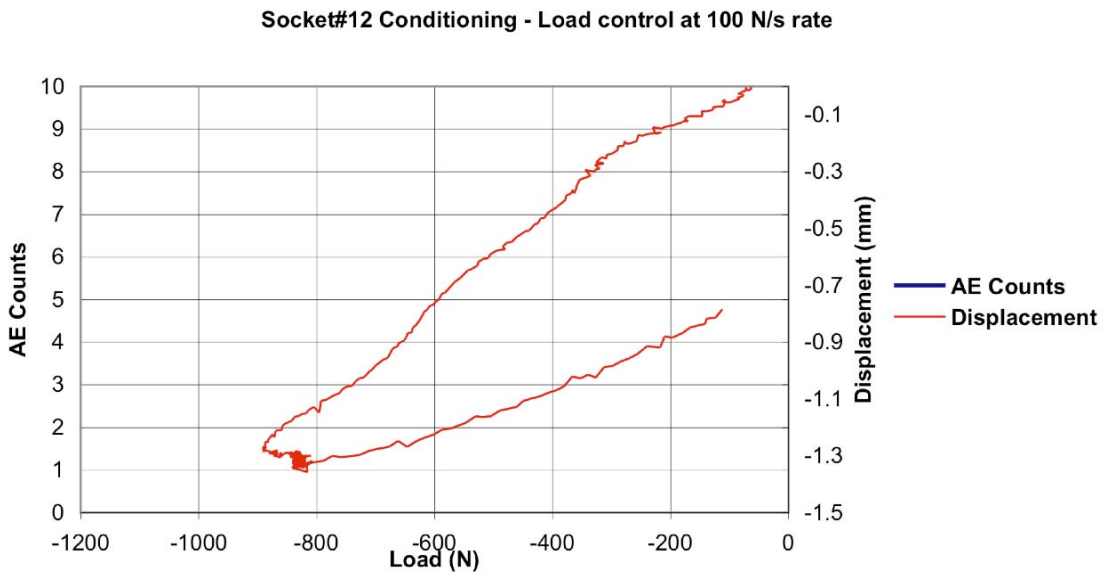


**Figure 40. Conditioning loading stage - Stroke and cumulative acoustic emission counts vs. applied load for socket #12.**

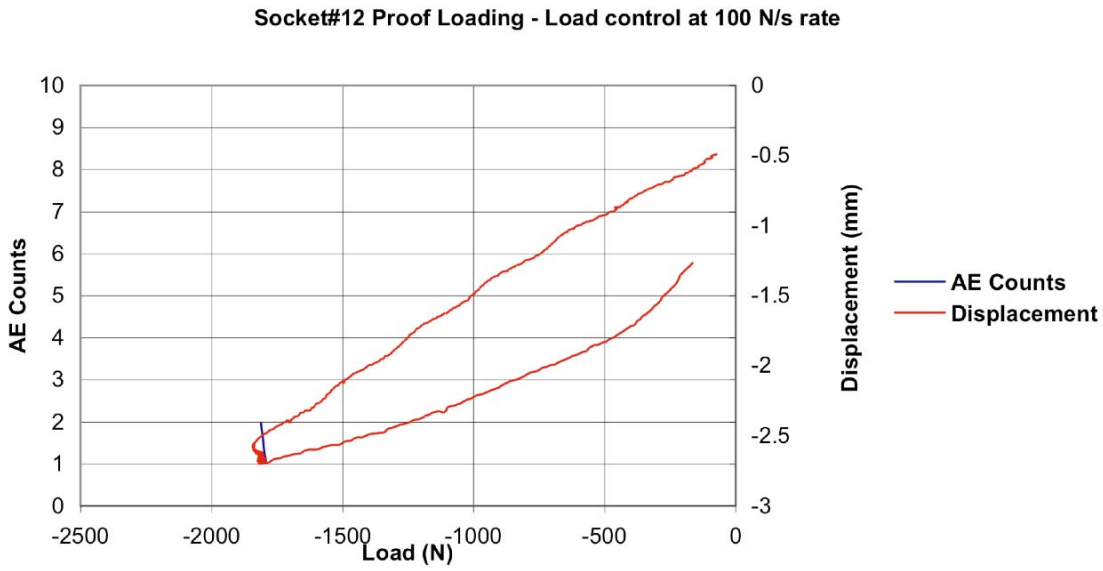


**Figure 41. Proof loading stage - Stroke and cumulative acoustic emission counts vs. applied load for socket #12.**



1505 Versailles Ct., Marietta, GA 30066
(678) 525 2724
www.dancila.com

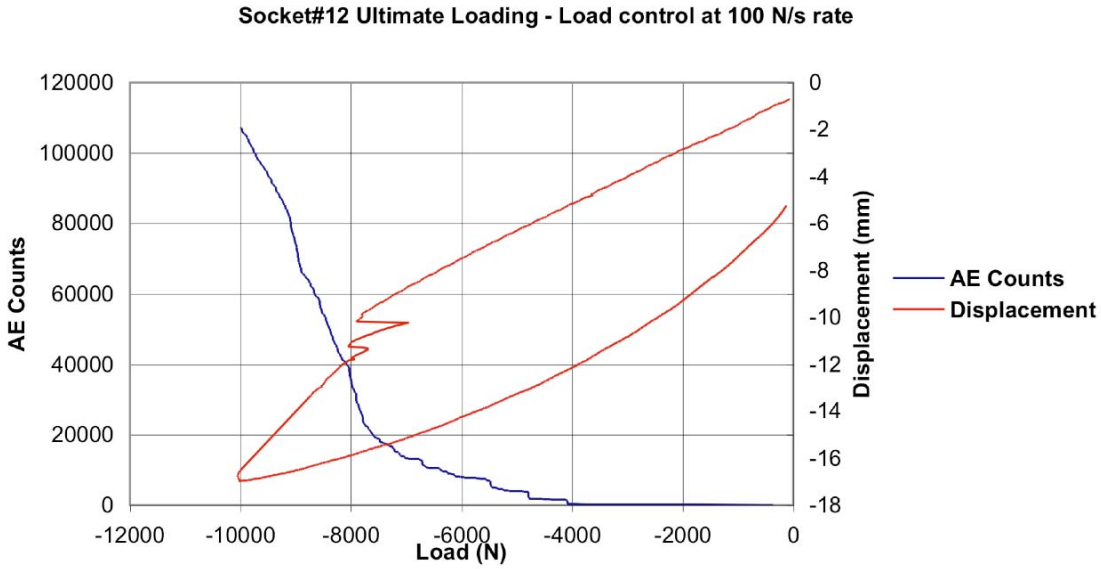


**Figure 42. Ultimate loading stage - Stroke and cumulative acoustic emission counts vs. applied load for socket #12.**



1505 Versailles Ct., Marietta, GA 30066
(678) 525 2724
www.dancila.com

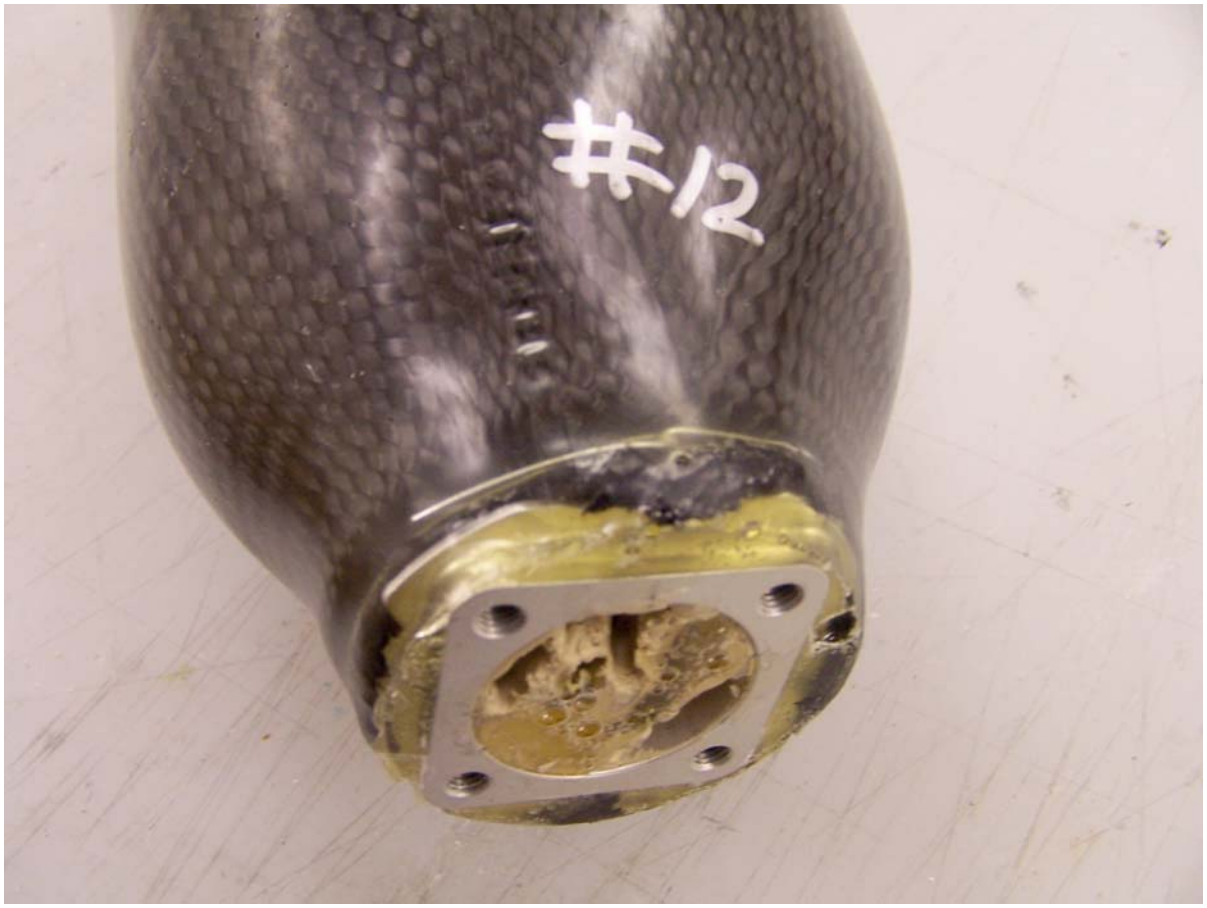


**Figure 43. Distal end close-up view for socket #12.**



1505 Versailles Ct., Marietta, GA 30066
(678) 525 2724
www.dancila.com